

GUGGENHEIM AERONAUTICAL LABORATORY

CALIFORNIA INSTITUTE OF TECHNOLOGY

STRESS DISTRIBUTION IN TWO  
INTERSECTING CYLINDERS UNDER PRESSURE

Thesis by

Lt. Cmdr. Vernon E. Teig, USN

Library  
U. S. Naval Postgraduate School  
Annapolis, Md.

PASADENA, CALIFORNIA

Thesis  
T23

Thesis  
23

STRESS DISTRIBUTION IN TWO INTERSECTING  
CYLINDERS UNDER PRESSURE

Thesis by

Lieutenant Commander Vernon E. Teig, U. S. Navy

Library  
U. S. Naval Postgraduate School  
Annapolis, Md.

In Partial Fulfillment of the Requirements

For the Degree of  
Aeronautical Engineer

California Institute of Technology

Pasadena, California

1949

## ACKNOWLEDGEMENT

The author is indebted to Dr. Ernest E. Sechler, Professor of Aeronautics, California Institute of Technology, for his valuable guidance in the formulation of this thesis, and to Mr. William H. Bowen, Superintendent, Guggenheim Aeronautical Laboratory, California Institute of Technology, for his able assistance and advice in the procurement and preparation of the test specimens and testing equipment. He also wishes to thank the other members of his supervising committee, Professors Housner and Fung for their comments and criticisms on the work.

Further indebtedness is acknowledged to Commander Leonard E. Harmon, U. S. Navy, who collaborated in conducting the experiments and in the preparation of all tables and graphs presented herein.

## SUMMARY

The experimental studies presented here were undertaken in an effort to determine the stress distribution in two circular cylinders intersecting at right angles and under internal pressure. The investigation was limited to tests of two specimens in the thick-walled cylinder range.

The experimental analysis led to the following conclusions:

1. The highest stress concentrations are located at an angle of about 14.5 degrees from the crotch centerline, measured in the plane of the intersection.
2. The critical stress causing rupture is the tangential stress in the plane of the ellipse.
3. For the  $R/t$  ratios tested, the strength reduction as compared with a straight closed cylinder is approximately 50%.
4. It appears probable that bending effects for these thick-walled cylinders are of relatively minor importance.

## TABLE OF CONTENTS

Part	Title	Page
	Introduction	1
I	Equipment and Procedure	3
II	Results and Discussion	7
III	Conclusions	14
IV	Recommendations	15
V	References and Bibliography	16
VI	Formulas and Sample Calculations	17
	Tables	A-1
	Figures	B-1

## LIST OF TABLES

		Page
Tables I through IX	Variation of Tangential and Axial Strains with Variation of Internal Pressure. Test No. I.	A-1
Tables X through XVIII	Variation of Tangential and Axial Strains with Variation of Internal Pressure. Test No. II	A-10
Table XIX	Relation of Load to $p \frac{R}{t}$	A-19

## LIST OF FIGURES

	Page
Fig. 1 First Specimen and Test Setup.	B-1
Fig. 2 Closeup View of First Specimen Showing Rupture.	B-2
Fig. 3 Second Specimen and Test Setup.	B-3
Fig. 4 Closeup View of Second Specimen Showing Rupture.	B-4
Fig. 5 Detail Design of Specimen.	B-5
Fig. 6 Assembly Drawing of Specimen.	B-6
Fig. 7 Positions of Gages on Specimens.	B-7
Fig. 8 Gage Orientation on First Specimen.	B-8
Fig. 9 Gage Orientation on Second Specimen.	B-9
Fig. 10 Load vs. Tangential Strain. Test No. I	B-10
Fig. 11 Load vs. Axial Strain. Test No. I	B-11
Fig. 12 Load vs. Tangential Strain. Test No. II	B-12
Fig. 13 Load vs. Axial Strain. Test No. II	B-13
Fig. 14 Load vs. Tangential Strain. Position No. 1	B-14
Fig. 15 " " " " " " 2	B-15
Fig. 16 " " " " " " 3	B-16
Fig. 17 " " " " " " 4	B-17
Fig. 18 " " " " " " 5	B-18
Fig. 19 " " " " " " 6	B-19
Fig. 20 " " " " " " 7	B-20
Fig. 21 " " " " " " 8	B-21
Fig. 22 " " " " " " 9	B-22

					Page
Fig. 23	Load vs. Axial Strain.		Position No. 1.		B-23
Fig. 24	" " " "		" " 2.		B-24
Fig. 25	" " " "		" " 3.		B-25
Fig. 26	" " " "		" " 4.		B-26
Fig. 27	" " " "		" " 5.		B-27
Fig. 28	" " " "		" " 6.		B-28
Fig. 29	" " " "		" " 7.		B-29
Fig. 30	" " " "		" " 8.		B-30
Fig. 31	" " " "		" " 9.		B-31
Fig. 32	Principal Strain vs. Axial Position, Test I				B-32
Fig. 33	Tangential	"	"	"	B-33
Fig. 34	Axial	"	"	"	B-34
Fig. 35	Principal	"	"	"	B-35
Fig. 36	Tangential	"	"	"	B-36
Fig. 37	Axial	"	"	"	B-37
Fig. 38	Principal	"	"	Position on Intersection, Test I	B-38
Fig. 39	Tangential	"	"	"	B-39
Fig. 40	Axial	"	"	"	B-40
Fig. 41	Principal	"	"	Axial Position, Test II	B-41
Fig. 42	Tangential	"	"	"	B-42
Fig. 43	Axial	"	"	"	B-43
Fig. 44	Principal	"	"	"	B-44
Fig. 45	Tangential	"	"	"	B-45



	Page
Fig. 46 Axial Strain vs. Axial Position, Test II	B-46
Fig. 47 Principal " " Position on Intersection, Test II	B-47
Fig. 48 Tangential " " " " " "	B-48
Fig. 49 Axial " " " " " "	B-49
Fig. 50 Sketches of Breaks in Welds, Tests I and II	B-50

## EXPLANATION OF SYMBOLS

$E$	Young's Modulus of Elasticity (assumed = $30 \times 10^6$ psi)
$R$	Strain gage reading
$b$	Strain gage constant (-200)
$p$	Internal pressure - lbs./sq.in.
$\epsilon_a$	Axial strain - in./in.
$\epsilon_r$	Radial strain - in./in.
$\epsilon_t$	Tangential strain - in./in.
$\epsilon_1$	Principal strain - in./in.
$\sigma_a$	Axial stress - lbs./sq.in.
$\sigma_r$	Radial stress - lbs./sq.in.
$\sigma_t$	Tangential stress - lbs./sq.in.
$\sigma_{1,2}$	Principal stresses - lbs./sq.in.
$\mu$	Poisson's ratio - (assumed = 0.3)

## INTRODUCTION

This investigation was prompted by certain problems which have arisen in systems employing high pressure piping. The construction of ducting for high speed wind tunnels involves cylindrical intersections of large diameter and similar problems, though on a smaller scale, may be found in various industrial applications. For piping which is highly stressed tangentially it has been the practice to furnish heavy ribs or other devices to take the bending stresses of the elliptical intersection. This procedure ignores bending stiffness of the pipe itself and some doubt has arisen as to the actual necessity for such ribs. Further, in some cases there was evidence that the reinforcing might in reality be harmful to the strength of the joint.

The tests presented here are steps toward a complete investigation of the problem. Some tests of this nature were made preliminary to the design and construction of the 20-inch supersonic wind tunnel of the Jet Propulsion Laboratory (CIT) (Ref. 1). The specimens tested in that project were of various shapes, materials, and Radius/thickness ratios. For the present approach to the problem it was decided to reduce the number of variable parameters to just one--the wall thickness. The steel to be used, the internal diameter, and other specifications were held constant. For this series it was originally planned to make tests on 90-degree elbows of at least four wall thicknesses, but difficulties in the manufacture of suitable specimens and time limitations forced a reduction in scope to only two specimens.

A search was made both in applicable textbooks and in the many engineering publications for previous work, either theoretical or experimental, on this subject. Considerable information was found on pipe bends, pipe elbows, and the like, but nothing on stresses to be found at or near a welded cylindrical intersection. This problem is of a type possessing mixed boundary conditions and as such is very difficult to solve from a purely theoretical approach.

The tests whose results are presented herein were conducted in the Structures Laboratory of the Guggenheim Graduate School of Aeronautics, California Institute of Technology.

### EQUIPMENT AND PROCEDURE

The test specimens were made of eight-inch National Extra Strong welded steel pipe, ASTM Spec. 53-47. This steel has a yield point of 30,000 psi. and ultimate strength of 48,000 psi. The pipe was first machined inside and out to remove any eccentricity and to obtain a uniform wall thickness. Inside diameter was held constant for both specimens and was 7.68 inches. The wall thickness of the first specimen was 0.4 inch and the second was 0.3 inch.

After machining, the pipe was cut and welded so as to form a 90-degree elbow as shown in Fig. 6. Care was taken in machining off excess weld metal in the joint in order to have smooth fillets of small radius so that the finished product would approximate as closely as possible a cylindrical intersection machined from a single billet. Standard eight-inch pipe caps were welded on the ends and threaded studs welded in these caps. The studs were drilled and tapped to provide pressure connections and were threaded to receive lugs intended for use in applying either tension or compression across the ends by means of a turnbuckle. The turnbuckle was not used, however. Complete details of manufacture and assembly are shown in Figs. 5 and 6.

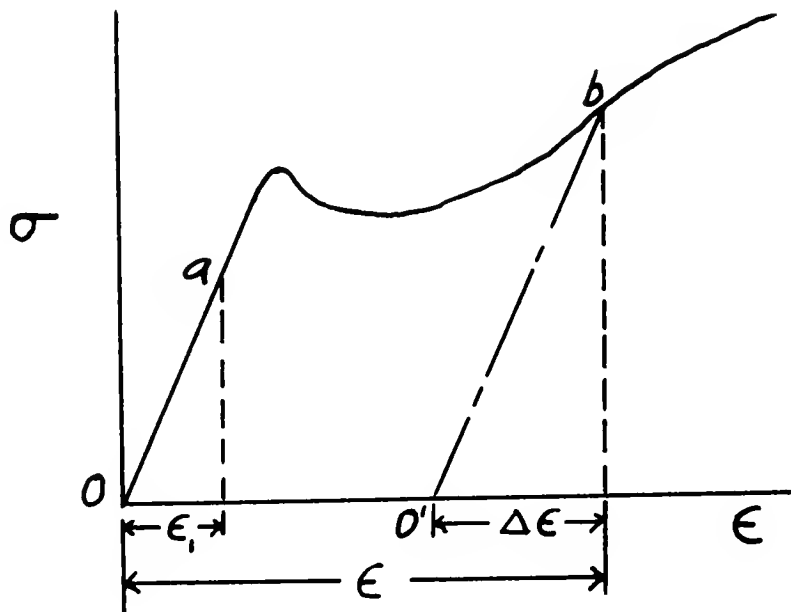
Pressure was applied by means of a Blackhawk hand-operated hydraulic pump. Pressure was measured by a standard high pressure gage. The variable resistance wire strain gages used were Baldwin-Southwark A-8 rectangular gages and AR-7 rectangular rosettes. The location and orientation of these gages is shown in Figs. 7, 8, and 9. Other equipment included a potentiometer and Wheatstone Bridge circuit, a switch

panel, 6-volt battery, and the necessary wiring and plumbing. The specimen was placed on wooden block supports spaced approximately 6 and 16 inches from each end.

The same procedure was followed in both tests. Within the elastic limit the following procedure was observed:

- (1) Zero readings were taken on all gages.
- (2) Load was applied and load readings taken.
- (3) Load was removed and a second zero reading taken.
- (4) Increased load was applied, readings taken, followed again by zero readings, etc.

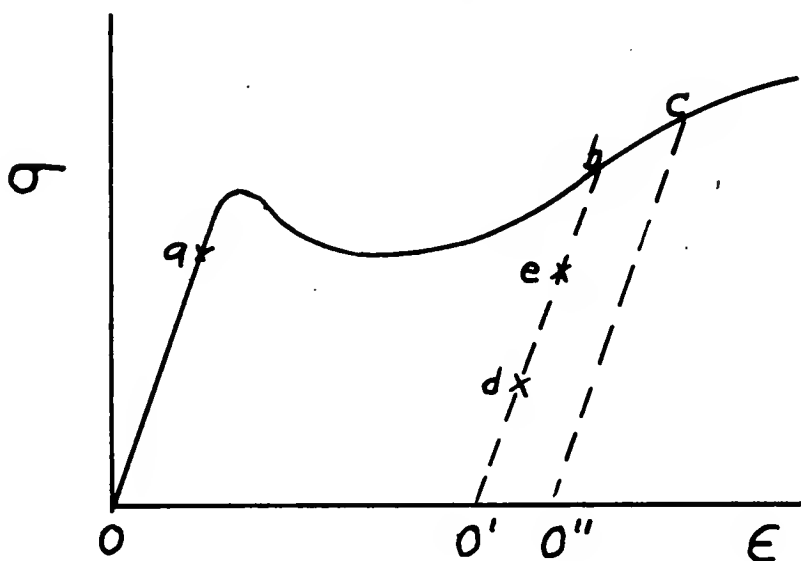
After the elastic limit had been exceeded, zero readings were taken only after the load readings. The reason for this can be seen by considering the curve below.



Assume that under the applied load, the metal at some given position reaches point "a" on the stress-strain diagram. This is below the elastic limit and when the load is removed both the stress and the

strain ( $\epsilon$ ) return to zero. Now if a sufficiently high load to cause yielding is applied, some point "b" on the curve will be reached. When the load is now removed, the line  $bo'$  will be followed ending at zero stress but with a permanent set  $o-o'$ . This permanent set can be computed by comparing strain gage readings at  $o$  and at  $o'$ . The strain at point "b" cannot now be referred directly to the zero strain at  $o$  but must be referred to the new "zero" at  $o'$ . Doing this gives the value of  $\Delta\epsilon$  and adding this strain increment to the permanent set  $o-o'$  gives the total strain  $\epsilon$  at point "b".

Theoretically the line  $bo'$  of the preceding diagram is parallel to  $oe$ . In order to check on the reliability of strain gage readings beyond the specimen elastic limit, this parallelism was utilized by taking readings at points  $d$  and  $e$  on the way up to point  $c$ .



the next higher load reading above  $b$ . Since stress was not measured directly, a stress versus strain curve could not be plotted. Points

d and e were plotted on the load versus strain curves where the same reasoning as above applies. Therefore it was assumed that if points o', d, e, and b on the load-strain curves plotted a straight line parallel to oa, the strain gages were giving useful readings.

Punch marks were made in the stud in each end cap and a trammel bar and points used to measure the distance between the punch marks both in the unloaded condition and for each loading applied.

At the higher loadings where considerable yielding occurred it was necessary to maintain pressure constant for some time until a condition of equilibrium was reached and readings held substantially constant.



## RESULTS AND DISCUSSION

The results of the two series of tests have been plotted on curves of loading versus tangential strain and axial strain for the several strain gage locations. The axial and tangential components were plotted since these were the strain components actually measured and also to facilitate comparison with the curves applying to a straight tube and the curves derived from previous tests on specimens having larger  $R/t$  ratios than those used in the present investigation. The principal strains and the principal axis orientation were computed within the elastic limit and are included in the tables. The maximum pressure held by the first specimen (0.4" wall) was 3350. psi. The maximum pressure held by the second specimen was 2950. psi.

The results of the two tests as shown in Tables I - XVIII and Figs. 22 and 27 show that the axial strains at position #5 are only very slightly smaller than the tangential strains at position #9 for all loadings under the elastic limit. Above the elastic limit, however, the tangential strains in the crotch increase much more rapidly than do those at any other point measured. For the locations investigated in these tests then, the critical strains occur in the crotch and are the tangential strains.

The type and location of ruptures obtained in the two tests were almost exactly identical as can be seen in Figs. 2, 4, and 50. In each case the failure was a crack perpendicular to the line of the weld at a distance of  $1\frac{1}{2}$ " up from the crotch centerline. In both cases audible cracks and snaps were heard at irregular intervals as

the internal pressure was increased. In the first test these noises started at a pressure of about 2600 psi and were accompanied by the appearance of fine, hair-line cracks in the weld and perpendicular to the line of the weld as shown in Fig. 50. In the second test no such cracks appeared, but roughened stress lines approximately parallel to the weld appeared in the parent metal near the weld.

In specimen #2, cracks between the parent metal and the weld metal started widening perceptibly at loads below the elastic limit. As in specimen #1, however, when rupture finally occurred, the break was in the weld and at right angles to both the line of the weld and the initial cracks. Since the two breaks were so exactly similar, it seems quite possible that a point of stress concentration existed between positions #6 and #9. This possibility should be investigated in any further tests of this nature. Further evidence of this high stress area was given by the extremely high strains measured at position #6. The tangential gage in the crotch failed fairly early, but up to the time of failure indicated strains even higher than those at position #6.

Rosettes 1, 2, and 4 all were located some distance from the weld. (Fig. 7) The test results from both specimens as plotted in Figs. 10 and 12 show that the tangential strains did not become large until high loadings were applied. When these strains did begin to increase, the magnitudes of the strains and the rates of increase at these three locations remained quite close to each other. The axial strains show no such uniformity but all remained relatively small as

compared with the tangential strains. A comparison of strains at these three locations with the theoretical strains in a straight pipe follows:  $p = 1,000$ . psi.

$$\begin{array}{l}
 \text{I: } \epsilon_{a_{th}} = .0608 \times 10^{-3} \quad \epsilon_{a_1} = .0865 \times 10^{-3} \quad \epsilon_{a_2} = .0318 \times 10^{-3} \quad \epsilon_{a_4} = .0764 \times 10^{-3} \\
 \epsilon_{\tau_{th}} = .2586 \times 10^{-3} \quad \epsilon_{\tau_1} = .1896 \times 10^{-3} \quad \epsilon_{\tau_2} = .2694 \times 10^{-3} \quad \epsilon_{\tau_4} = .3274 \times 10^{-3} \\
 \text{II: } \epsilon_{a_{th}} = .0822 \times 10^{-3} \quad \epsilon_{a_1} = .1392 \times 10^{-3} \quad \epsilon_{a_2} = .0299 \times 10^{-3} \quad \epsilon_{a_4} = .0946 \times 10^{-3} \\
 \epsilon_{\tau_{th}} = .3490 \times 10^{-3} \quad \epsilon_{\tau_1} = .3305 \times 10^{-3} \quad \epsilon_{\tau_2} = .3048 \times 10^{-3} \quad \epsilon_{\tau_4} = .4313 \times 10^{-3}
 \end{array}$$

Previous testing and experience had indicated an appreciable bending effect in this type of joint as evidenced by an opening of the original ninety-degree angle. For both specimens tested in this investigation no measurable amount of bending was found until the rupture point was reached. This would seem to indicate, at least for  $R/t$  ratios close to these, that the bending effects are much less important than had been believed and that for a properly welded joint there is sufficient inherent stiffness to eliminate the necessity for stiffening webs.

In making these tests it was desirable to get strain readings insofar as possible right up to the point of rupture. It was not known to what extent the strain gage readings would prove reliable once the yield point of the steel was passed. As a result of these tests it appears that the gage readings gave reliable qualitative results throughout the range of readings. Since the physical properties of the strain gages themselves are not known, it is impossible to state definitely at what total strain the gage accuracy underwent a change. Quantitatively, therefore, the

results are of an unknown degree of accuracy. It is probable that the close agreement of the curves for the two test specimens at each location would not have been obtained if the gages had become unreliable at the high loadings. In order to check the gage action at the higher loads, intermediate readings were taken between the unloaded condition and the high loads as previously explained in "PROCEDURE". These points as plotted in Figs. 16, 19, 22, 23, 25, 27, 28, and 31 give a straight line parallel to that obtained within the elastic region and the gages were therefore assumed to be giving useful readings. At some locations gages were broken under high loadings. This fact was immediately apparent due to the inability to obtain a balance in the bridge circuit.

From the strain readings taken, stresses at the various locations were computed within the elastic region and recorded in Tables I-XVIII. Since the strain gages can measure only two-dimensional strains, stresses were computed using two-dimensional theory. The third-dimensional strains while known to be present could not be accounted for in these tests. When yielding first occurred anywhere in the specimen, the resultant permanent deformation imposed residual stresses throughout the specimen when the load was removed. This was shown by an apparent permanent set indicated by all gages at approximately the same loading even though local load stresses had not risen sufficiently to reach the yield stress of the metal. This is the reason why all the load-strain curves deviate from a linear relation at about the same loading. Above the elastic limit the strains measured cannot be

transformed to other axes since the usual transformation equations are invalid outside the elastic range. Considerable work is now being done toward developing stress and strain relations for use in the plastic region (Ref. 2), but no attempt was made to apply any of those theories here.

The curves plotted from the results of the tests on the two specimens agree quite closely with three exceptions. The tangential strain curves at position #8 diverge, and the axial strain curves for positions 7 and 8 also diverge. The reason for this divergence is not known but may be due to the change in thickness ratio. Further tests on specimens of various  $R/t$  ratios would indicate whether the divergence is a trend established by the change in wall thickness.

For the wall thicknesses used in these tests it is believed that gravity effects were of very minor importance. In any further tests using thin-walled specimens of similar dimensions it would be better to provide supports which distribute the load uniformly along the length of the specimen rather than supporting it at four points as was done here.

Considering the fact that first yielding occurred at approximately 54% of maximum load in the first test and at about 42% of maximum load in the second test, use of the theory of limit design in actual construction is indicated. At the same time the large difference in yield loads observed compared with the theoretical yield load for a straight pipe should be considered.

Specimen I:  $P_{\text{yield-str. pipe}} = 3288. \text{ psi.}$   
 $P_{\text{yield-actual}} = 1800. \text{ psi.}$

Specimen II:  $P_{\text{yield-str. pipe}} = 2435. \text{ psi.}$   
 $P_{\text{yield-actual}} = 1200. \text{ psi.}$

This shows a reduction in strength of 45% for the first specimen, and 51% for the second.

A measurement of the intersection cross section shape was made after rupture in the tests described in Ref. 1. The original elliptical cross section was found to have been deformed into an egg shape with the greatest outward deviation located approximately midway between the crotch and the 90 degree point of the intersection. This contour is typical of deformations suffered by such intersections and was observed in the present tests.

Figs. 32 to 49 were plotted to show the measured strain distribution both along the cylinder axis and along the elliptical intersection. Examination of these figures (for instance Fig. 39 and Fig. 40) shows that axial strains are highest at position #5 and tangential strains are highest in the crotch. All strains are relatively low at the outside of the elbow for all loadings. There are relatively high

tangential and axial strains in the region between positions 6 and 9 so that the principal strains will be highest in that region.

### CONCLUSIONS

1. The results of this investigation indicate that the highest stress concentration in a right angle cylindrical intersection under internal pressure occurs at an angle of about 14.5 degrees from the notch centerline measured in the plane of the ellipse.
2. The critical stress causing rupture is the tangential stress in the plane of the ellipse.
3. For the  $R/t$  ratios tested, the strength reduction as compared with a straight closed cylinder is approximately 50%.
4. It appears probable that bending effects for these thick walled cylinders are of relatively minor importance.



RECOMMENDATIONS

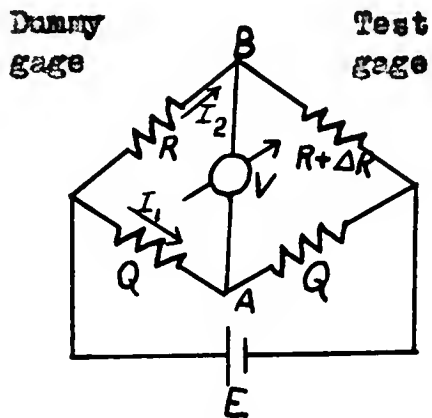
1. An analysis of the tangential stresses in the plane of the elliptical intersection should be made.
2. A study should be made of the variation of these tangential stresses through the wall thickness.
3. Analytical studies of bending effects and shearing stresses should be made.
4. In any further experimental work, the critical area as determined in this investigation should be thoroughly examined by strain gages or other means.
5. Further experimental work should check on the differing axial strains observed in the two specimens on the outside of the elbow.

REFERENCES AND BIBLIOGRAPHY

1. Sandberg, William A., "Tests of Welded Pipe Fittings", Progress Report No. 11-2. Jet Propulsion Laboratory, California Institute of Technology, October 6, 1948.
2. Onsted, Harold and Serrurier, Mark, "Stress Analysis of Southern California Cooperative Wind Tunnel", CWT Report T-22, So. Calif. CWT, Pasadena, California.
3. Articles on the Theory of Plasticity by H. F. Bohnenblust and Pol Durez; William Prager; J. E. Dorn and A. J. Latter; E. A. Davis; and by A. H. Philippidis in Journal of Applied Mechanics, Vol. 15, No. 3, September 1948.
4. Sechler, E. E., "Elasticity in Engineering", California Institute of Technology, Pasadena, California. (Class notes)

REDUCTION OF STRAIN GAGE DATA

The test gage mounted on the specimen and a dummy gage mounted on identical, unstrained material are included in a Wheatstone Bridge



circuit. The opposite sides of the circuit are two precision resistances of magnitude Q.

Under load the potentiometer is varied so that no current flows between points A and B. We wish to determine

the relation between the voltage V, across AB and the unit strain,  $\epsilon$ , in the test specimen.

From the circuit diagram, we determine that

$$I_1(2Q) = E \qquad I_2(2R + \Delta R) = E \qquad V = I_1Q - I_2R$$

Hence

$$V = \frac{E}{2} - \frac{ER}{2R + \Delta R} = \frac{E}{4} \frac{\Delta R}{R} \left[ 1 + \frac{\Delta R}{2R} \right]^{-1} \approx \frac{E}{4} \frac{\Delta R}{R}$$

To eliminate the ratio  $\Delta R/R$ , the following relation for resistivity of a conductor is employed.

$$R = K \frac{L}{A}$$

where K is a resistivity constant, L the length of the conductor, and A its cross-sectional area. Then

$$\ln R = \ln K + \ln L - \ln A$$

Hence

$$\frac{\Delta R}{R} = \frac{\Delta L}{L} - \frac{\Delta A}{A}$$

For a cylindrical conductor

$$\frac{\Delta A}{A} = 2 \frac{\Delta r}{r} = -2\nu \frac{\Delta L}{L} = -2\nu \epsilon \quad \begin{array}{l} r \text{ is the radius} \\ \text{of the cross section} \end{array}$$

Therefore

$$\frac{\Delta R}{R} = (1 + 2\nu)\epsilon$$

$\nu$  is the Poisson's ratio for the strain gage material.

Substituting directly into the equation for the voltage reading  $V$ ,

Hence

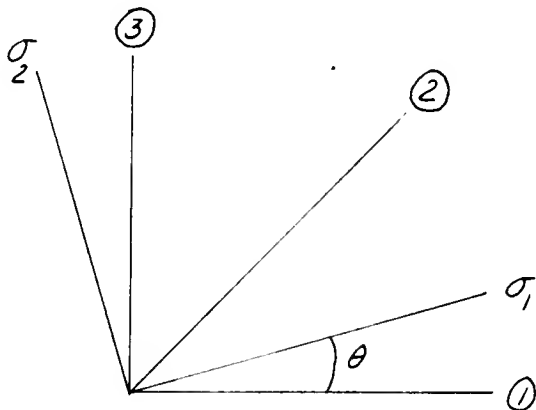
$$v = \frac{E}{4} (1 + 2\nu)\epsilon$$
$$\epsilon = \frac{4v}{(1 + 2\nu)E}$$

This equation is usually employed in the form

$$\epsilon = \frac{4 \text{ (milli volts)}}{(\text{gage factor})(\text{battery reading})}$$

where  $\epsilon$  is obtained in inches per inch times  $10^{-3}$ .

Within the elastic region the average of zero readings taken before and after loading was used in getting the gage readings. Application of gage factor and battery reading gave apparent strains in the case of the rosettes, so these readings were further corrected as follows:



$$\Delta \epsilon_1 = R_1 - \frac{1}{b} R_3$$

$$\Delta \epsilon_2 = 1.02 R_2 - \frac{1}{b} (R_1 + R_3)$$

$$\Delta \epsilon_3 = R_3 - \frac{1}{b} R_1$$

$b = -200$  where  $b$  is a factor furnished by the manufacturer for each gage lot.

Having the strains at a given point, the axial and tangential stresses were computed from the usual two-dimensional equations:

$$\sigma_a = \frac{E}{1-\mu^2} [\epsilon_a + \mu \epsilon_t] \quad \sigma_t = \frac{E}{1-\mu^2} [\epsilon_t + \mu \epsilon_a]$$

These stresses could be computed only up to the load where yielding first occurred at any point in the specimen.

To compute principal stresses the following equations were used:

$$\sigma_{1,2} = \frac{E}{2(1-\mu)(1+b)} \left[ (R_1 + R_3) \pm \frac{(1-\mu)(1+b)}{(1+\mu)(1-b)} \cdot r \right]$$

where  $r = \left| \frac{R_1 + R_3 - 2R_2}{\sin 2\theta} \right|$

$$\tan 2\theta = - \frac{R_1 + R_3 - 2R_2}{R_1 - R_3}$$

Having the principal stresses, principal strains could then be computed.

$$\epsilon_1 = \frac{1}{E} (\sigma_1 - \mu\sigma_2)$$

Principal stresses and strains were computed only within the elastic region.

For test number one it was necessary to transform the measured strains at positions 5 and 7 to get the tangential strains due to the orientation of those two gages. (Fig. 8). This was done by using Mohr's circle. The transformation was performed only within the elastic region.

TABLE I

VARIATION OF TANGENTIAL AND AXIAL STRAINS WITH VARIATION OF INTERNAL PRESSURE

Test I

Position #1

Gages 2,3

Press.	← R →				← Δ ε →				← σ →				← ε →		
	Axial	Tang.	Diag.		Axial	Tang.	Princ.	θ	Princ.	Axial	Tang.	Axial	Tang.	Axial	Tang.
500	.0430	.1133	-		.0436	.1135	-	-	-	2560	4170	.0436	.1135	.0436	.1135
750	.0645	.1416	-		.0652	.1419	-	-	-	3550	5320	.0652	.1419	.0652	.1419
1000	.0856	.1892	-		.0865	.1896	-	-	-	4725	7100	.0865	.1896	.0865	.1896
1250	.1068	.2381	-		.1080	.2386	-	-	-	5910	8930	.1080	.2386	.1080	.2386
1500	.1284	.2890	-		.1298	.2896	-	-	-	7140	10830	.1298	.2896	.1298	.2896
1600	.1325	.3003	-		.1340	.3010	-	-	-	7400	11240	.1340	.3010	.1340	.3010
1700	.1398	.3160	-		.1414	.3167	-	-	-	7800	11840	.1414	.3167	.1414	.3167
1800	.1468	.3335	-		.1485	.3342	-	-	-	-	-	.1460	.7388	.1460	.7388
1900	.1546	.3552	-		.1564	.3560	-	-	-	-	-	.1704	.7403	.1704	.7403
2000	.1627	.3856	-		.1646	.3864	-	-	-	-	-	.2075	.7209	.2075	.7209
2050	.1674	.3899	-		.1693	.3907	-	-	-	-	-	.2227	.7092	.2227	.7092
2150	.1809	.4807	-		.1833	.4816	-	-	-	-	-	.2449	.7873	.2449	.7873
750	.0616	.1480	-		.0623	.1483	-	-	-	-	-	.1239	.4540	.1239	.4540
1700	.1420	.3337	-		.1437	.3344	-	-	-	-	-	.2053	.6401	.2053	.6401
2200	.1850	.4263	-		.1871	.4356	-	-	-	-	-	.2581	.7481	.2581	.7481
2300	.1941	.4474	-		.1963	.4484	-	-	-	-	-	.2861	.7438	.2861	.7438
2400	.1993	.4922	-		.2018	.4932	-	-	-	-	-	.2938	.8333	.2938	.8333
2500	.2135	.4801	-		.2159	.4812	-	-	-	-	-	.2953	.9880	.2953	.9880
2600	.0804	.3915	-		.0824	.3955	-	-	-	-	-	.3602	2.2024	.3602	2.2024
2800	.2096	.5993	-		.2126	.6003	-	-	-	-	-	.9139	4.1237	.9139	4.1237
3000	.2146	.6726	-		.2161	.6937	-	-	-	-	-	1.1340	5.5106	1.1340	5.5106
3250	.2411	.7970	-		.2451	.7982	-	-	-	-	-	1.3111	6.8218	1.3111	6.8218

Pressures and stresses in lb./sq.in. Strains given in inches per inch x 10<sup>3</sup>

TABLE II

Position #2

Test I

Press.	← R →		← Δ ε →		θ	← σ →		← ε →		
	Axial	Tang.	Axial	Tang.		Princ.	Axial	Tang.	Axial	Tang.
500	.0181	.1318	.0188	.1319	.1322	2-42	4540	1889	.0188	.1319
750	.0234	.1908	.0244	.1909	.1909	0-39	6534	2690	.0244	.1909
1000	.0305	.2693	.0318	.2694	.2690	0-15	9189	3707	.0318	.2694
1250	.0474	.3300	.0480	.3302	.3306	2-10	11382	4855	.0480	.3302
1500	.0576	.4050	.0596	.4053	.4058	1-58	13964	5973	.0596	.4053
1600	.0522	.4300	.0543	.4303	.4302	0-47	14722	6045	.0543	.4303
1700	.0531	.4600	.0554	.4603	.4601	0-47	15719	6380	.0554	.4603
1800	.0580	.4807	.0604	.4810	-	-	-	-	.0546	.4994
1900	.0657	.4976	.0682	.4979	-	-	-	-	.0512	.5335
2000	.0644	.5211	.0670	.5214	-	-	-	-	.0448	.6029
2050	.0690	.5319	.0717	.5322	-	-	-	-	.0379	.6365
2150	.0608	.5297	.0634	.5300	-	-	-	-	.0191	.8161
750	.0197	.2410	.0209	.2411	-	-	-	-	-.0234	.5272
1700	.0528	.4400	.0550	.4403	-	-	-	-	.0107	.7264
2200	.0693	.5643	.0721	.5646	-	-	-	-	.0302	.8649
2300	.0718	.4518	.0741	.4522	-	-	-	-	.0188	1.5388
2400	.0754	.5411	.0781	.5415	-	-	-	-	.0171	2.1654
2500	.0878	.5583	.0906	.5587	-	-	-	-	.0362	2.7001
2600	.0955	.6440	.0987	.6445	-	-	-	-	-.0780	3.8779
2800	.1176	.6632	.1209	.6688	-	-	-	-	-.2543	5.5926
3000	.1336	.8351	.1378	.8358	-	-	-	-	-.4013	7.8630
3250	.1358	.9513	.1406	.9520	-	-	-	-	-.4910	9.4319





TABLE IV

Position #4

Test I

Gages 10,11,12

Press.	← R →		← Δε →				← σ →				← ε →	
	Axial	Tang.	Diag.	Axial	Tang.	Princ.	θ	Princ.	Axial	Tang.	Axial	Tang.
500	.0369	.1582	.1411	.0377	.1584	.1723	-17-51	5916	2805	5.590	.0377	.1584
750	.0565	.2183	.2070	.0576	.2186	.2443	-20-22	8369	4060	7.840	.0576	.2186
1000	.0748	.3270	.2862	.0764	.3274	.3533	-17-03	12148	5750	11.530	.0764	.3274
1250	.0996	.3977	.3467	.1016	.3982	.4274	-16-40	14808	7290	14.120	.1016	.3982
1500	.1150	.4890	.4240	.1174	.4896	.5257	-16-34	18136	8720	17.280	.1174	.4896
1600	.1502	.5220	.4620	.1528	.5228	.5611	-17-04	19632	10190	18.710	.1528	.5228
1700	0.1549	0.5520	0.4820	.1577	.5528	.5905	-16-28	20655	10650	19.780	.1577	.5528
1800	.1429	.5841	.5168	.1498	.5848	-	-	-	-	-	.1562	.5833
1900	.1595	.6040	.5370	.1625	.6048	-	-	-	-	-	.1532	.6169
2000	.1650	.6164	.5539	.1681	.6172	-	-	-	-	-	.1345	.7743
2050	.1738	.6133	.5646	.1769	.6142	-	-	-	-	-	.1422	.8531
2150	.1893	.6289	.5878	.1924	.6298	-	-	-	-	-	.1570	1.3555
750	.0650	.2287	.2057	.0661	.2290	-	-	-	-	-	.0302	0.9547
1700	.1481	.5132	.4655	.1507	.5139	-	-	-	-	-	.1148	1.2396
2200	.1944	.6584	.5990	.1977	.6554	-	-	-	-	-	.1725	1.3850
2300	.1821	.5772	.5305	.1850	.5781	-	-	-	-	-	.4297	2.0265
2400	.2165	.6072	.5714	.2195	.6083	-	-	-	-	-	.7248	2.7650
2500	.2469	.6392	.6210	.2501	.6322	-	-	-	-	-	.9061	3.3265
2600	.2667	.7040	.6368	.2702	.7053	-	-	-	-	-	1.0969	3.9296
2800	.2931	.7206	.652	.2967	.7221	-	-	-	-	-	1.5359	5.2937
3000	.3268	.7730	.6833	.3307	.7746	-	-	-	-	-	2.1318	6.9961
3250	.3630	.8555	.6837	.3673	.8573	-	-	-	-	-	2.6431	8.6785

TABLE V

Position #5

Test I

Press.	← R →		Normal to Weld	← Δε →		θ	Princ.	← σ →		Axial	Tang.	← ε →
	Axial	Along Weld		Axial	Tang.			Princ.	Axial			
500	0.2150	0.1288	0.2170	0.1293	.2344	66-45	8847	8474	0.2210	6420	0.2210	.1293
750	0.3265	0.1955	0.3286	0.1970	.3555	67-01	13415	12816	.3356	9758	.3356	.1970
1000	0.4380	0.2633	0.4440	0.2655	.4783	66-31	18070	17306	.4503	13158	.4503	.2655
1250	0.5324	0.3163	0.5420	.3190	.5834	66-16	21996	21076	.5473	15892	.5473	.3190
1500	0.6515	0.3854	0.6590	.3887	.7120	66-43	26814	25634	0.6698	19350	.6698	.3887
1600	0.7020	0.415	0.7140	.4185	.7694	66-19	28979	27748	0.7216	20880	.7216	.4185
1700	0.7370	0.4330	0.7580	.4343	.8128	65-32	30596	29381	0.7576	21917	.7576	.4343
1800	0.7797	0.4558	0.7959	.4599	-	-	-	-	.8016	-	.8933	.4476
1900	0.8272	0.4849	0.8498	.4892	-	-	-	-	.8504	-	1.1027	.4711
2000	0.8738	0.5068	0.8907	.5115	-	-	-	-	.8983	-	1.3280	.4510
2050	0.8844	0.5203	0.9001	.5249	-	-	-	-	.9092	-	1.4455	.4866
2150	0.9243	0.5438	0.9376	.5486	-	-	-	-	.9502	-	1.8839	.6597
750	0.3123	0.1795	0.3096	.1811	-	-	-	-	.3209	-	1.2546	.2922
1700	0.7164	0.4150	0.7269	.4187	-	-	-	-	.7364	-	1.6701	.5298
2200	0.9250	0.5356	0.9381	.5404	-	-	-	-	.9509	-	1.9229	.6762
2300	0.9648	0.5649	1.0095	.5700	-	-	-	-	.9920	-	2.9586	1.1058
2400	1.0026	0.5841	1.0292	.5615	-	-	-	-	1.0307	-	3.6251	1.3387
2500	1.0108	0.5920	1.0229	.7058	-	-	-	-	1.0391	-	4.2130	1.7047
2600	1.0683	0.6175	1.0510	.6229	-	-	-	-	1.0980	-	5.0013	1.8820
2800	1.0585	0.6775	1.0585	.6829	-	-	-	-	1.0884	-	6.8464	2.4601
3000	1.0871	0.7703	1.0629	.7770	-	-	-	-	1.1180	-	8.9184	2.9686
3250	1.1626	0.9040	1.0636	.9095	-	-	-	-	1.1956	-	10.7605	3.5506



TABLE VII

Pages 19, 20, 21

Position #7

Test I

Press.	← R →		← Δ ε →		← σ →		← ε →			
	Axial	Along Weld to Normal	Axial	Tang.	Princ.	θ	Princ.	Tang.		
500	.0700	-.0385	.0716	-.0381	.1015	-63-06	2823	2479	.0716	-.0381
750	.1045	-.0615	.1069	-.0608	.1451	-63-55	4090	3518	.1069	-.0608
1000	.1340	-.0818	.1372	-.0809	.2019	-62-06	5594	4983	.1372	-.0809
1250	.1732	-.1040	.1772	-.1029	.2488	-64-00	6779	5827	.1772	-.1029
1500	.2276	-.1344	.2328	-.1386	.3206	-64-42	8681	7469	.2328	-.1386
1600	.2382	-.1400	.2437	-.1442	.3368	-64-30	9144	7901	.2437	-.1442
1700	.2477	-.1452	.2534	-.1438	.3508	-64-30	9534	8113	.2534	-.1438
1800	.2549	-.1508	.2608	-.1492	-	-	-	-	.3051	-.1899
1900	.2690	-.1542	.2753	-.1525	-	-	-	-	.3469	-.2175
2000	.2753	-.1650	.2817	-.1633	-	-	-	-	.4062	-.3066
2050	.2941	-.1581	.3010	-.1500	-	-	-	-	.4235	-.3159
2150	.3064	-.1632	.3135	-.1614	-	-	-	-	.4603	-.4078
750	.1011	-.0599	.1034	-.0623	-	-	-	-	.2502	-.3087
1700	.2411	-.0599	.2471	-.0584	-	-	-	-	.3939	-.3048
2200	.3175	-.1641	.3249	-.1622	-	-	-	-	.4706	-.4109
2300	.3123	-.1560	.3197	-.1520	-	-	-	-	.4601	-.5308
2400	.3228	-.1614	.3304	-.1595	-	-	-	-	.4598	-.6319
2500	.3268	-.1598	.3346	-.1578	-	-	-	-	.4973	-.7219
2600	.3380	-.1544	.3462	-.1523	-	-	-	-	.5333	-.8354
2800	.3486	-.1458	.3572	-.1435	-	-	-	-	.6613	-1.0814
3000	.3630	-.1373	.3722	-.1344	-	-	-	-	.7355	-1.3375
3250	.4287	-.1021	.4397	-.0991	-	-	-	-	.8197	-1.4149

TABLE VIII

Gages 22&23

Position #8

Test I

Press.	$\leftarrow R \rightarrow$		Diag.	$\leftarrow \Delta \epsilon \rightarrow$		$\theta$	$\leftarrow \sigma \rightarrow$		$\leftarrow \epsilon \rightarrow$	
	Axial	Tang.		Axial	Tang.		Princ.	Princ.	Axial	Tang.
500	.0058	-.0613	-	.0058	-.0613	0	-415	-415	.0058	-.0613
750	.0054	-.0875	-	.0054	-.0875	0	-686	-686	.0054	-.0875
1000	.0018	-.1263	-	.0018	-.1263	0	-1190	-1190	.0018	-.1263
1250	.0118	-.1675	-	.0118	-.1675	0	-1266	-1266	.0118	-.1675
1500	.0218	-.1956	-	.0218	-.1956	0	-1216	-1216	.0218	-.1956
1600	.0352	-.2100	-	.0352	-.2100	0	-916	-916	.0352	-.2100
1700	.0419	-.2280	-	.0419	-.2280	0	-874	-874	.0419	-.2280
1800	.0417	-.2425	-	-	-.2425	-	-	-	.1019	-.2680
1900	.0474	-.2563	-	-	-.2563	-	-	-	.1469	-.2941
2000	.0597	-.2696	-	-	-.2696	-	-	-	.2184	-.3303
2050	.0640	-.2696	-	-	-.2696	-	-	-	.2329	-.3382
2150	.0720	-.2891	-	-	-.2891	-	-	-	.3098	-.3850
750	-.0003	-.0825	-	-	-.0825	-	-	-	.2375	-.1784
1700	.0283	-.2000	-	-	-.2000	-	-	-	.2661	-.2959
2200	.0646	-.2606	-	-	-.2606	-	-	-	.3148	-.3556
2300	.0789	-.2942	-	-	-.2942	-	-	-	.4184	-.4651
2400	.0903	-.3029	-	-	-.3029	-	-	-	.5437	-.6020
2500	.1060	-.3259	-	-	-.3259	-	-	-	.7146	-.8523
2600	.1161	-.3248	-	-	-.3248	-	-	-	.7247	-.8512
2800	.1401	-.3318	-	-	-.3318	-	-	-	.9385	-1.2150
3000	.1855	-.3549	-	-	-.3549	-	-	-	1.1440	-1.7719
3250	.2273	-.3218	-	-	-.3218	-	-	-	1.2880	-2.0626

TABLE IX

Gages 1-24

Test I	← R →				← Δε →				← σ →				← ε →				
	Press.	Axial	Tang.	Diag.	Axial	Tang.	Princ.	θ	Princ.	Axial	Tang.	Princ.	θ	Axial	Tang.	Princ.	θ
500	0.0468	0.2245	-	-	0.0468	0.2245	0.2245	090	7860	3762	7860	-	090	0.0468	0.2245	7860	090
750	0.0646	0.3290	-	-	0.0646	0.3290	0.3290	090	11500	5385	11500	-	090	0.0646	0.3290	11500	090
1000	0.0585	0.4560	-	-	0.0585	0.4560	0.4560	090	15600	6440	15600	-	090	0.0585	0.4560	15600	090
1250	0.1178	0.5720	-	-	0.1178	0.5720	0.5720	090	20000	9535	20000	-	090	0.1178	0.5720	20000	090
1500	0.1340	0.6980	-	-	0.1340	0.6980	0.6980	090	24300	11320	24300	-	090	0.1340	0.6980	24300	090
1600	0.1235	0.7580	-	-	0.1235	0.7580	0.7580	090	26200	11560	26200	-	090	0.1235	0.7580	26200	090
1700	0.1310	0.8120	-	-	0.1310	0.8120	0.8120	090	28050	12350	28050	-	090	0.1310	0.8120	28050	090
1800	0.1441	0.8602	-	-	.1441	0.8602	-	-	-	-	-	-	-	.1246	1.0058	-	-
1900	0.1366	0.9786	-	-	.1366	0.9786	-	-	-	-	-	-	-	.1843	2.0139	-	-
2000	0.1198	1.0962	-	-	.1198	1.0962	-	-	-	-	-	-	-	.2643	3.7938	-	-
2050	0.1084	1.1037	-	-	.1084	1.1037	-	-	-	-	-	-	-	.3632	4.1425	-	-
2150	0.1140	1.1809	-	-	.1140	1.1809	-	-	-	-	-	-	-	.5995	6.6369	-	-
750	0.0346	.3310	-	-	.0346	.3310	-	-	-	-	-	-	-	.5201	5.7870	-	-
1700	.0958	.8170	-	-	.0958	.8170	-	-	-	-	-	-	-	.5813	6.2730	-	-
2200	.1198	1.0619	-	-	.1198	1.0619	-	-	-	-	-	-	-	.5911	6.3979	-	-
2300	.0827	NG	-	-	.0827	-	-	-	-	-	-	-	-	.9537	-	-	-
2400	.1373	NG	-	-	.1373	-	-	-	-	-	-	-	-	1.1481	-	-	-
2500	.1609	NG	-	-	.1609	-	-	-	-	-	-	-	-	1.1530	-	-	-
2600	.1669	NG	-	-	.1669	-	-	-	-	-	-	-	-	1.0149	-	-	-
2800	.1644	NG	-	-	.1644	-	-	-	-	-	-	-	-	.4478	-	-	-
3000	.1006	NG	-	-	.1006	-	-	-	-	-	-	-	-	-.2094	-	-	-
3250	.0175	NG	-	-	.0175	-	-	-	-	-	-	-	-	-.6431	-	-	-

TABLE NO. X  
 VARIATION OF TANGENTIAL AND AXIAL STRAINS WITH VARIATION OF INTERNAL PRESSURE

Test II	Position #1										Gages 2,3	
	← R →		← Δε →		← σ →		← ε →		← ε →		← ε →	
Press.	Axial	Tang.	Diag.	Axial	Tang.	Princ.	θ	Princ.	Axial	Tang.	Axial	Tang.
400	.0600	.1385	-	.0670	.1388	-	-	-	3580	5239	.0670	.1388
600	.0815	.1970	-	.0825	.1974	-	-	-	4672	7326	.0825	.1974
800	.1142	.2680	-	.1155	.2686	-	-	-	6465	9996	.1155	.2686
1000	.1376	.3298	-	.1392	.3305	-	-	-	7860	12275	.1392	.3305
1100	.1535	.3677	-	.1553	.3685	-	-	-	8767	13686	.1553	.3685
1200	.1657	.4020	-	.1677	.4028	-	-	-	-	-	.1795	.3631
1250	.1724	.4182	-	.1745	.4191	-	-	-	-	-	.1905	.3906
1300	.1848	.4316	-	.1870	.4325	-	-	-	-	-	.2070	.3978
500	.0705	.1632	-	.0713	.1636	-	-	-	-	-	.0913	.1289
900	.1254	.3019	-	.1269	.3025	-	-	-	-	-	.1469	.2678
1400	.1940	.4794	-	.1964	.4804	-	-	-	-	-	.2531	.3806
1600	.2226	.5814	-	.2255	.5825	-	-	-	-	-	.3474	.3389
600	.0869	.2171	-	.0880	.2175	-	-	-	-	-	.2099	.0261
1200	.1718	.4421	-	.1740	.4430	-	-	-	-	-	.2959	.1994
1800	.1989	.6038	-	.2019	.6048	-	-	-	-	-	.6174	1.7911
2000	.2622	.8185	-	.2663	.8198	-	-	-	-	-	1.1349	4.1168
2200	.2623	.9078	-	.2668	.9091	-	-	-	-	-	1.4475	6.6002
2400	.2727	1.0532	-	.2780	1.0546	-	-	-	-	-	1.7004	9.4359
2600	.2848	1.1135	-	.2904	1.1149	-	-	-	-	-	1.8471	12.5249
2800	.2852	NO	-	-	-	-	-	-	-	-	-	-

Pressures and stresses in lb./sq.in. Strains given in inches per inch x 10<sup>3</sup>



TABLE XI

Test II	Position #2										Pages 4,5,6		
	← R →		← Δε →		← Princ. θ →		← σ →		← ε →		Axial	Tang.	
Press.	Axial	Diag.	Axial	Tang.	Princ.	θ	Princ.	Axial	Tang.	Axial	Tang.	Axial	Tang.
400	.0112	.1296	.0739	.0118	.1297	.1296	-1-28	4401	1672	4392	.0118	.1297	
600	.0172	.1824	.1164	.0181	.1825	.1841	-5-41	6234	2404	6195	.0181	.1825	
800	.0228	.2475	.1564	.0240	.2476	.2497	-5-21	8450	3241	8401	.0240	.2476	
1000	.0284	.3047	.1918	.0299	.3048	.3070	-5-11	10397	3999	10346	.0299	.3048	
1100	.0307	.3374	.2152	.0324	.3376	.3408	-5-45	11524	4408	11450	.0324	.3376	
1200	.0358	.3708	.2357	.0377	.3710	-	-	-	-	-	.0377	.3668	
1250	.0375	.3804	.2408	.0394	.3806	-	-	-	-	-	.0394	.3797	
1300	.0375	.3944	.2456	.0395	.3946	-	-	-	-	-	.0395	.3968	
500	.0140	.1506	.0941	.0148	.1507	-	-	-	-	-	.0148	.1529	
900	.0253	.2773	.1742	.0267	.2774	-	-	-	-	-	.0267	.2796	
1400	.0392	.4182	.2618	.0413	.4184	-	-	-	-	-	.0413	.4508	
1600	.0443	.4806	.3925	.0467	.4808	-	-	-	-	-	.0467	.6006	
600	.0166	.1751	.1109	.0175	.1752	-	-	-	-	-	.0175	.2950	
1200	.0296	.3525	.2184	.0314	.3526	-	-	-	-	-	.0314	.4724	
1800	.0653	.5121	.3289	.0679	.5124	-	-	-	-	-	.0679	.7023	
2000	.0794	.6330	.4089	.0826	.6334	-	-	-	-	-	.0826	4.3461	
2200	.1129	.7303	.4958	.1166	.7309	-	-	-	-	-	.1166	6.8078	
2400	.1365	.8720	.5836	.1409	.8727	-	-	-	-	-	.1409	9.2633	
2600	.1419	.9022	.6138	.1464	.9029	-	-	-	-	-	.1464	11.1987	
2800	.1772	.9618	.6995	.1820	.9627	-	-	-	-	-	.1820	12.4117	



TABLE XIII

Position #4

Pages 10,11,12

Test II

Press.	$\leftarrow R \rightarrow$		$\leftarrow \Delta \epsilon \rightarrow$		$\theta$	Princ.	$\leftarrow \sigma \rightarrow$		$\leftarrow \epsilon \rightarrow$		
	Axial	Tang.	Axial	Tang.			Axial	Tang.	Axial	Tang.	
400	.0366	.1817	.0375	.1819	.2038	-19-57	6873	3036	6366	.0375	.1819
600	.0567	.2586	.0580	.2589	.2907	-20-18	9844	4474	9110	.0580	.2589
800	.0729	.3511	.0747	.3515	.3925	-19-46	13273	5938	12327	.0747	.3515
1000	.0924	.4308	.0946	.4313	.4860	-20-30	16418	7385	15156	.0946	.4313
1100	.1023	.4780	.1047	.4785	.5354	-19-58	18124	8186	16311	.1047	.4785
1200	.1162	.5226	.1188	.5232	-	-	-	-	-	.1022	.5148
1250	.1212	.5345	.1239	.5351	-	-	-	-	-	.1017	.5217
1300	.1259	.5470	.1286	.5476	-	-	-	-	-	.0998	.5286
500	.0462	.2125	.0473	.2127	-	-	-	-	-	.0185	.1937
900	.0864	.3890	.0883	.3894	-	-	-	-	-	.0595	.3704
1400	.1404	.5819	.1433	.5826	-	-	-	-	-	.0795	.5115
1600	.1927	.6107	.1958	.6117	-	-	-	-	-	-.0536	.5417
600	.0649	.2404	.0661	.2407	-	-	-	-	-	-.1833	.1707
1200	.1375	.4740	.1399	.4747	-	-	-	-	-	-.1095	.4047
1800	.2279	.6714	.2313	.6725	-	-	-	-	-	.6633	2.4305
2000	.3182	.7103	.3218	.7119	-	-	-	-	-	1.6984	4.8164
2200	.3792	.8006	.3832	.8025	-	-	-	-	-	2.5154	7.0360
2400	.4330	.9358	.4377	.9380	-	-	-	-	-	3.5395	9.9191
2600	.4897	1.0230	.4948	1.0254	-	-	-	-	-	4.8255	13.2397
2800	.5078	1.0089	.5128	1.0114	-	-	-	-	-	6.9492	18.8651

TABLE XIV

Gages 13,14,15

Position #5

Test II

Press.	← R →		← Δε →		← σ →		← ε →			
	Axial Tang.	Diag.	Axial Tang.	Princ. θ	Princ.	Axial Tang.	Axial Tang.			
400	.2625	.1332	.2447	.2632	.1345	.2783 +72-02	10010	7039	.2632	.1345
600	.3728	.1923	.3520	.3738	.1942	.3841 +71-32	14246	10099	.3738	.1942
800	.5032	.2584	.4749	.5045	.2609	.5364 +71-13	19215	13594	.5045	.2609
1000	.6292	.3195	.5919	.6308	.3226	.6625 +71-24	23989	16874	.6308	.3226
1100	.6909	.3459	.6490	.6926	.3494	.7364 +71-26	26290	18371	.6926	.3494
1200	.7570	.3778	.7105	.7589	.3816	-	-	-	.9014	.3298
1250	.7700	.3827	.7258	.7719	.3866	-	-	-	.9568	.3201
1300	.7945	.3898	.7434	.7964	.3938	-	-	-	1.0488	.3248
500	.3039	.1523	.2876	.3047	.1538	-	-	-	.5571	.0848
900	.5576	.2826	.5277	.5590	.2854	-	-	-	.8114	.2164
1400	.8687	.4258	.8154	.8708	.4301	-	-	-	1.4479	.3315
1600	.9385	.4719	.8862	.9409	.4766	-	-	-	3.0029	.5085
600	.3329	.1861	.3163	.3338	.1878	-	-	-	2.3958	.2197
1200	.6525	.3559	.6259	.6543	.3952	-	-	-	2.7163	.3911
1800	.9330	.5298	.8630	.9356	.5345	-	-	-	4.7072	.8899
2000	.9076	.5814	.8339	.9105	.5859	-	-	-	6.2507	1.0764
2200	.9146	.7028	.8174	.9181	.7074	-	-	-	8.7857	1.6676
2400	.9861	.8362	.8385	.9903	.8411	-	-	-	11.6937	2.8194
2600	1.0498	.9176	.9190	1.0544	.9228	-	-	-	14.6300	4.8068
2800	NG	.9635	.9618	-	-	-	-	-	-	-



TABLE XVI

Pages 19,20,21

Position #7

Test II

Press.	$\leftarrow R \rightarrow$		$\leftarrow \Delta \epsilon \rightarrow$		Princ.	$\theta$	Princ.	$\leftarrow \sigma \rightarrow$		$\leftarrow \epsilon \rightarrow$	
	Axial	Tang.	Axial	Tang.				Axial	Tang.	Axial	Tang.
400	-.0066	-.0336	-.0068	-.0336	.0435	+ 38-55	605	-557	-1174	-.0068	-.0336
600	-.0112	-.0475	-.0114	-.0476	.0626	+ 39-21	862	-847	-1681	-.0114	-.0476
800	-.0175	-.0640	-.0178	-.0641	.0836	+ 39-29	1118	-1220	-2288	-.0178	-.0641
1000	-.0224	-.0759	-.0228	-.0760	.1026	+ 39-58	1391	-1503	-2730	-.0228	-.0760
1100	-.0244	-.0838	-.0248	-.0839	.1147	+ 38-58	1570	-1648	-3010	-.0248	-.0839
1200	-.0242	-.0896	-.0246	-.0897	-	-	-	-	-	-.0298	-.1084
1250	-.0269	-.0860	-.0273	-.0861	-	-	-	-	-	-.0318	-.1169
1300	-.0276	-.0930	-.0281	-.0931	-	-	-	-	-	-.0316	-.1277
500	-.0103	-.0359	-.0105	-.0360	-	-	-	-	-	-.0140	-.0706
900	-.0203	-.0678	-.0206	-.0679	-	-	-	-	-	-.0241	-.1025
1400	-.0333	-.1031	-.0338	-.1033	-	-	-	-	-	-.0387	-.1686
1600	-.0493	-.0998	-.0498	-.1000	-	-	-	-	-	-.0634	-.2847
600	-.0156	-.0389	-.0158	-.0390	-	-	-	-	-	-.0294	-.2237
1200	-.0413	-.0802	-.0417	-.0804	-	-	-	-	-	-.0553	-.2651
1800	-.0743	-.1020	-.0748	-.1024	-	-	-	-	-	-.2306	-.4977
2000	-.1085	-.0854	-.1089	-.0859	-	-	-	-	-	-.4937	-.7576
2200	-.1139	-.0573	-.1142	-.0579	-	-	-	-	-	-.8624	-.9176
2400	-.1261	-.0255	-.1262	-.0261	-	-	-	-	-	-1.0256	-.8471
2600	-.1211	.0154	-.1210	.0148	-	-	-	-	-	-1.1384	-.6243
2800	-.0847	.0710	-.0843	.0706	-	-	-	-	-	-1.5323	-.1973

TABLE XVII  
 Position #8  
 Cages 22 & 23

Test II	$R$		Diag.	$\Delta \epsilon$		$\theta$	Princ.	$\sigma$	$\epsilon$		
	Axial	Tang.		Axial	Tang.				Axial	Tang.	
400	-.0390	-.0307	-	-.0390	-.0307	-	-	-1589	-1398	-.0390	-.0307
600	-.0579	-.0432	-	-.0579	-.0432	-	-	-2338	-1998	-.0579	-.0432
800	-.0730	-.0597	-	-.0730	-.0597	-	-	-2997	-2690	-.0730	-.0597
1000	-.0934	-.0741	-	-.0934	-.0741	-	-	-3811	-3366	-.0934	-.0741
1100	-.1023	-.0801	-	-.1023	-.0801	-	-	-4164	-3653	-.1023	-.0801
1200	-.1083	-.0856	-	-.1083	-.0856	-	-	-	-	-.1270	-.0846
1250	-.1145	-.0896	-	-.1145	-.0896	-	-	-	-	-.1355	-.0848
1300	-.1171	-.0918	-	-.1171	-.0918	-	-	-	-	-.1370	-.0833
500	-.0443	-.0353	-	-.0443	-.0353	-	-	-	-	-.0642	-.0268
900	-.0868	-.0674	-	-.0868	-.0674	-	-	-	-	-.1067	-.0588
1400	-.1255	-.0963	-	-.1255	-.0963	-	-	-	-	-.1465	-.0732
1600	-.1479	-.0923	-	-.1479	-.0923	-	-	-	-	-.2295	-.0248
600	-.0635	-.0361	-	-.0635	-.0361	-	-	-	-	-.1451	.0314
1200	-.1248	-.0754	-	-.1248	-.0754	-	-	-	-	-.2064	-.0079
1800	-.1697	-.0787	-	-.1697	-.0787	-	-	-	-	-.3453	.3800
2000	-.1945	-.0733	-	-.1945	-.0733	-	-	-	-	-.4368	-.0032
2200	-.1808	-.0610	-	-.1808	-.0610	-	-	-	-	-.6109	.0402
2400	-.1527	-.0502	-	-.1527	-.0502	-	-	-	-	-.7606	.1302
2600	-.1447	-.0276	-	-.1447	-.0276	-	-	-	-	-.9359	.2580
2800	-.1137	-.0113	-	-.1137	-.0113	-	-	-	-	-1.2371	.5097

TABLE XVIII

Position #9

Test II

Press.	← R →		← ΔE →		← σ →		← ε →	
	Axial	Tang.	Axial	Tang.	Princ.	Axial	Axial	Tang.
400	.0379	.2609	.0379	.2609	-	3831	.0379	.2609
600	.0586	.3790	.0586	.3790	-	5681	.0586	.3790
800	.0790	.5128	.0790	.5128	-	7675	.0790	.5128
1000	.1023	.6519	.1023	.6519	-	9822	.1023	.6519
1100	.1174	.7238	.1174	.7238	-	11028	.1174	.7238
1200	.0953	.8185	.0953	.8185	-	-	.2061	1.1963
1250	.0911	.8575	.0911	.8575	-	-	.2821	1.4422
1300	.0774	.9016	.0774	.9016	-	-	.4146	1.8942
500	.0483	.3181	.0483	.3181	-	-	.3855	1.3107
900	.0890	.6071	.0890	.6071	-	-	.4262	1.5997
1400	.1186	1.0540	.1186	1.0540	-	-	.8126	4.1393
1600	.1198	NG	.1198	-	-	-	1.3072	-
600	.0375	NG	.0375	-	-	-	1.2249	-
1200	.0563	NG	.0563	-	-	-	1.2437	-
1800	.1484	NG	.1484	-	-	-	1.4052	-
2000	.0664	NG	.0664	-	-	-	.7650	-
2200	.0468	NG	.0468	-	-	-	-.0689	-
2400	-.0429	NG	-.0429	-	-	-	-.7222	-
2600	-.0440	NG	-.0440	-	-	-	-.7927	-
2800	-.0856	NG	-.0856	-	-	-	-1.0672	-



TABLE NO. XIX

Relation of load to  $p \cdot \frac{R}{t}$

$$\text{Test I: } \frac{R}{t} = \frac{3.84}{.4} = 9.6$$

$$\text{Test II: } \frac{R}{t} = \frac{3.84}{.3} = 12.8$$

Test I		Test II	
P	$P \cdot \frac{R}{t}$	P	$P \cdot \frac{R}{t}$
500	4800	400	5120
750	7200	600	7680
1000	9600	800	10240
1250	12000	1000	12800
1500	14400	1100	14080
1600	15360	1200	15360
1700	16320	1250	16000
1800	17280	1300	16640
1900	18240	1400	17920
2000	19200	1600	20480
2050	19680	1800	23040
2150	20640	2000	25600
2200	21120	2200	28160
2300	22080	2400	30720
2400	23040	2600	33280
2500	24000	2800	35840
2600	24960		
2800	26880		
3000	28800		
3250	31200		



B-1



Fig. 1 First specimen and test setup.



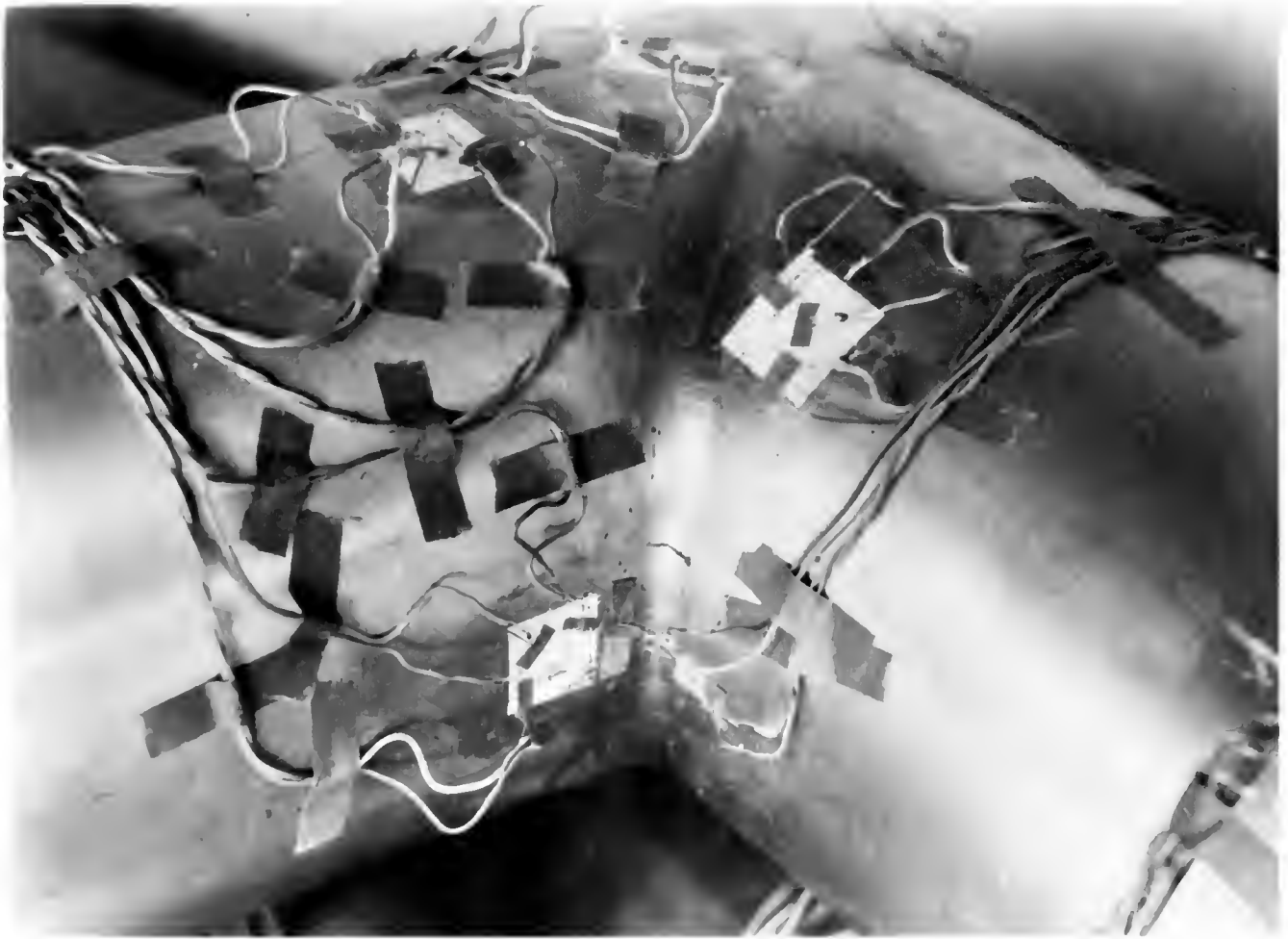


Fig. 2 Closeup view of first specimen showing rupture.

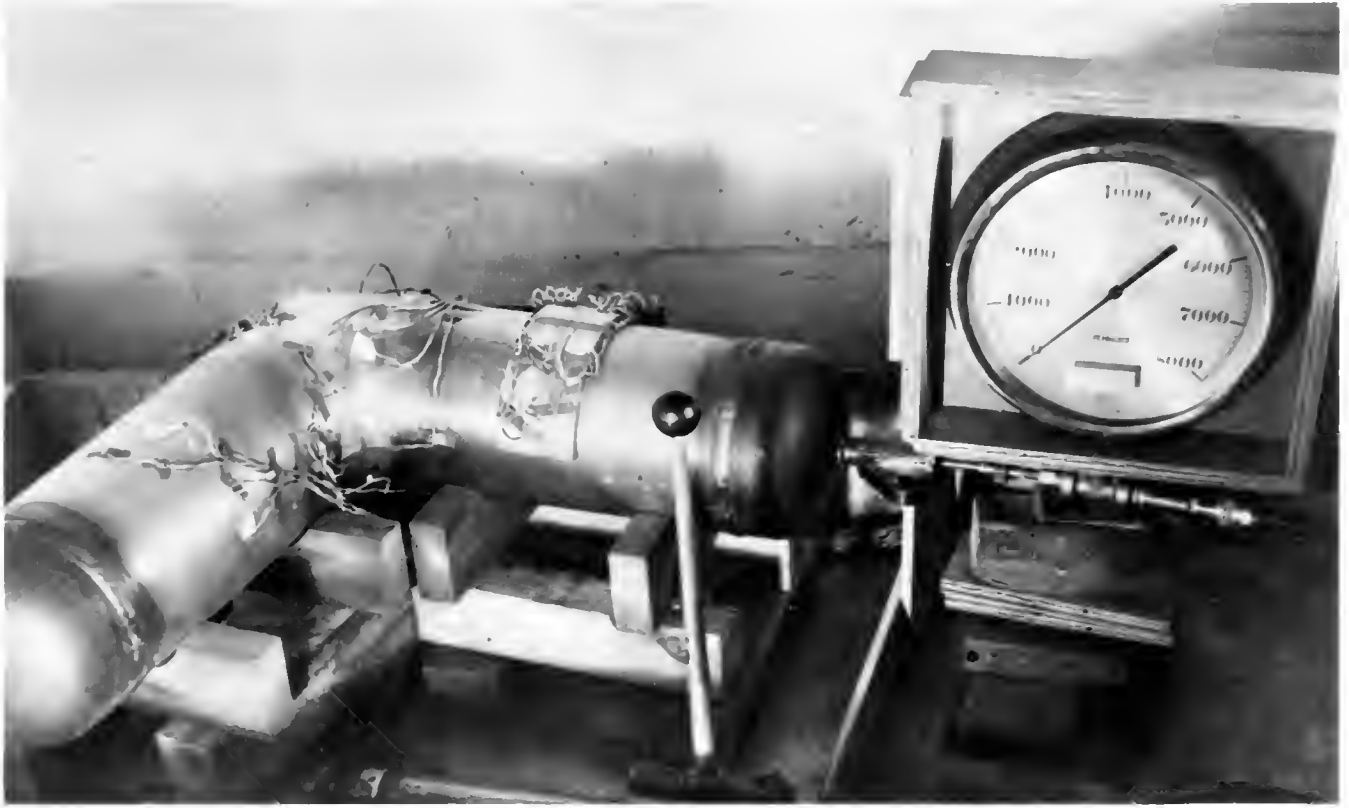


Fig. 3 Second specimen and test setup.

B-4



Fig. 4 Closeup view of second specimen showing rupture.

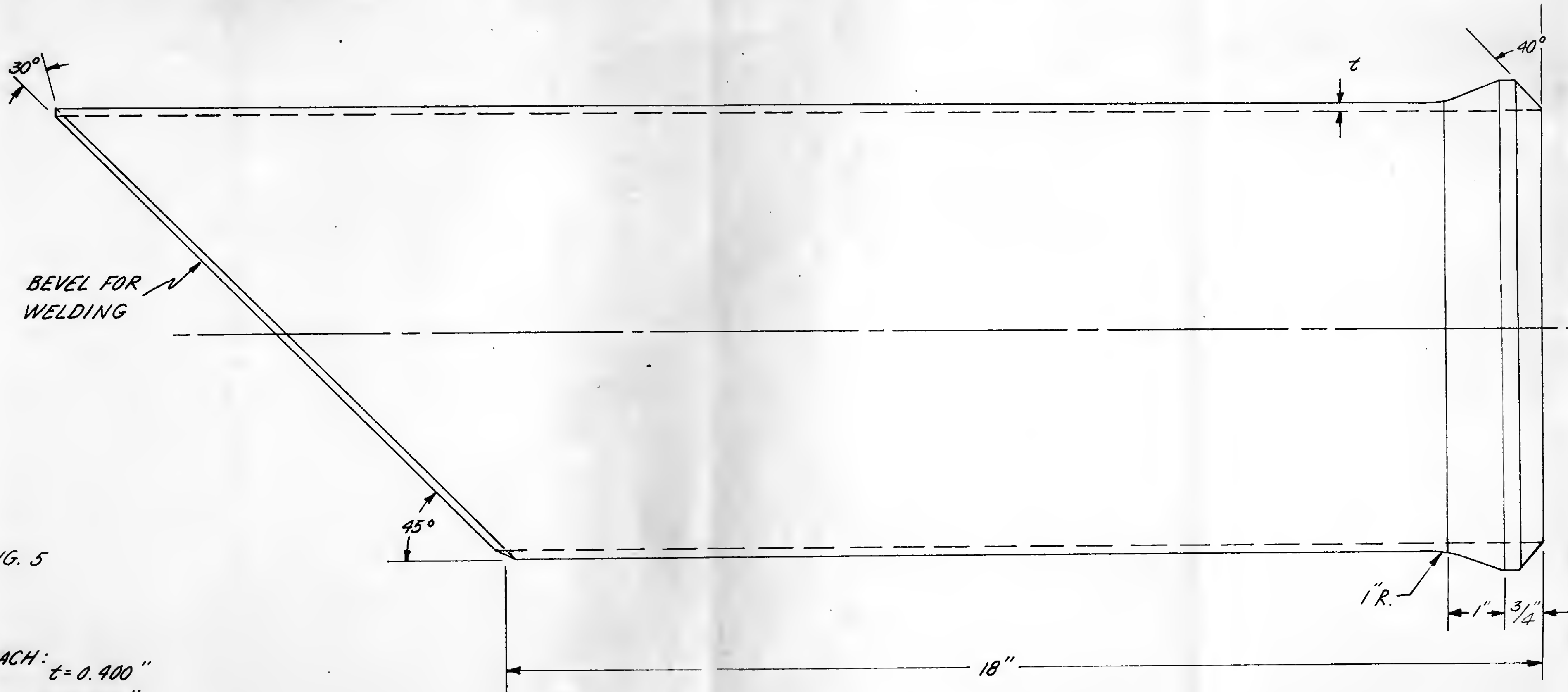


FIG. 5

NOTE:

2 EACH:  $t = 0.400$ "  
 $t = 0.300$ "

MACHINE INSIDE AND OUT  
 TO GIVE UNIFORM WALL  
 THICKNESS WITH TOLERANCE  
 $\pm .002$ "

MAINTAIN I. D. AS SMALL  
 AS POSSIBLE

8" STEEL TUBING	MACHINE						TOLERANCES = .010 OR $\frac{1}{32}$ UNLESS OTHERWISE NOTED
MATERIAL	FINISH	HEAT TREAT	DRAFTSMAN	CHECKED	APPROVED	ENGINEER	
GUGGENHEIM AERONAUTICAL LABORATORY CALIFORNIA INSTITUTE OF TECHNOLOGY			SPECIMENS FOR PRESSURE TESTS OF 90° CYLINDRICAL CORNER				
						NAME	DRAWING NO.



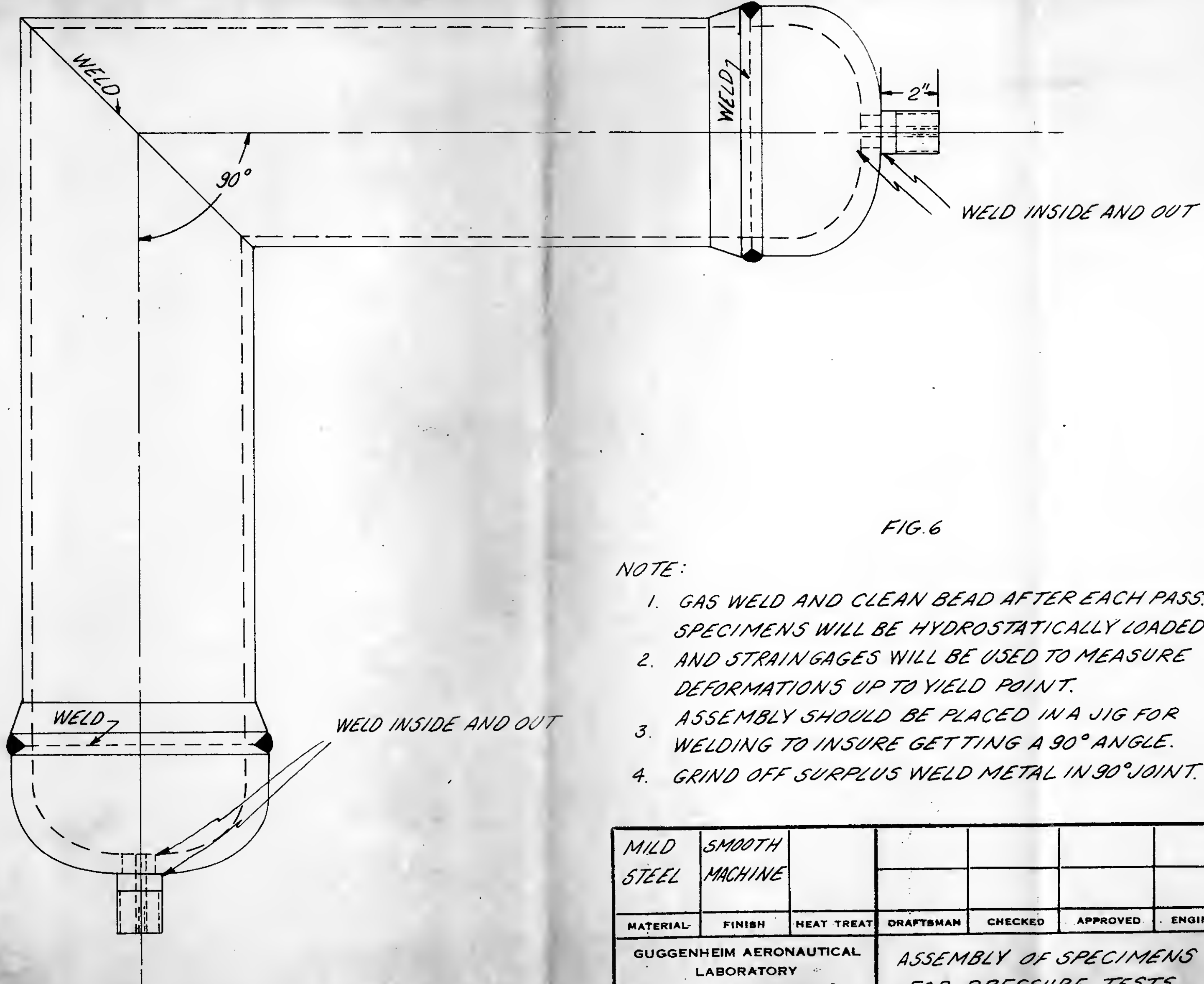


FIG. 6

NOTE:

1. GAS WELD AND CLEAN BEAD AFTER EACH PASS. SPECIMENS WILL BE HYDROSTATICALLY LOADED
2. AND STRAIN GAGES WILL BE USED TO MEASURE DEFORMATIONS UP TO YIELD POINT.
3. ASSEMBLY SHOULD BE PLACED IN A JIG FOR WELDING TO INSURE GETTING A 90° ANGLE.
4. GRIND OFF SURPLUS WELD METAL IN 90° JOINT.

MILD STEEL	SMOOTH MACHINE						TOLERANCES = .010 OR $\frac{1}{32}$ UNLESS OTHERWISE NOTED
							SCALE: $\frac{1}{4}$
MATERIAL	FINISH	HEAT TREAT	DRAFTSMAN	CHECKED	APPROVED	ENGINEER	
GUGGENHEIM AERONAUTICAL LABORATORY CALIFORNIA INSTITUTE OF TECHNOLOGY			ASSEMBLY OF SPECIMENS FOR PRESSURE TESTS				
						NAME	DRAWING NO.

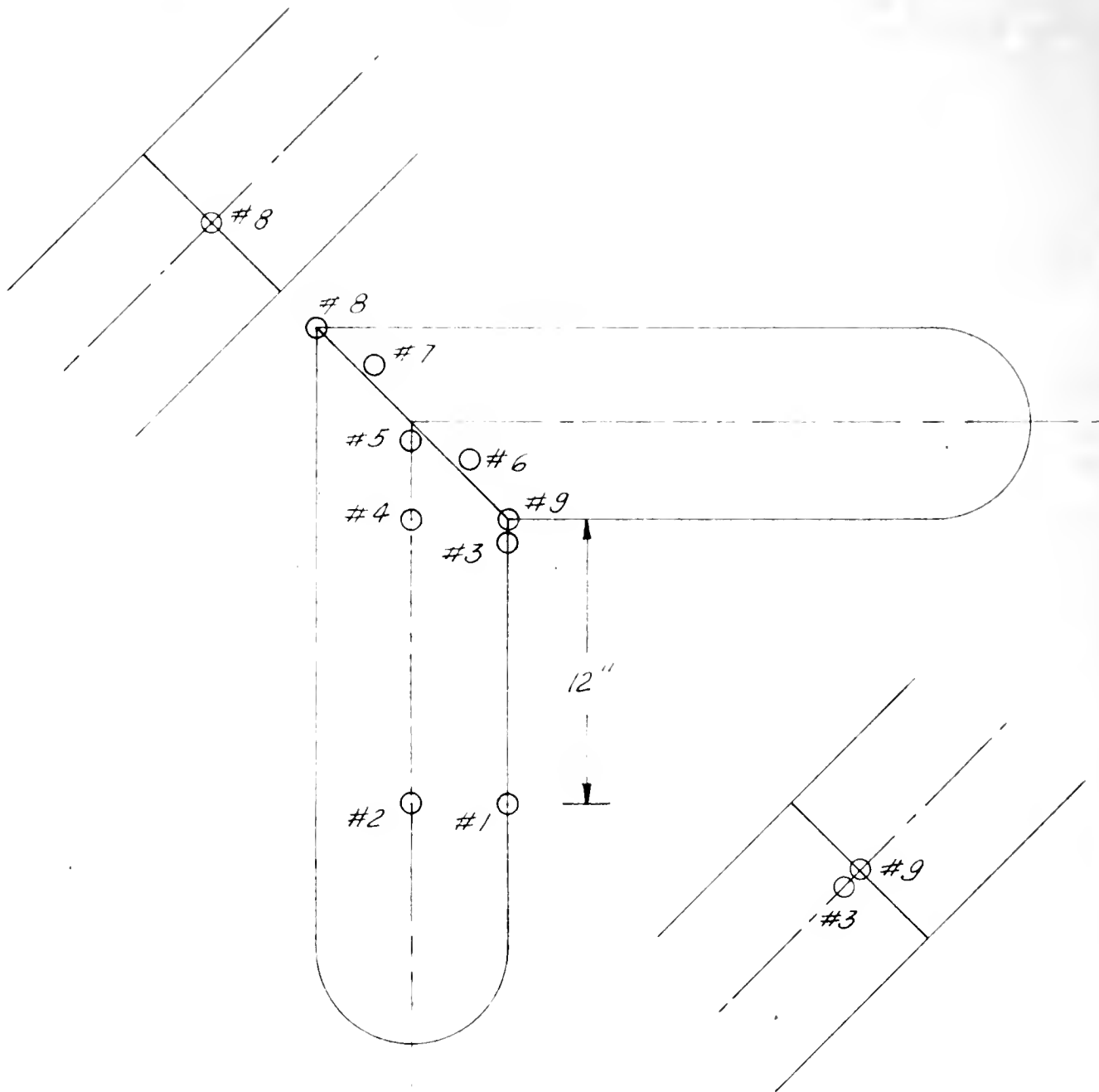


FIG. 7

LOCATION OF STRAIN GAGES  
TESTS I AND II

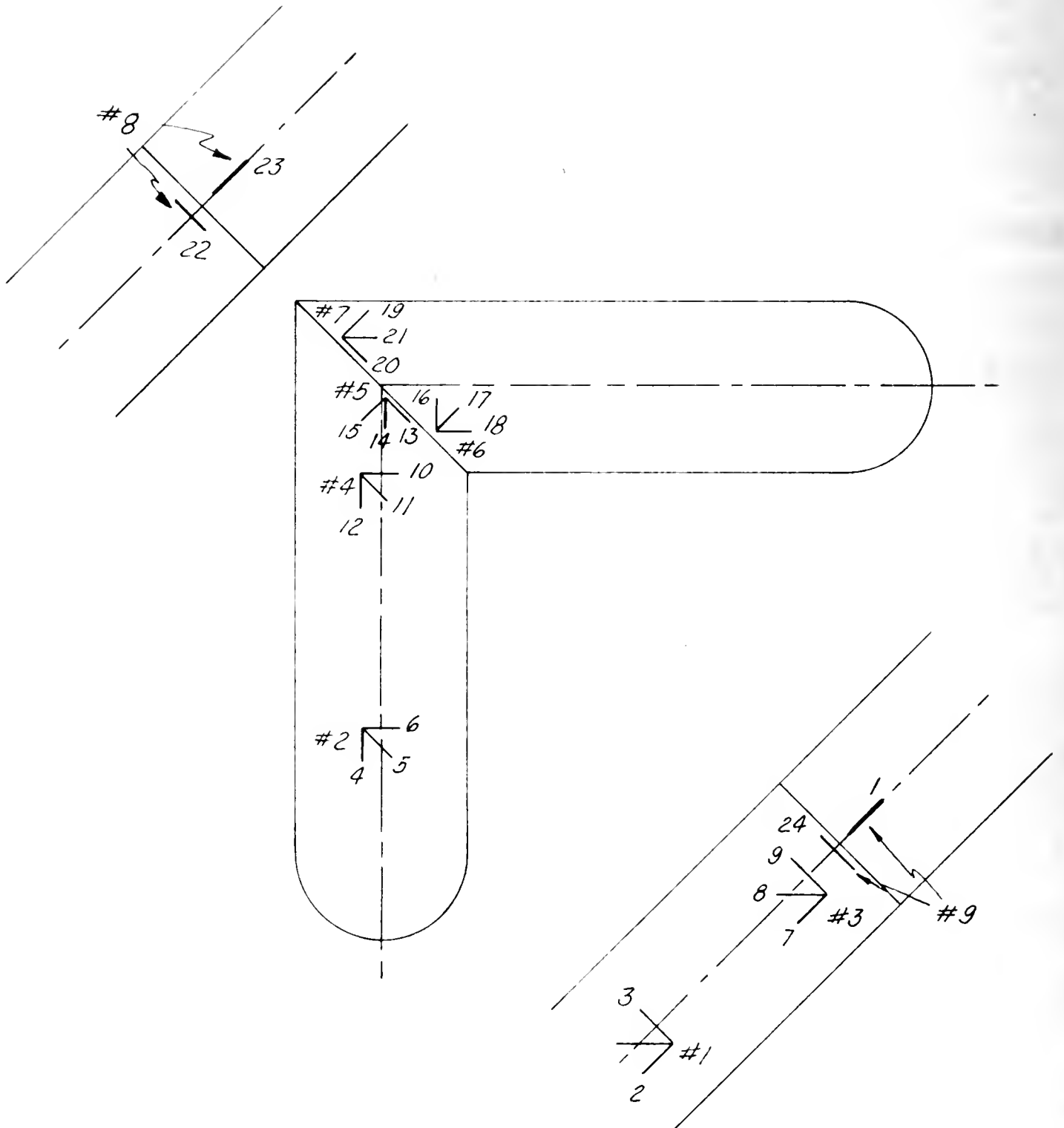


FIG. 8  
ORIENTATION OF STRAIN GAGES, TEST I

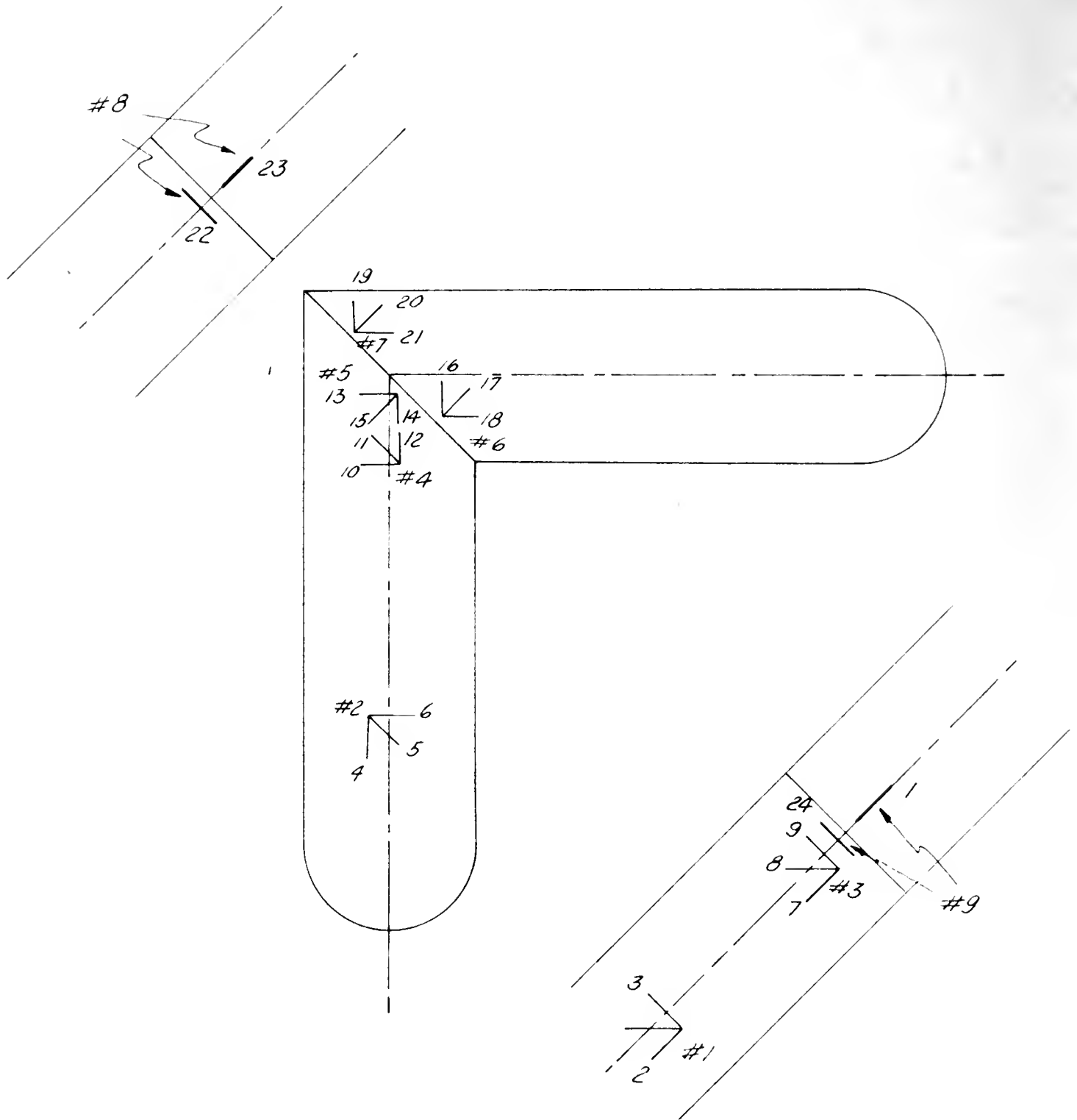
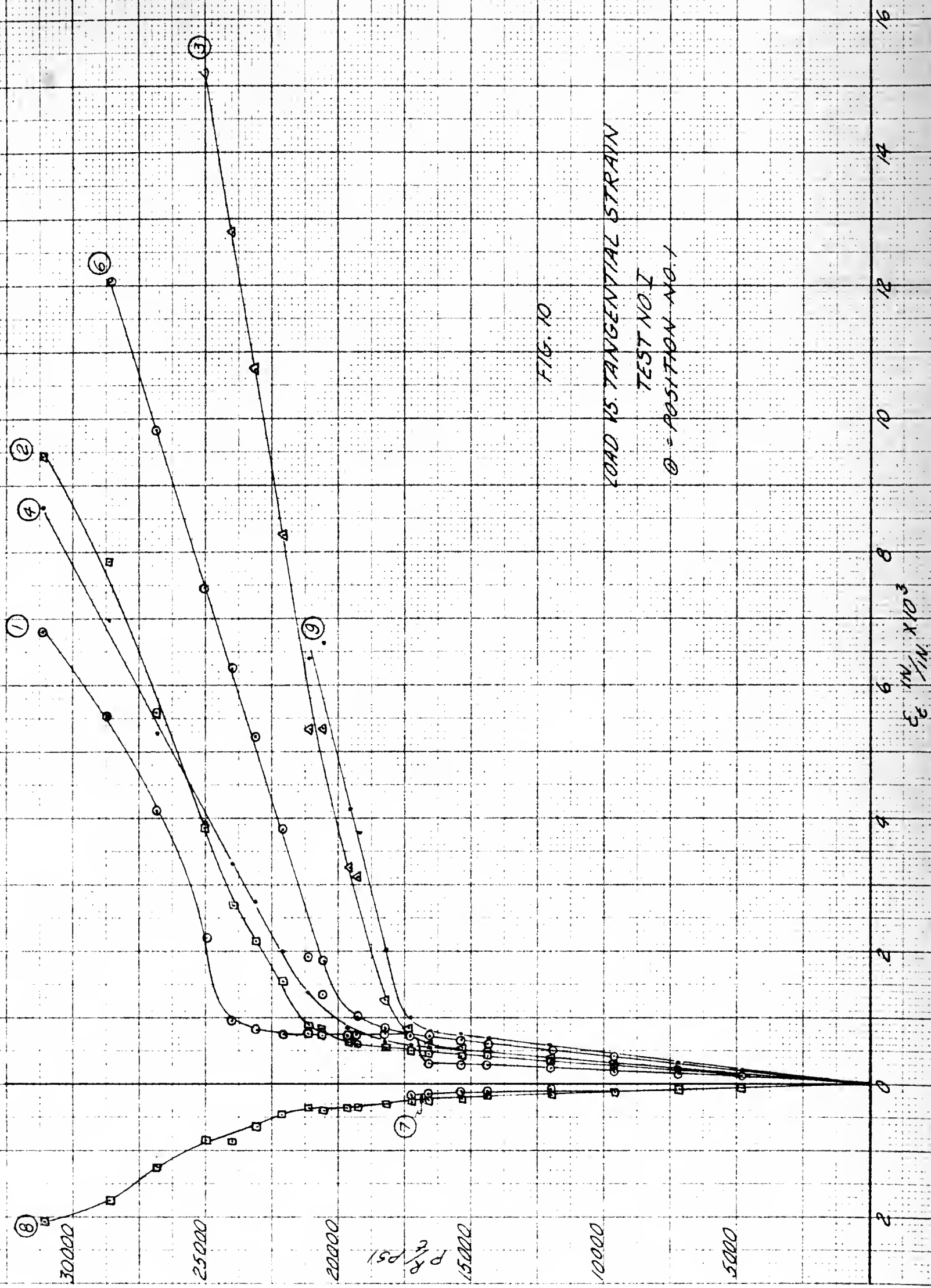
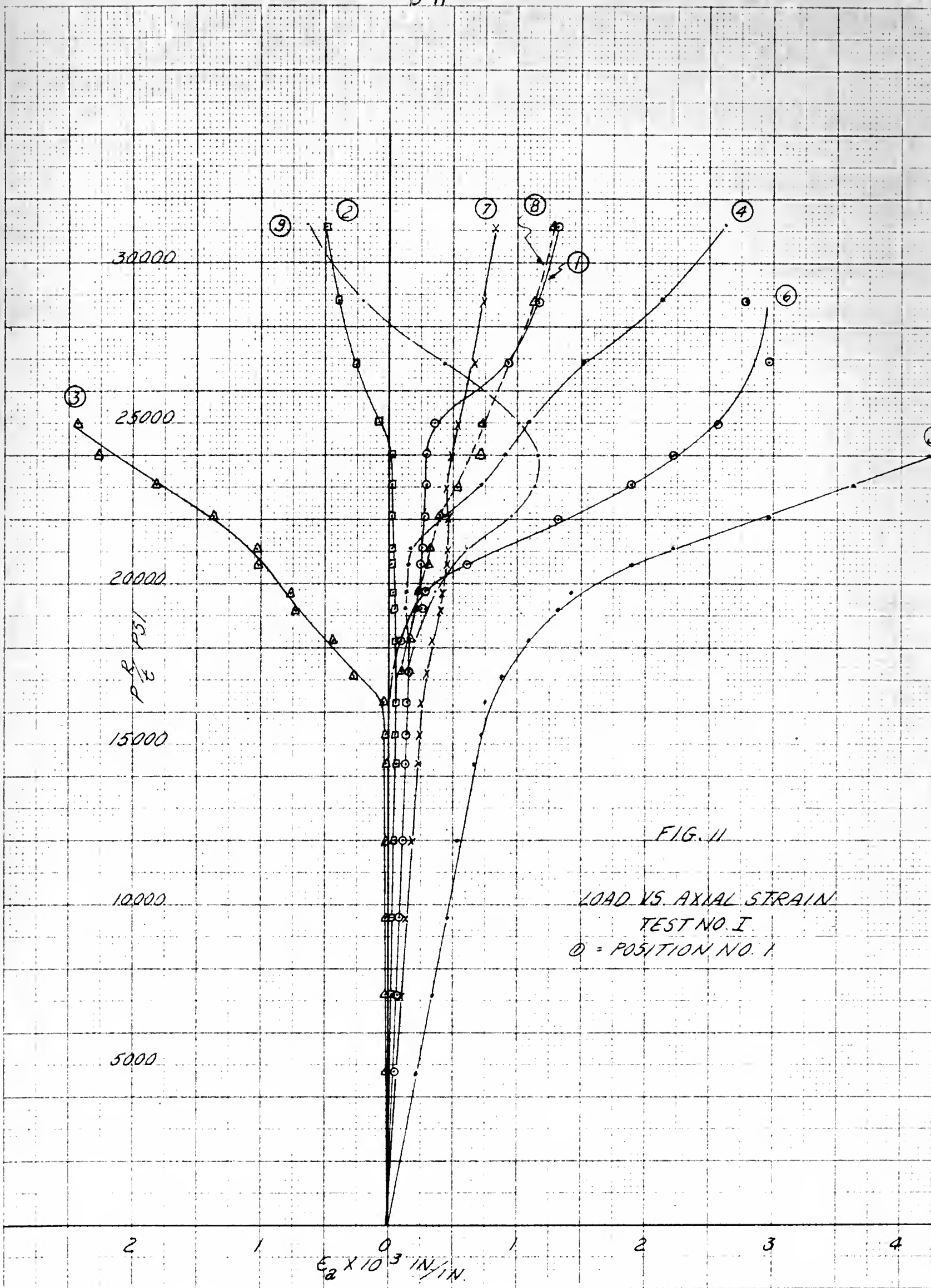


FIG. 9

ORIENTATION OF STRAIN GAGES, TEST II





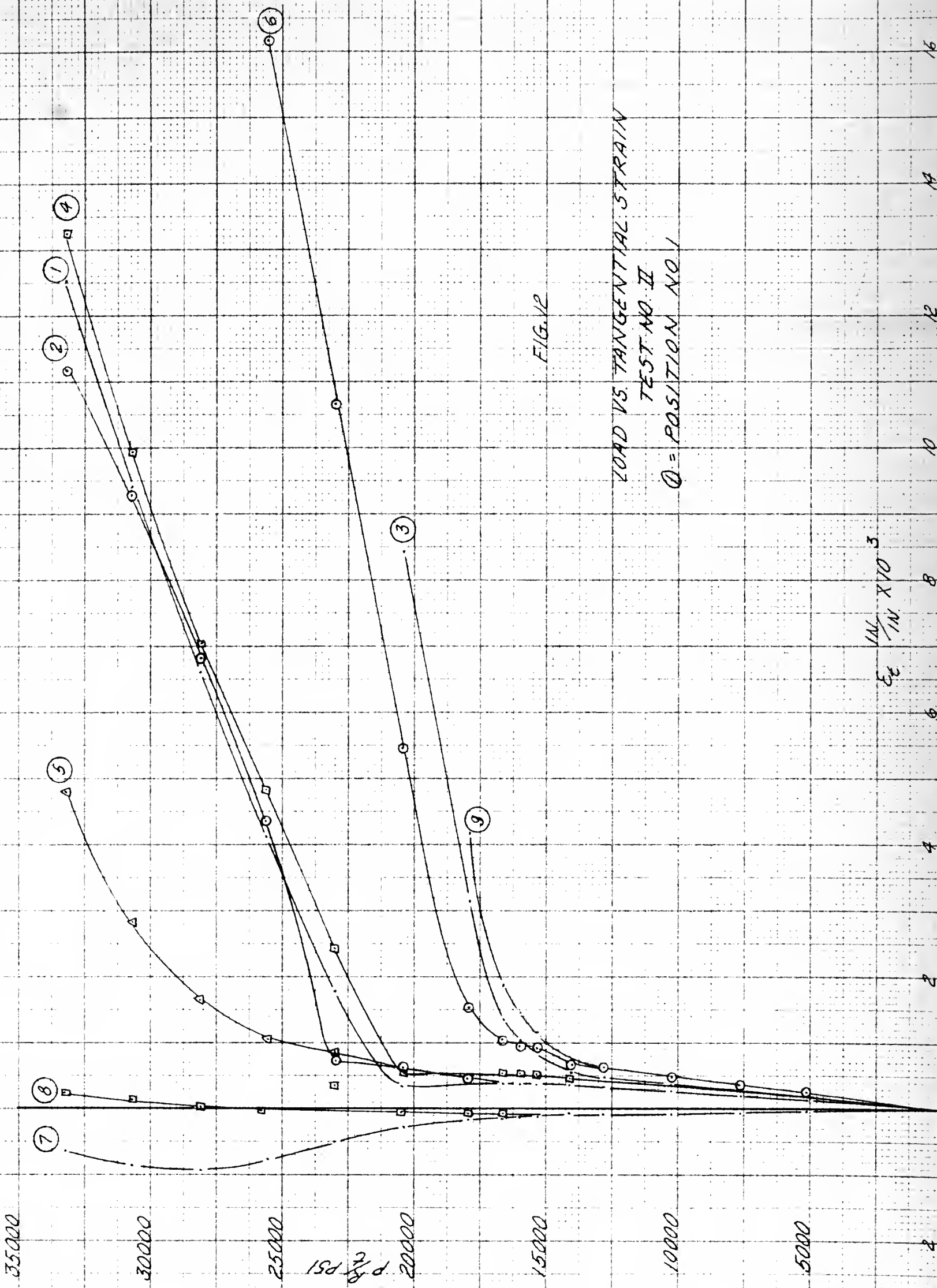


FIG. 12

LOAD VS. TANGENTIAL STRAIN  
 TEST NO. II  
 ① = POSITION NO. 1

Eε IN / IN X 10<sup>3</sup>

P / PSI

2 2 4 6 8 10 12 14 16

35000  
 30000  
 25000  
 20000  
 15000  
 10000  
 5000

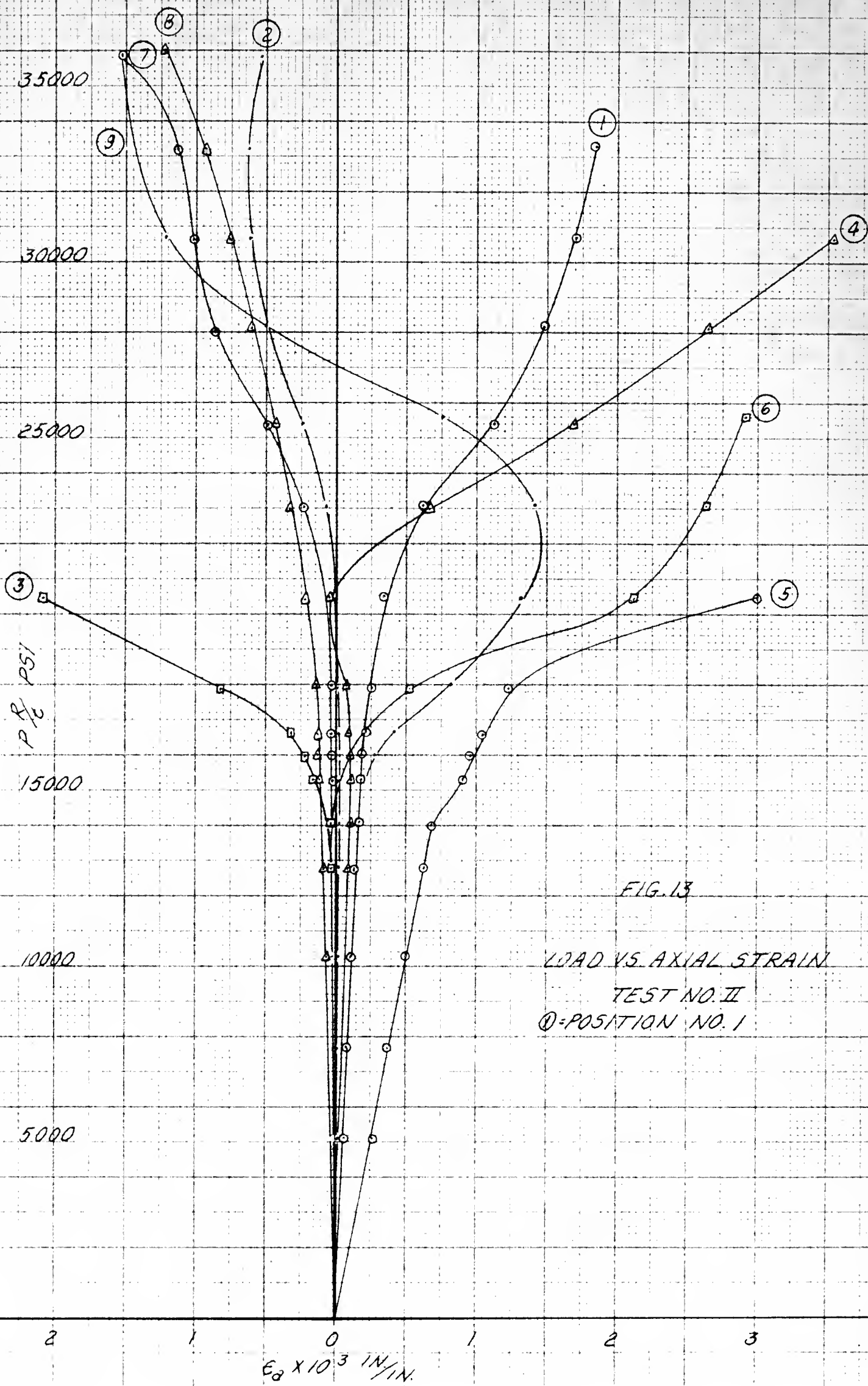
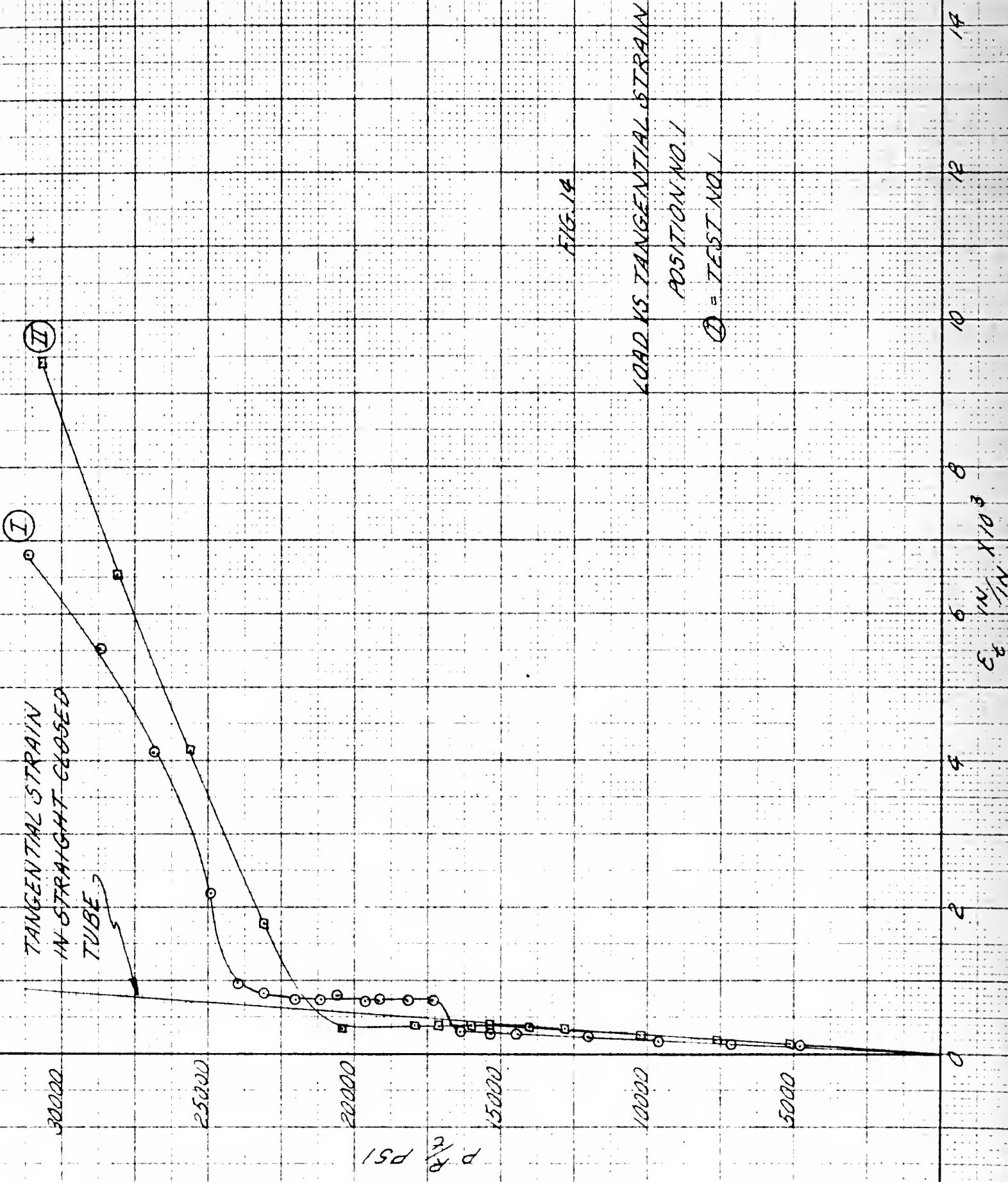
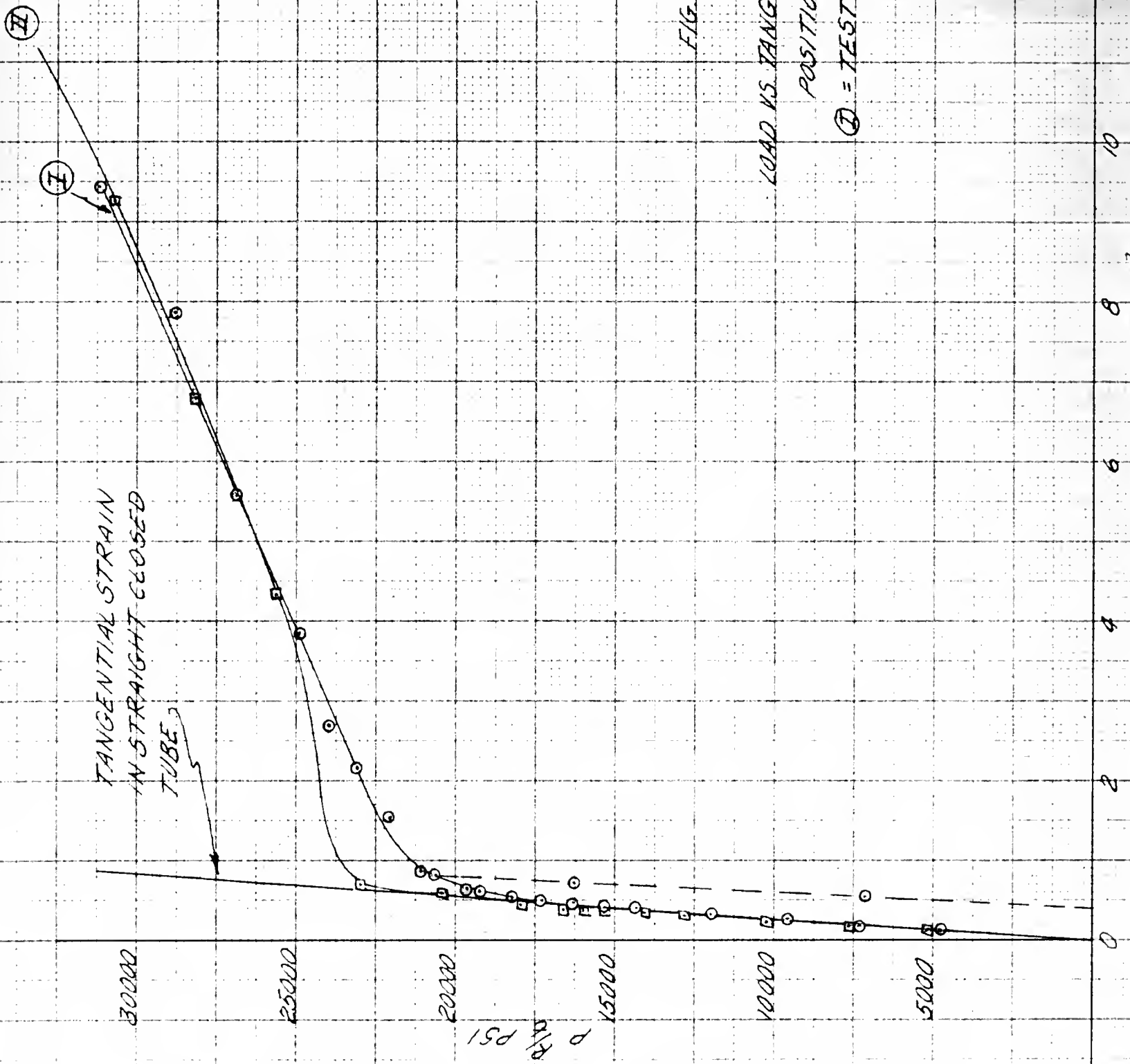


FIG. 13

LOAD VS. AXIAL STRAIN  
TEST NO. II  
① = POSITION NO. 1







TANGENTIAL STRAIN  
IN STRAIGHT CLOSED  
TUBES

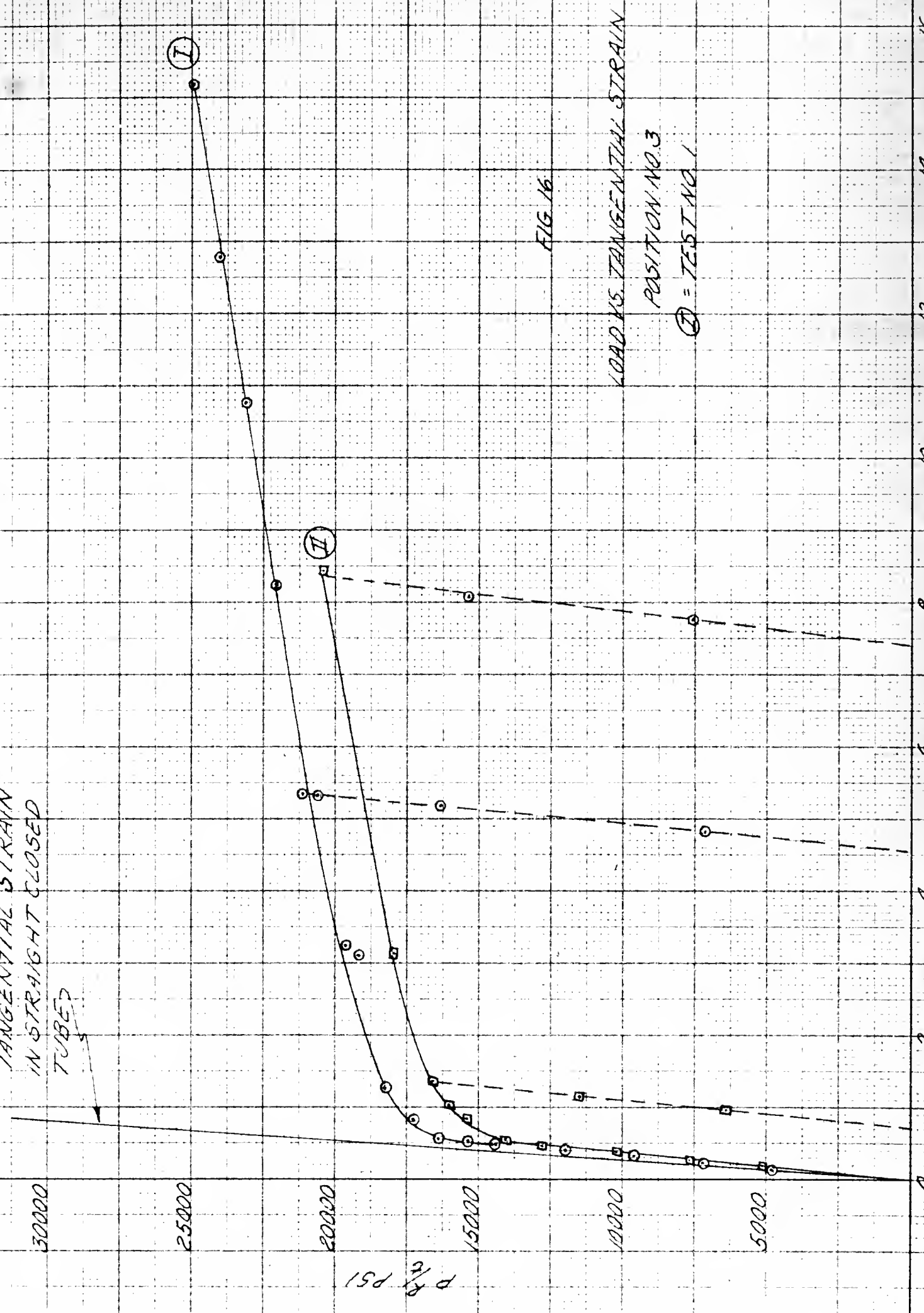


FIG. 16

LOAD VS. TANGENTIAL STRAIN  
POSITION NO. 3  
① = TEST NO. 1

$\epsilon_t \times 10^{-3}$

P/PsI

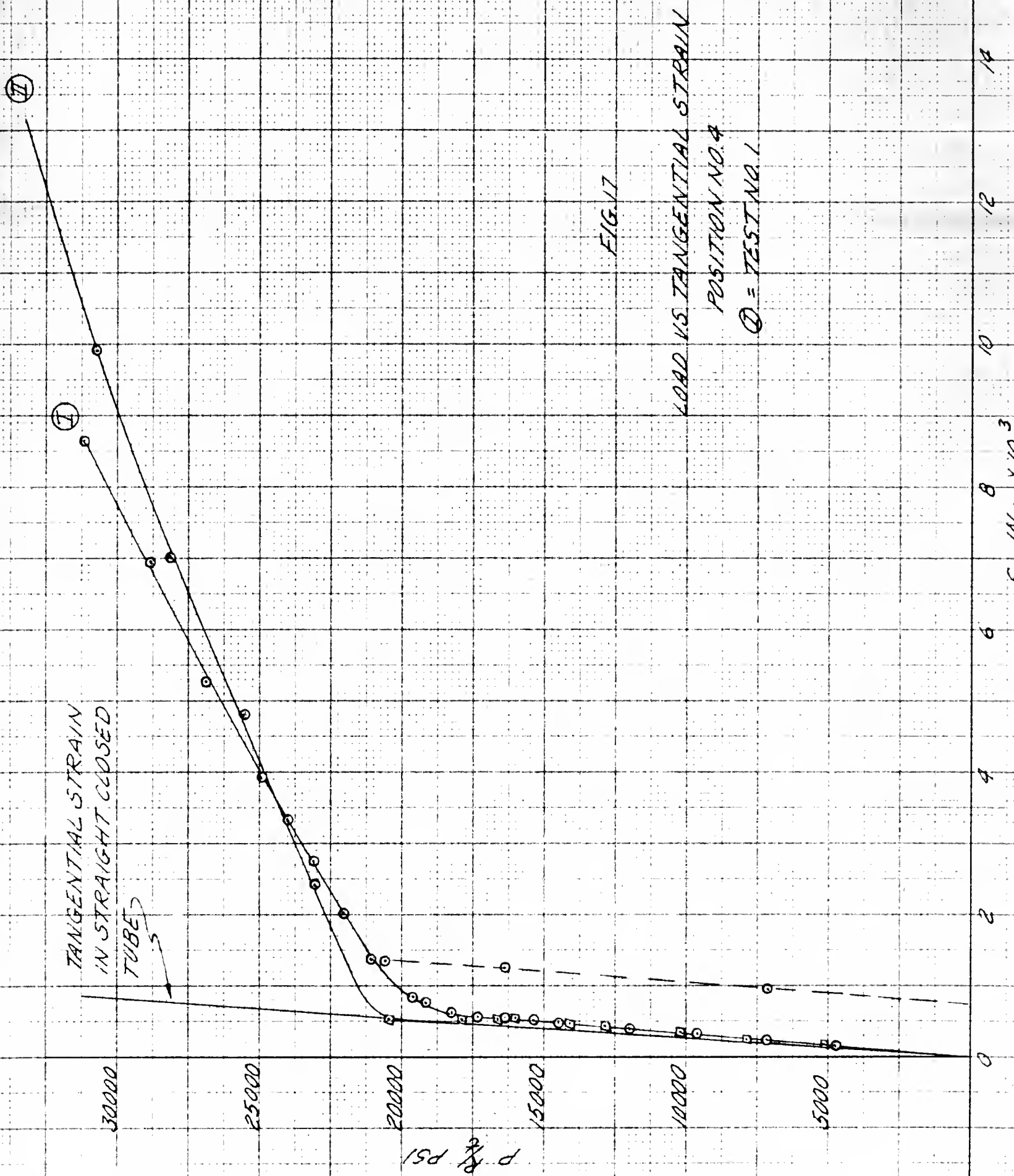


FIG. 17

LOAD VS. TANGENTIAL STRAIN  
POSITION NO. 4  
① = TEST NO. 1

TANGENTIAL STRAIN  
IN STRAIGHT CLOSED  
TUBE

30000

25000

20000

15000

10000

5000

P % PSI

FIG. 18

LOAD VS. TANGENTIAL STRAIN

POSITION NO. 5

① = TEST NO. 1

$\epsilon$  IN/IN  $\times 10^3$

14

12

10

8

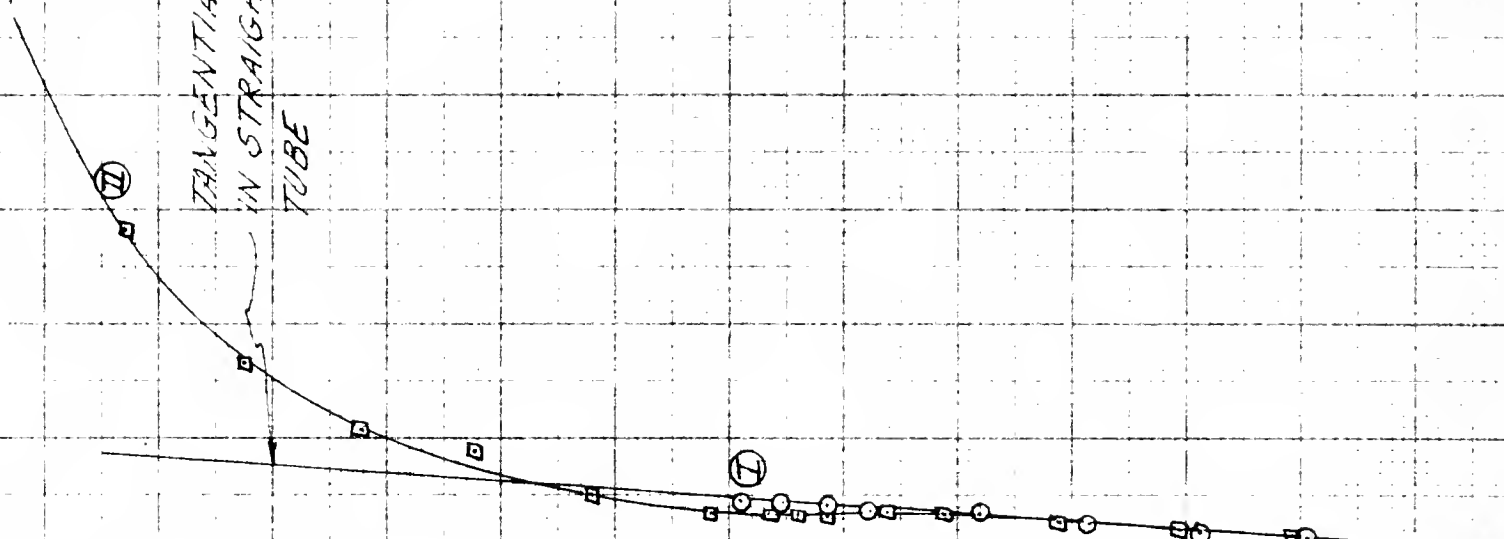
6

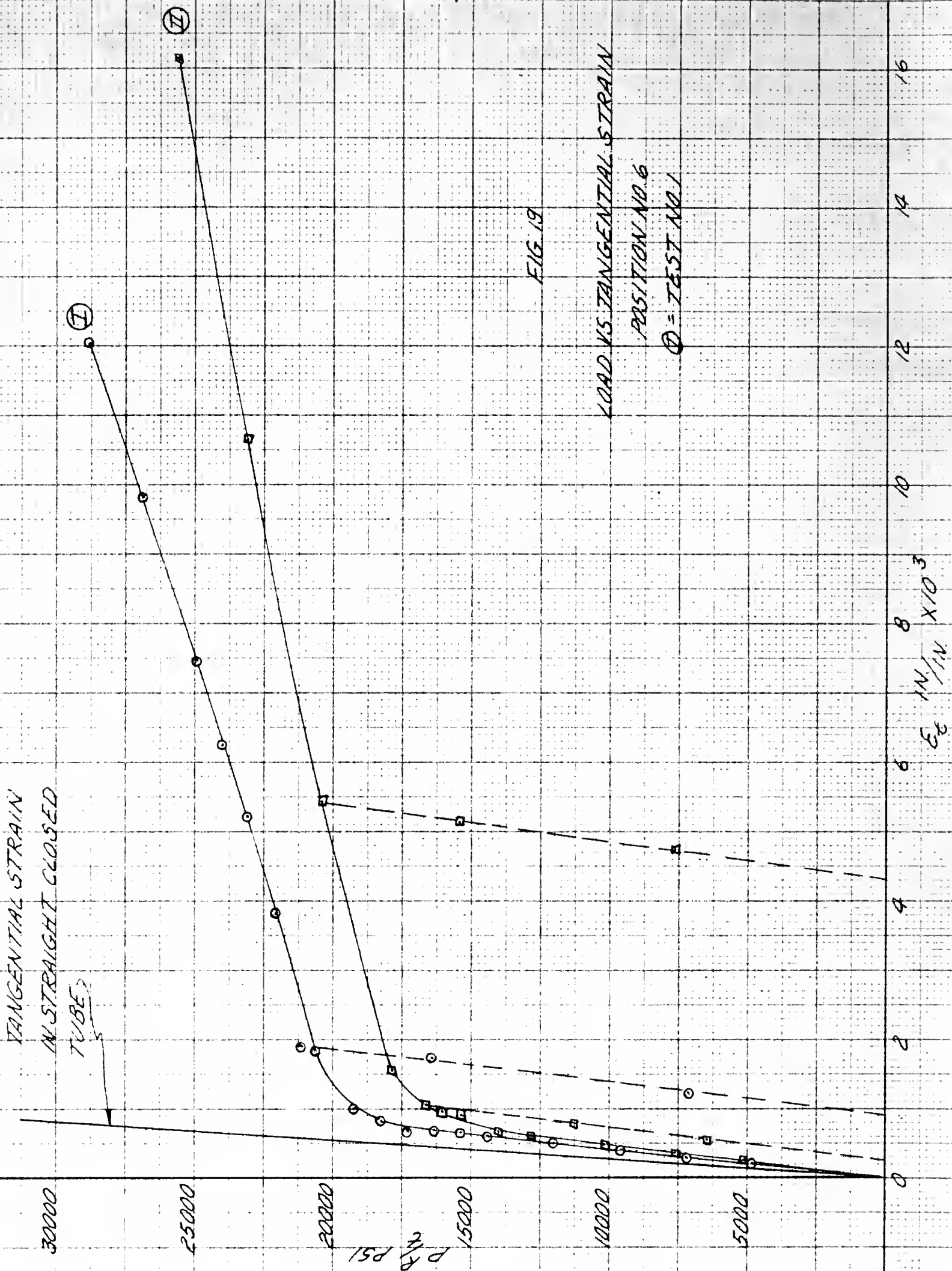
4

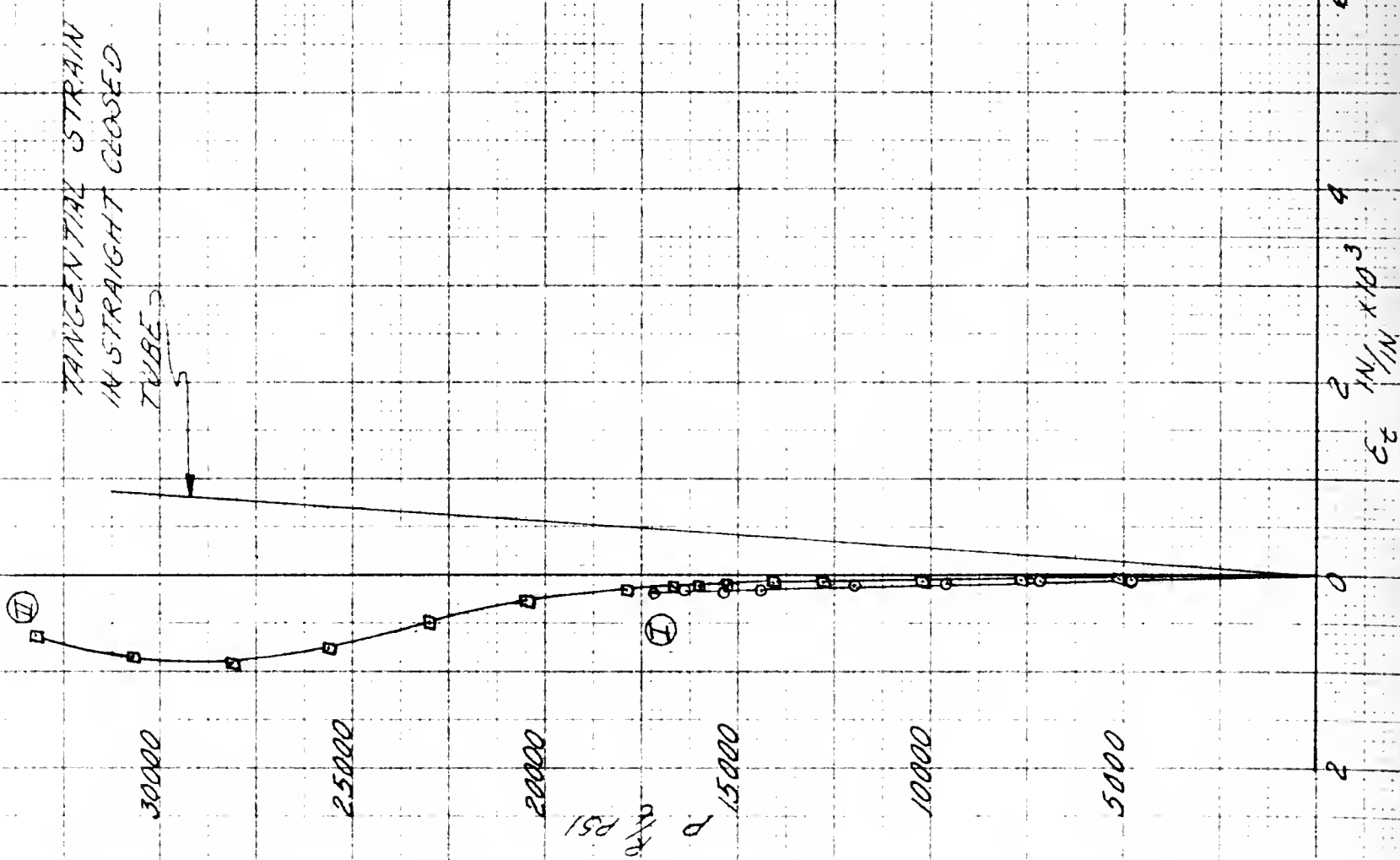
2

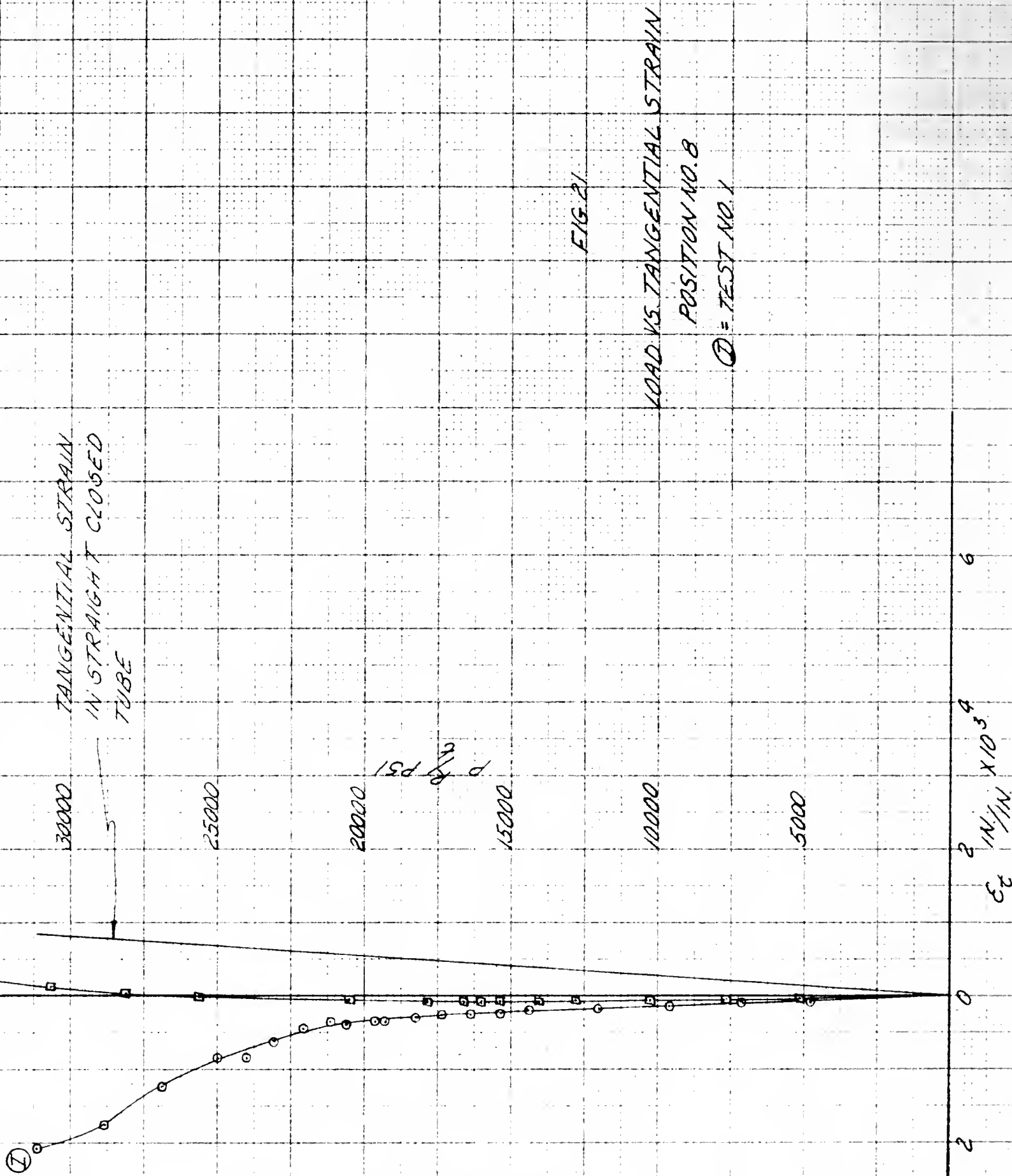
0

2











TANGENTIAL STRAIN  
IN STRAIGHT CLOSED  
TUBE

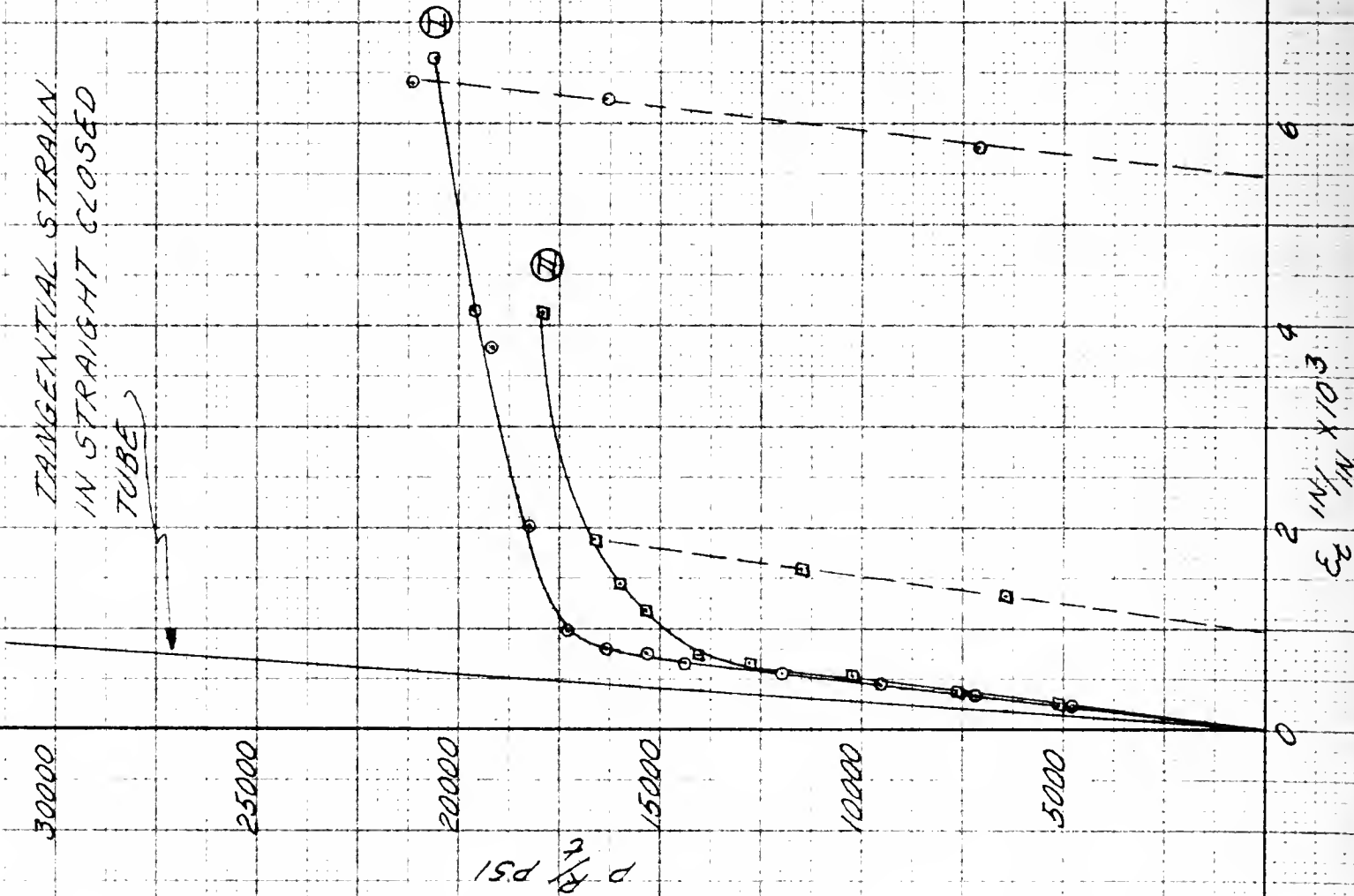


FIG. 22

LOAD VS. TANGENTIAL STRAIN

POSITION NO. 9

⊙ = TEST NO. 1

$E_T$   
in/in  $\times 10^3$

2

0

2

4

6

8

10

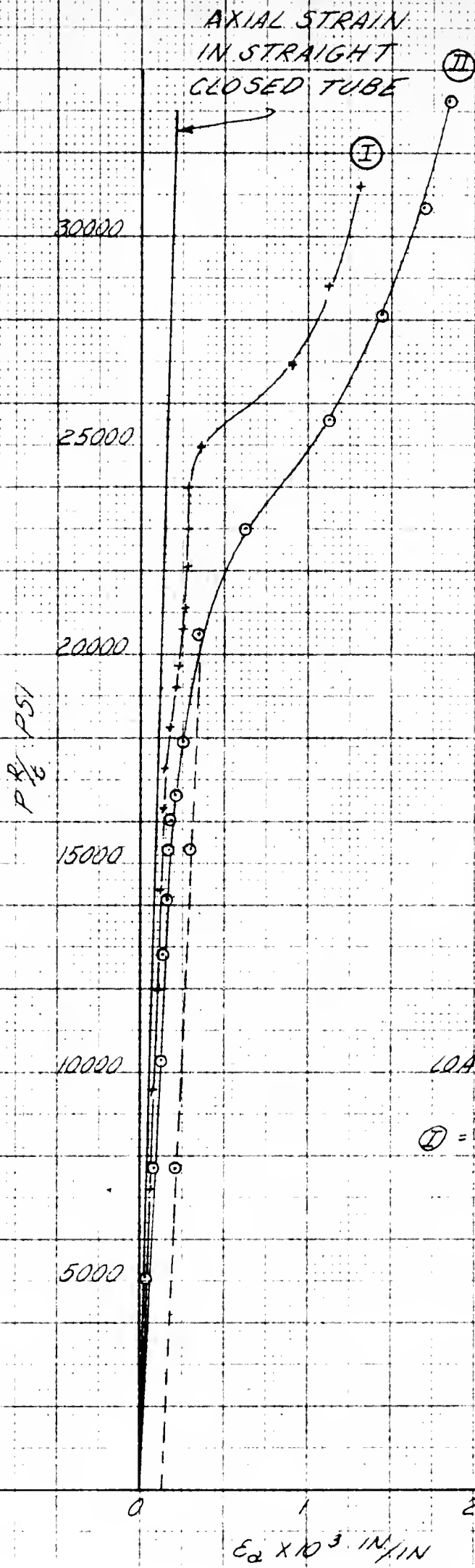


FIG. 23

LOAD VS. AXIAL STRAIN  
POSITION NO. 1

⊙ = TEST NO. 1

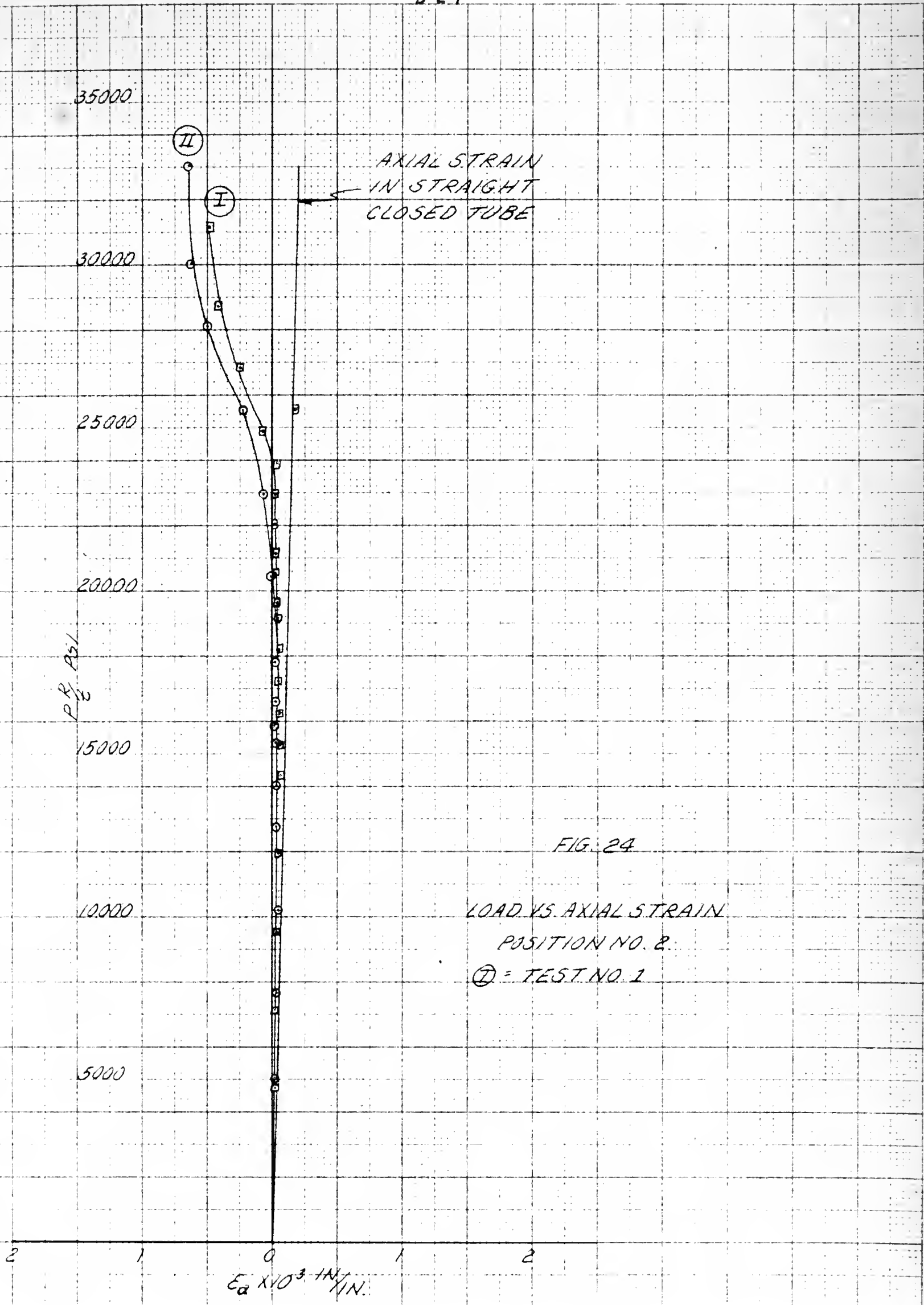


FIG. 24

LOAD VS. AXIAL STRAIN  
POSITION NO. 2.  
⊙ = TEST NO. 1

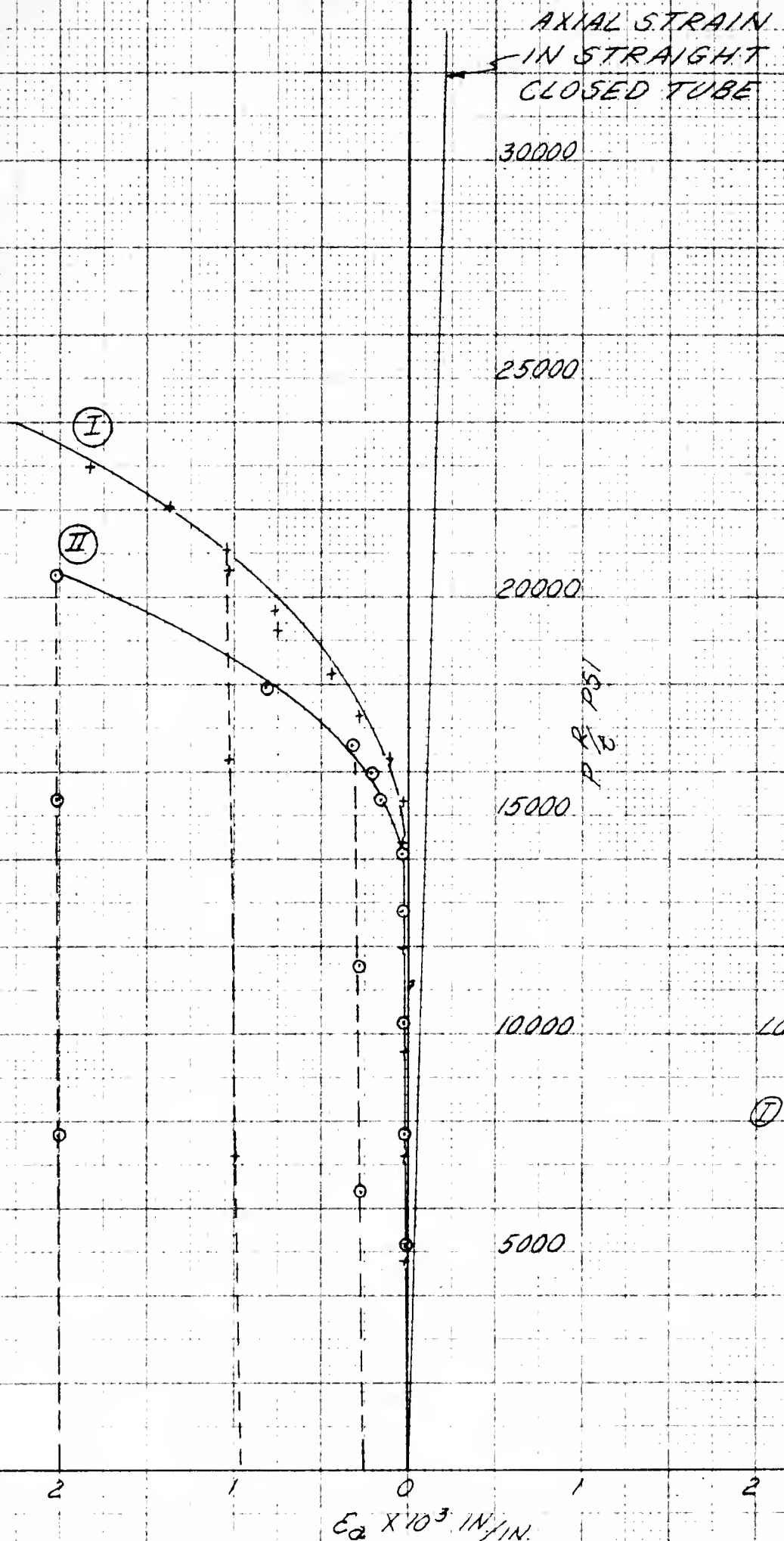
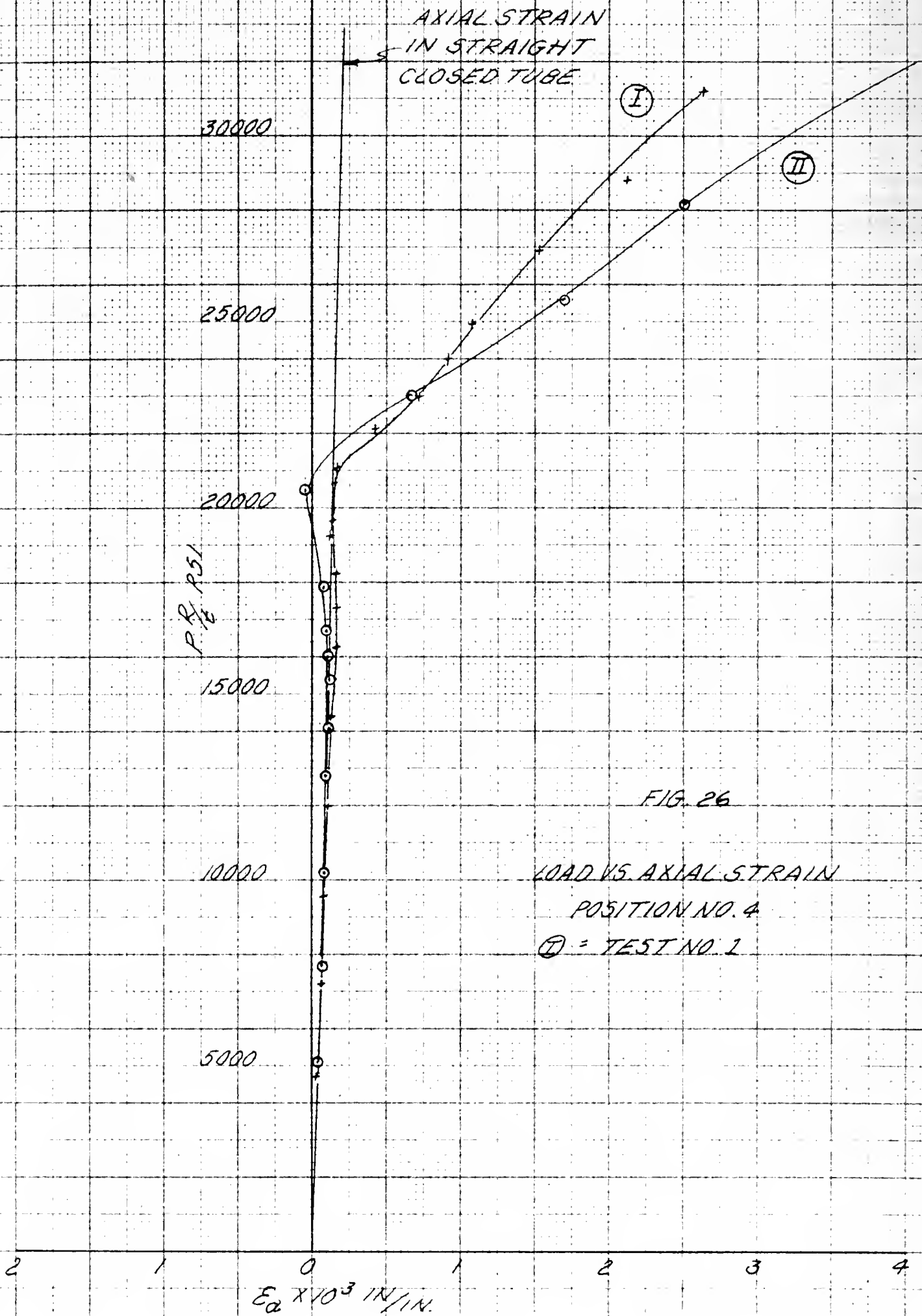
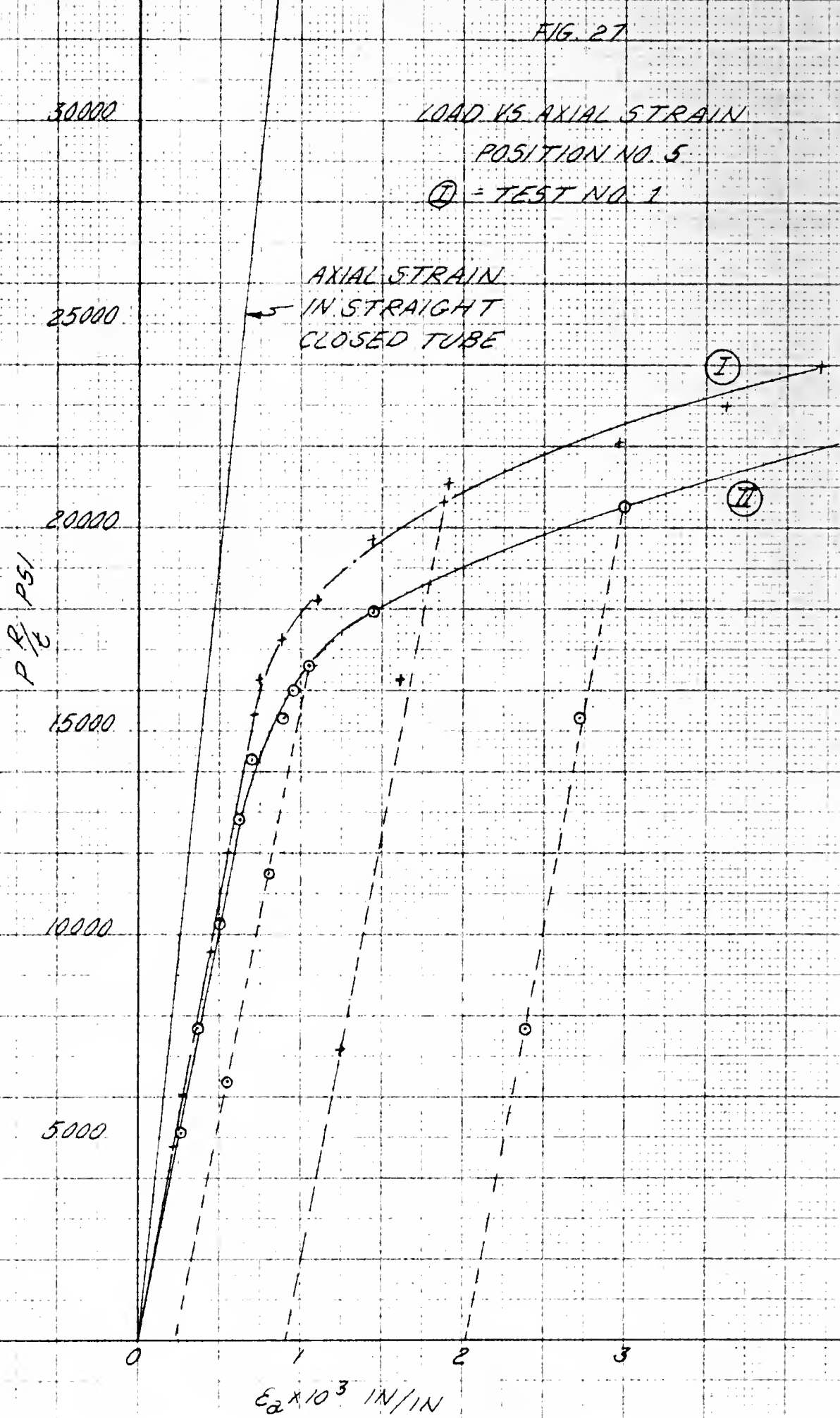


FIG. 25

LOAD VS. AXIAL STRAIN  
POSITION NO. 3  
Ⓘ = TEST NO. 1





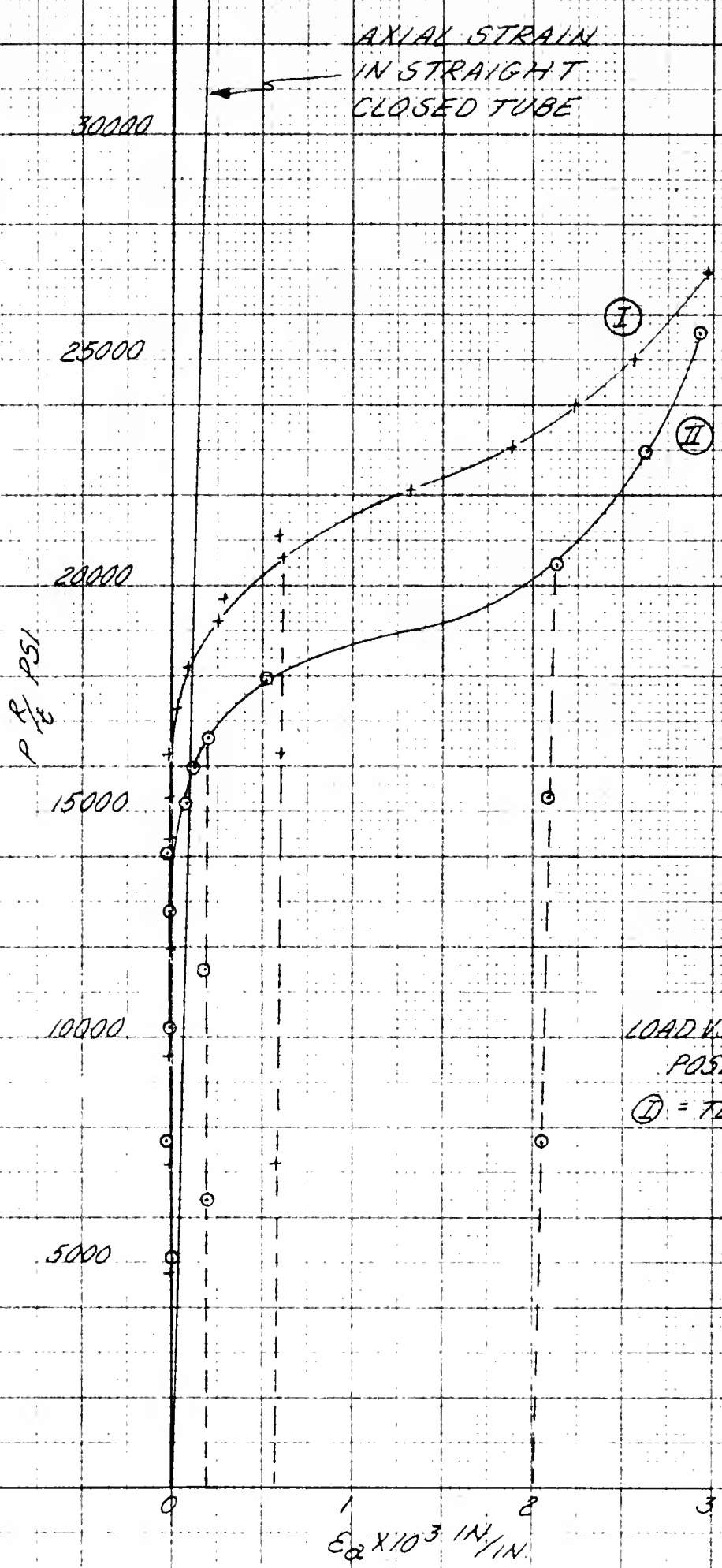


FIG. 28

LOAD VS AXIAL STRAIN  
POSITION NO. 6  
① = TEST NO. 1

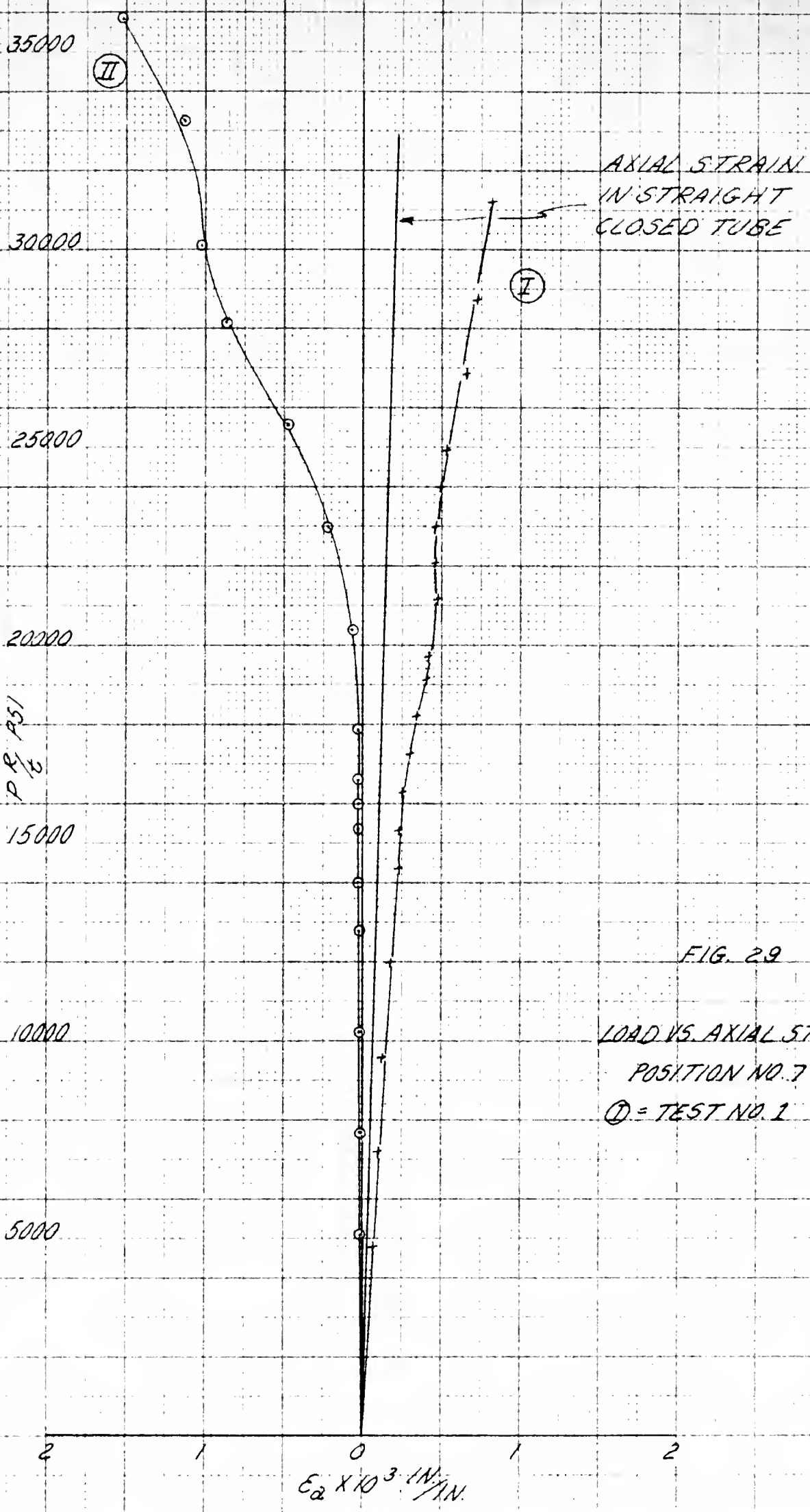


FIG. 29

LOAD VS. AXIAL STRAIN  
POSITION NO. 7  
① = TEST NO. 1



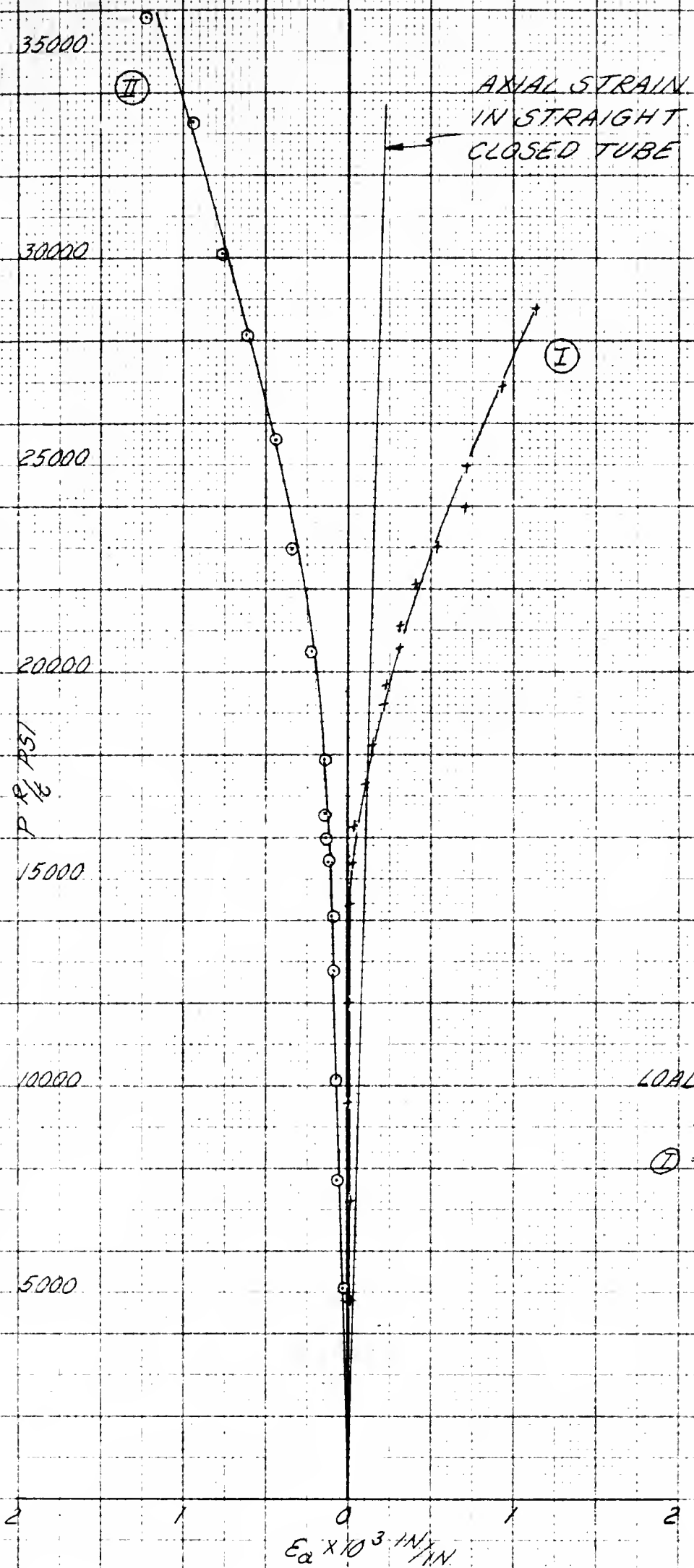


FIG. 30

LOAD VS. AXIAL STRAIN  
POSITION NO. 8  
Ⓢ = TEST NO. 1

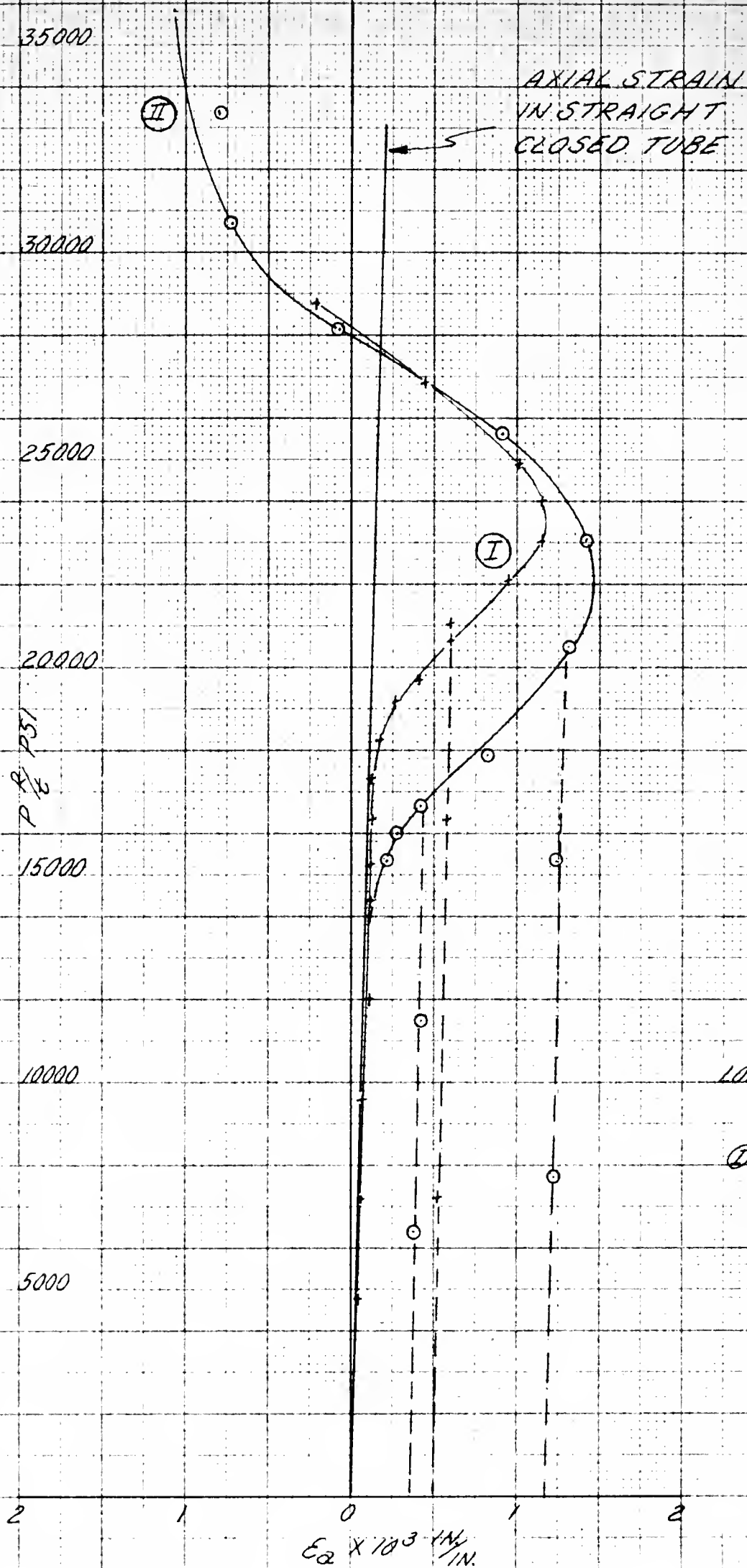


FIG. 31

LOAD VS. AXIAL STRAIN  
POSITION NO. 9  
① = TEST NO. 1

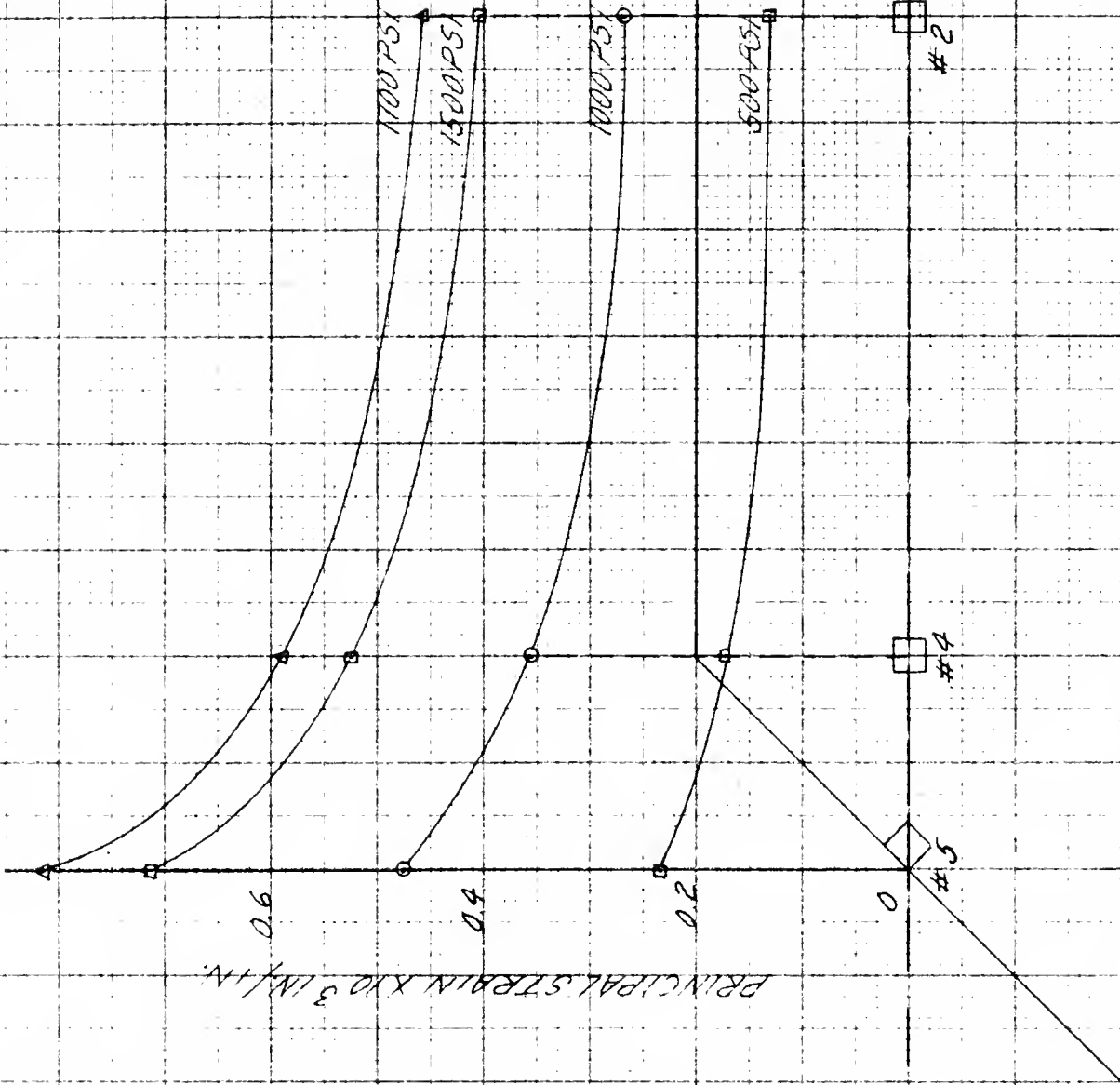


FIG. 32

PRINCIPAL STRAIN VS AXIAL POSITION

TEST NO. I

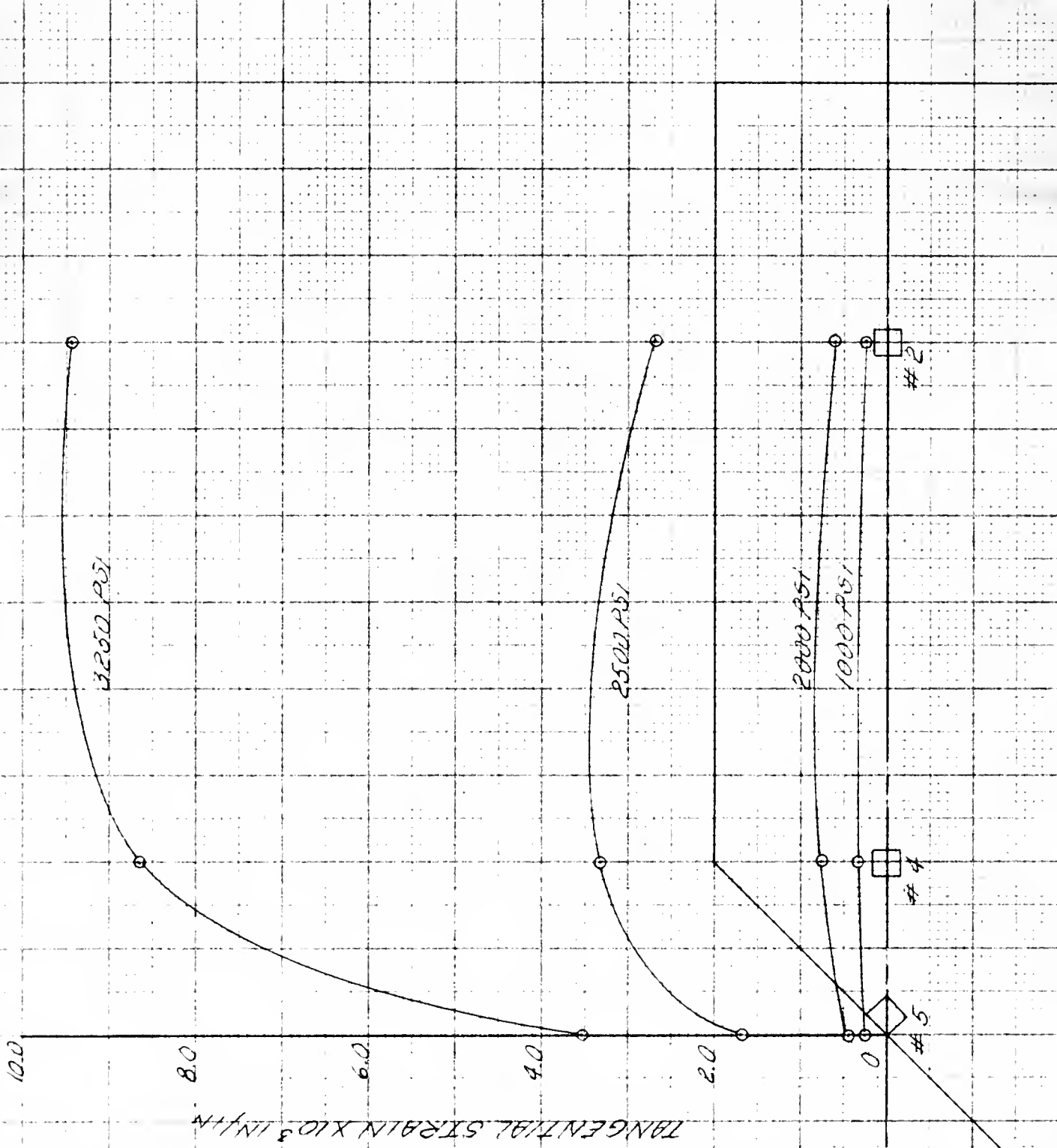


FIG. 33  
TANGENTIAL STRAIN VS. AXIAL POSITION  
TEST NO. 1

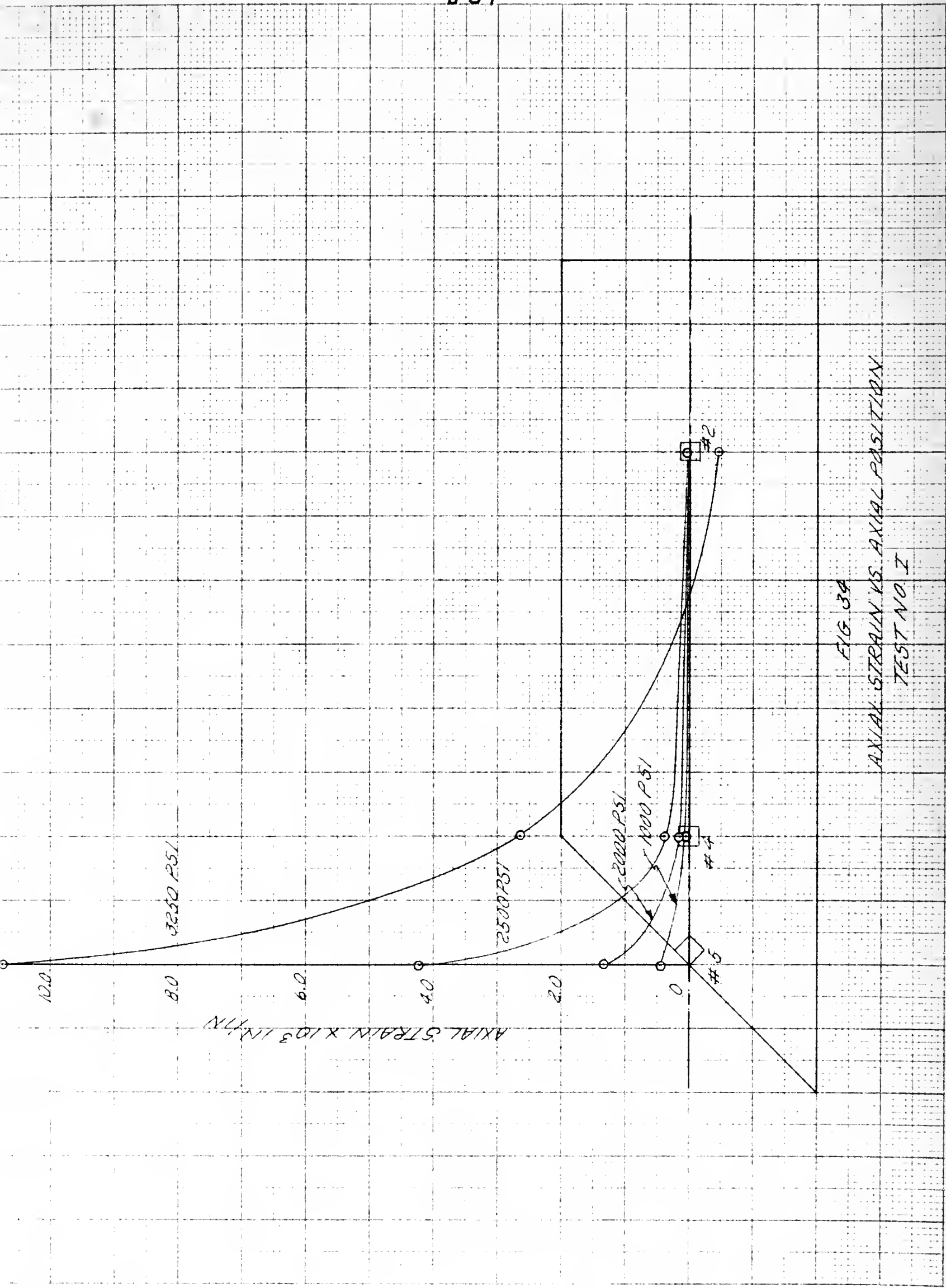


FIG. 34  
AXIAL STRAIN VS. AXIAL POSITION  
TEST NO. 1

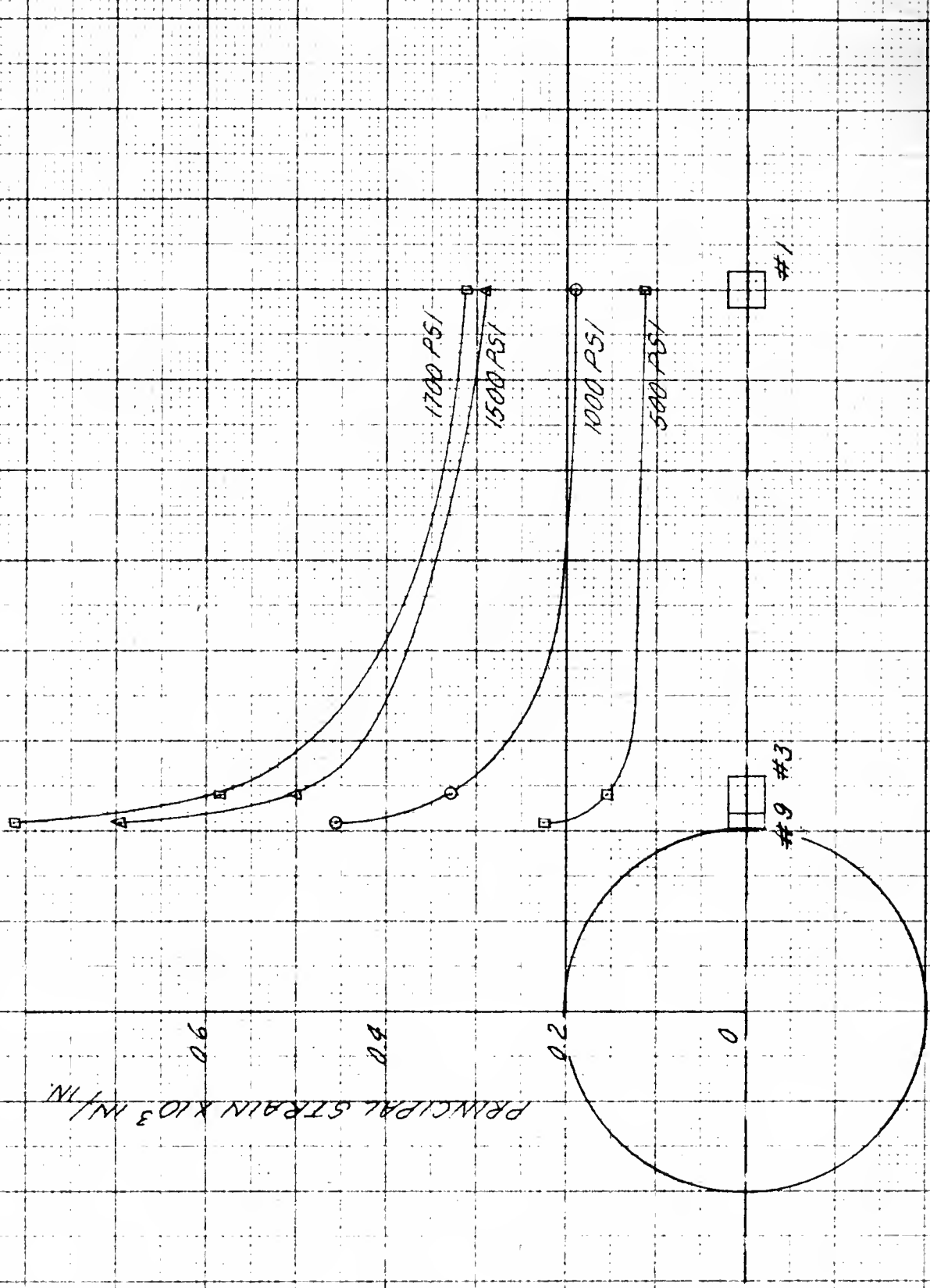
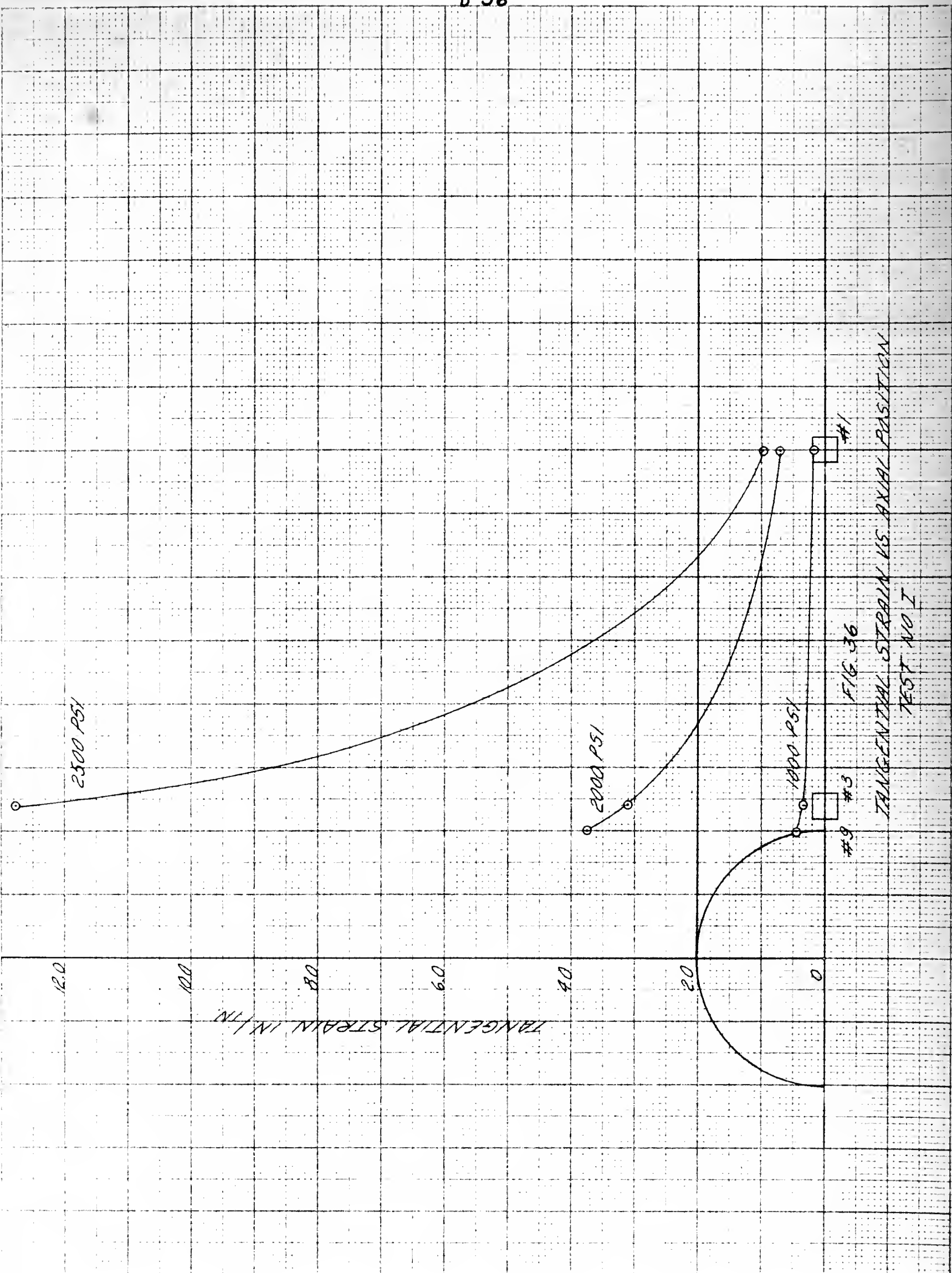


FIG. 35  
PRINCIPAL STRAIN VS AXIAL POSITION  
TEST NO. I



AXIAL STRAIN  $\times 10^3$  IN/IN

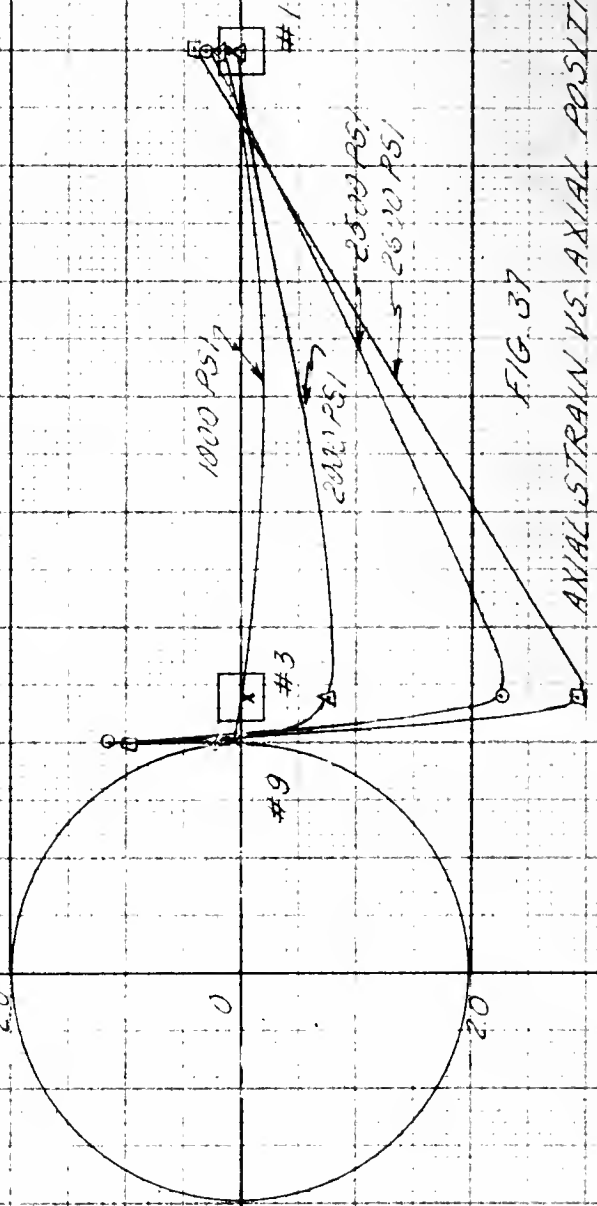


FIG. 37  
AXIAL STRAIN VS. AXIAL POSITION  
TEST NO. I



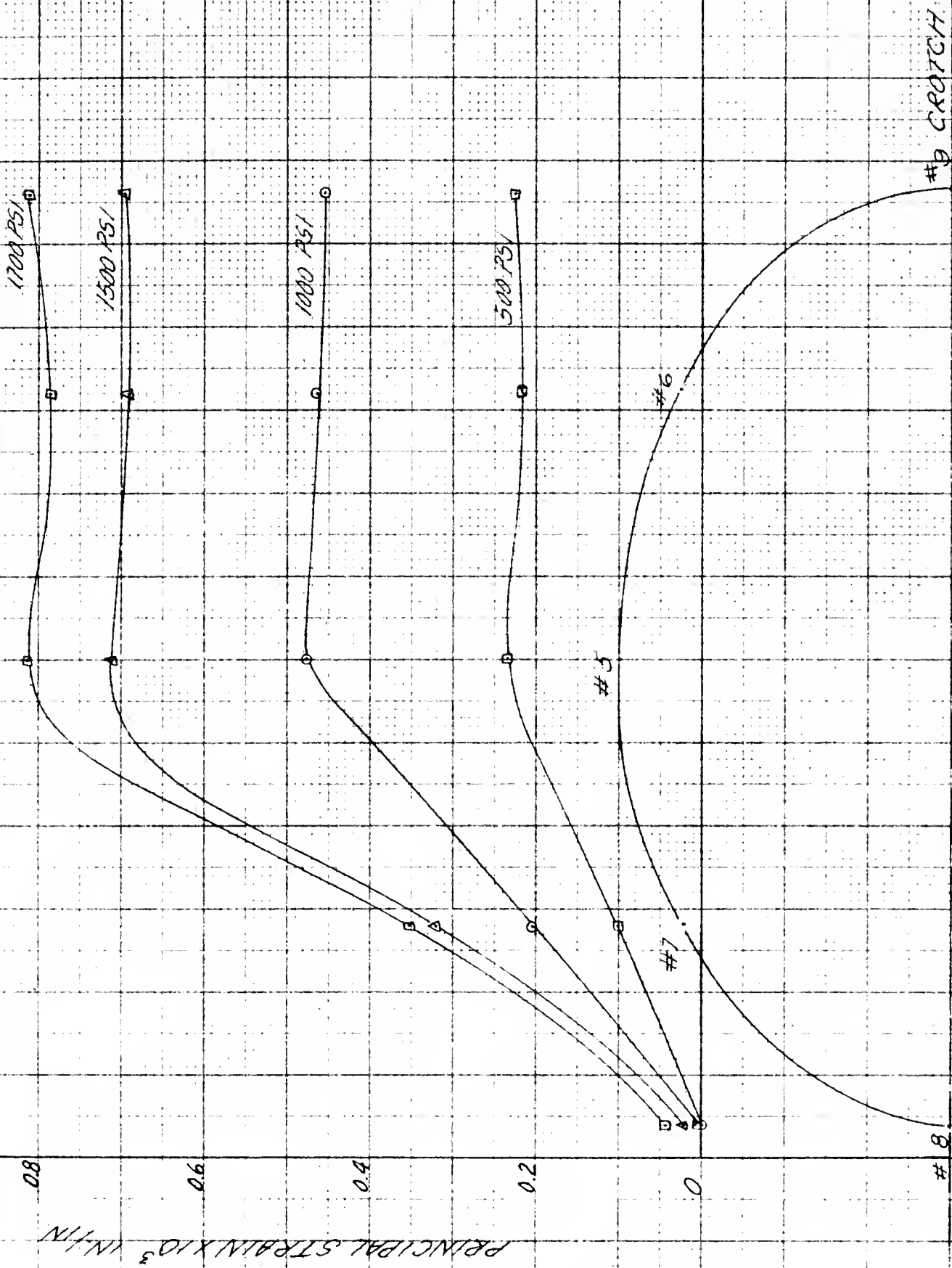


FIG. 38  
PRINCIPAL STRAIN VS. POSITION ON INTERSECTION  
TEST NO. I

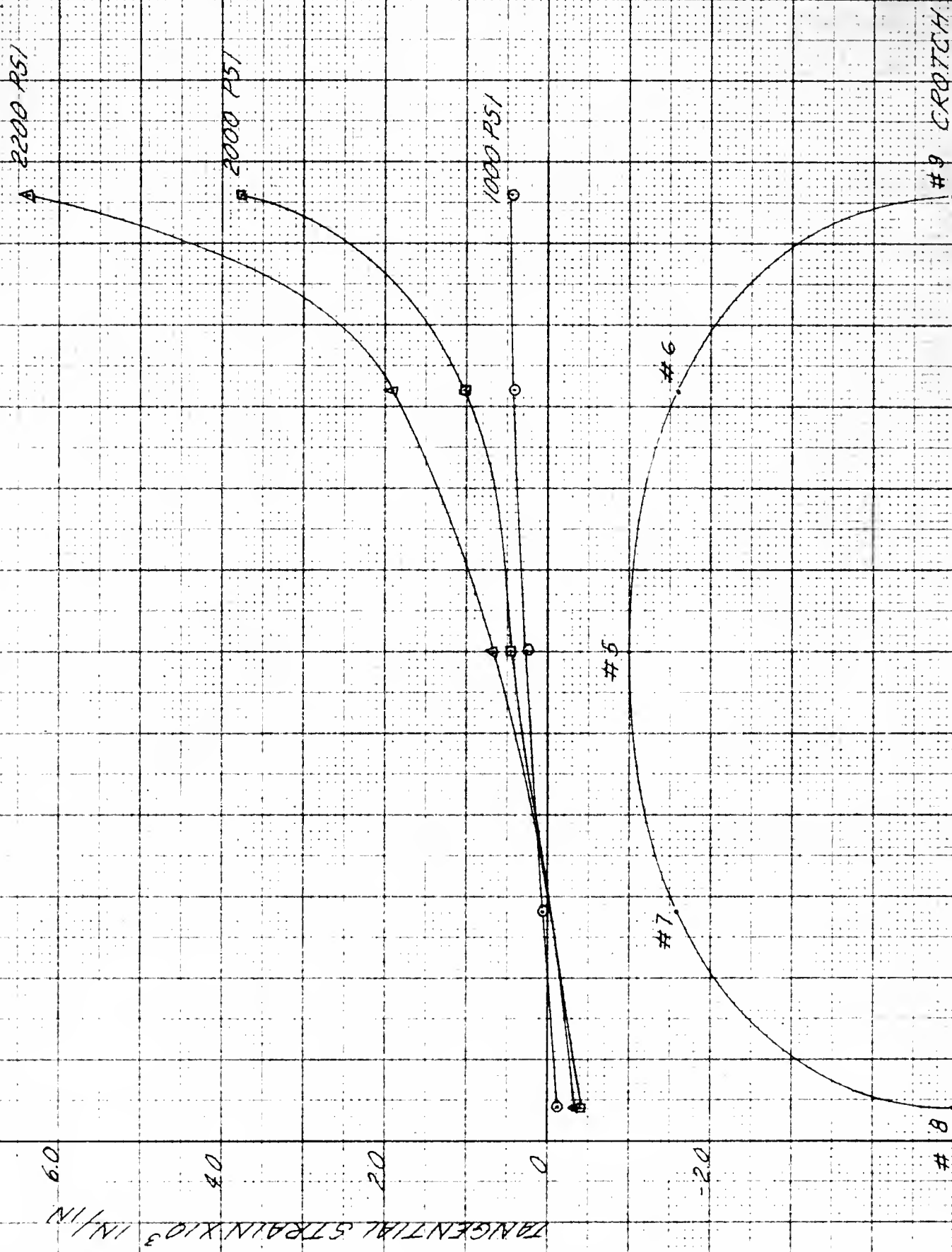


FIG. 39  
TANGENTIAL STRAIN VS. POSITION ON WATER SECTION  
TEST NO. 1

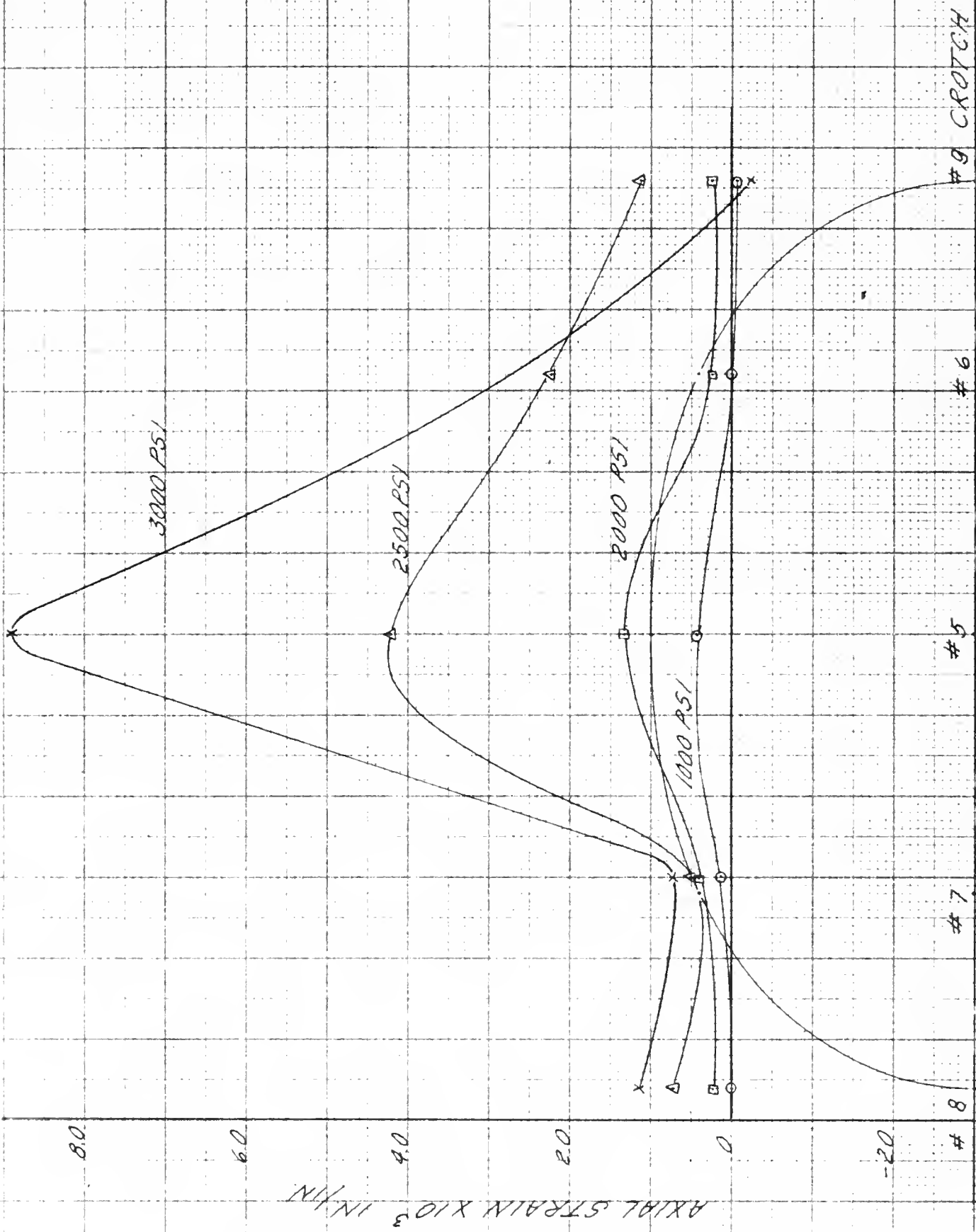


FIG. 40  
AXIAL STRAIN VS POSITION OF INTERSECTION  
TEST NO. 1

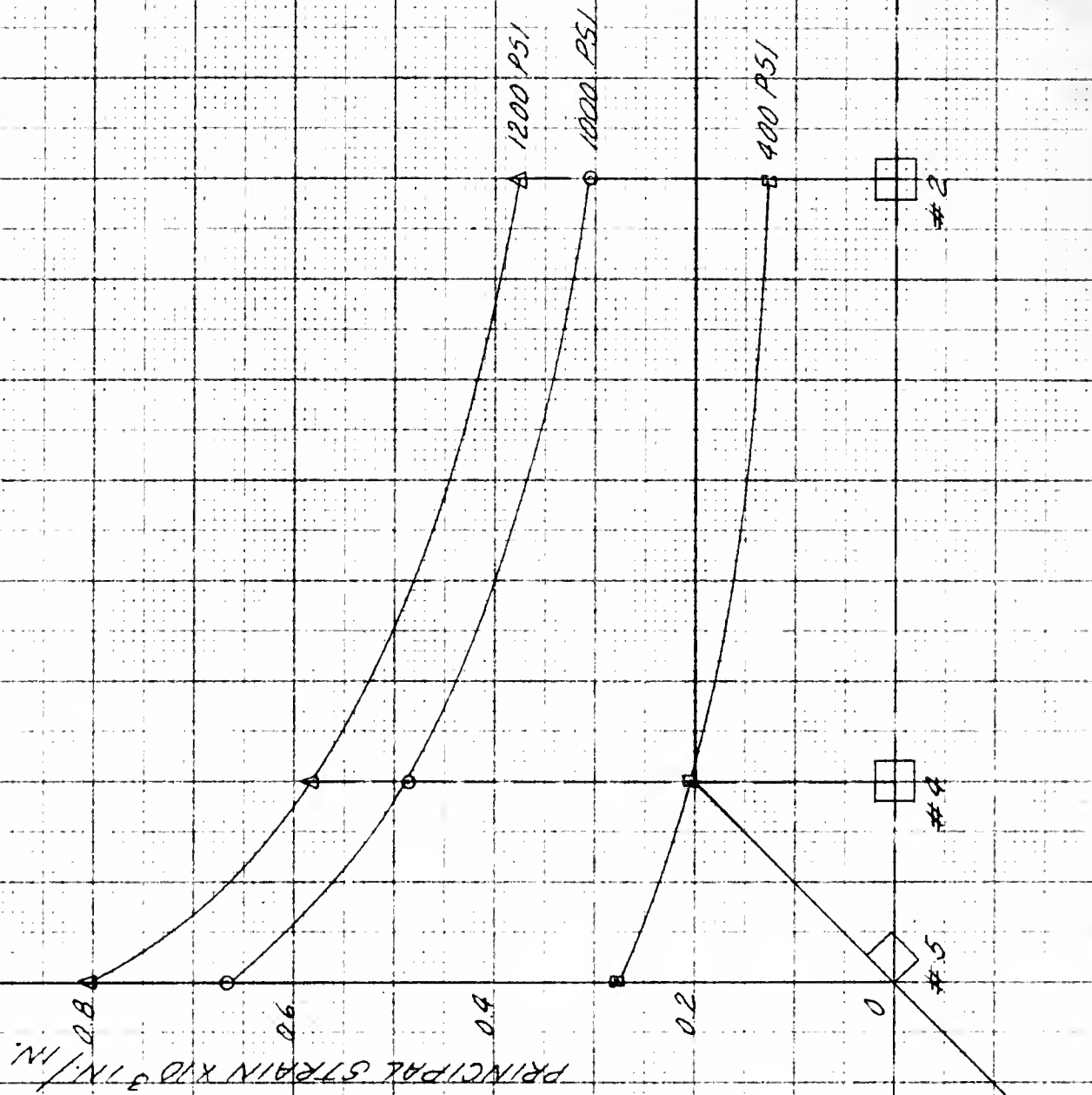
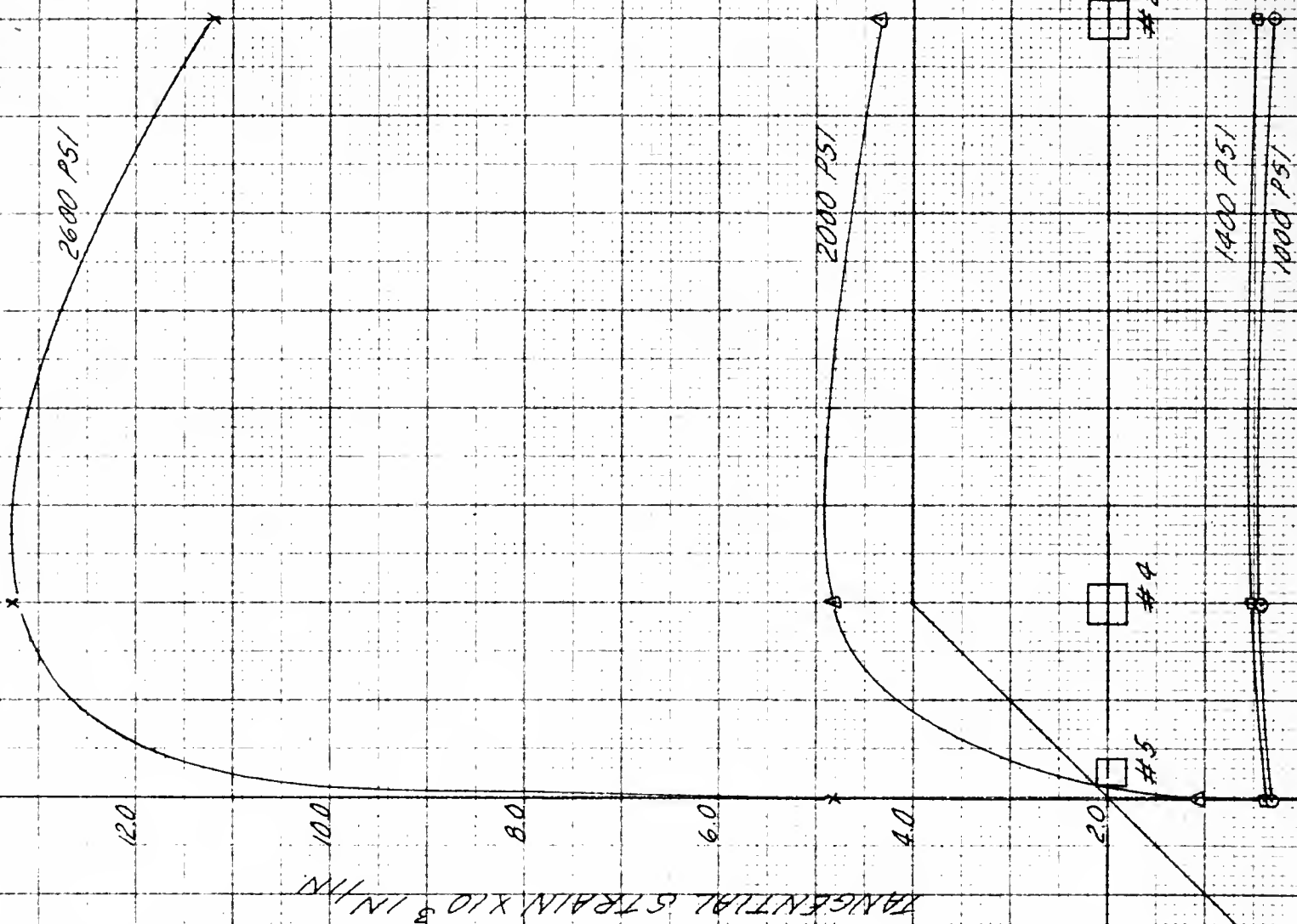


FIG. 41  
PRINCIPAL STRAIN VS. AXIAL POSITION  
TEST NO. II

FIG. 42  
TANGENTIAL STRAIN  
VS. AXIAL POSITION  
TEST NO. II



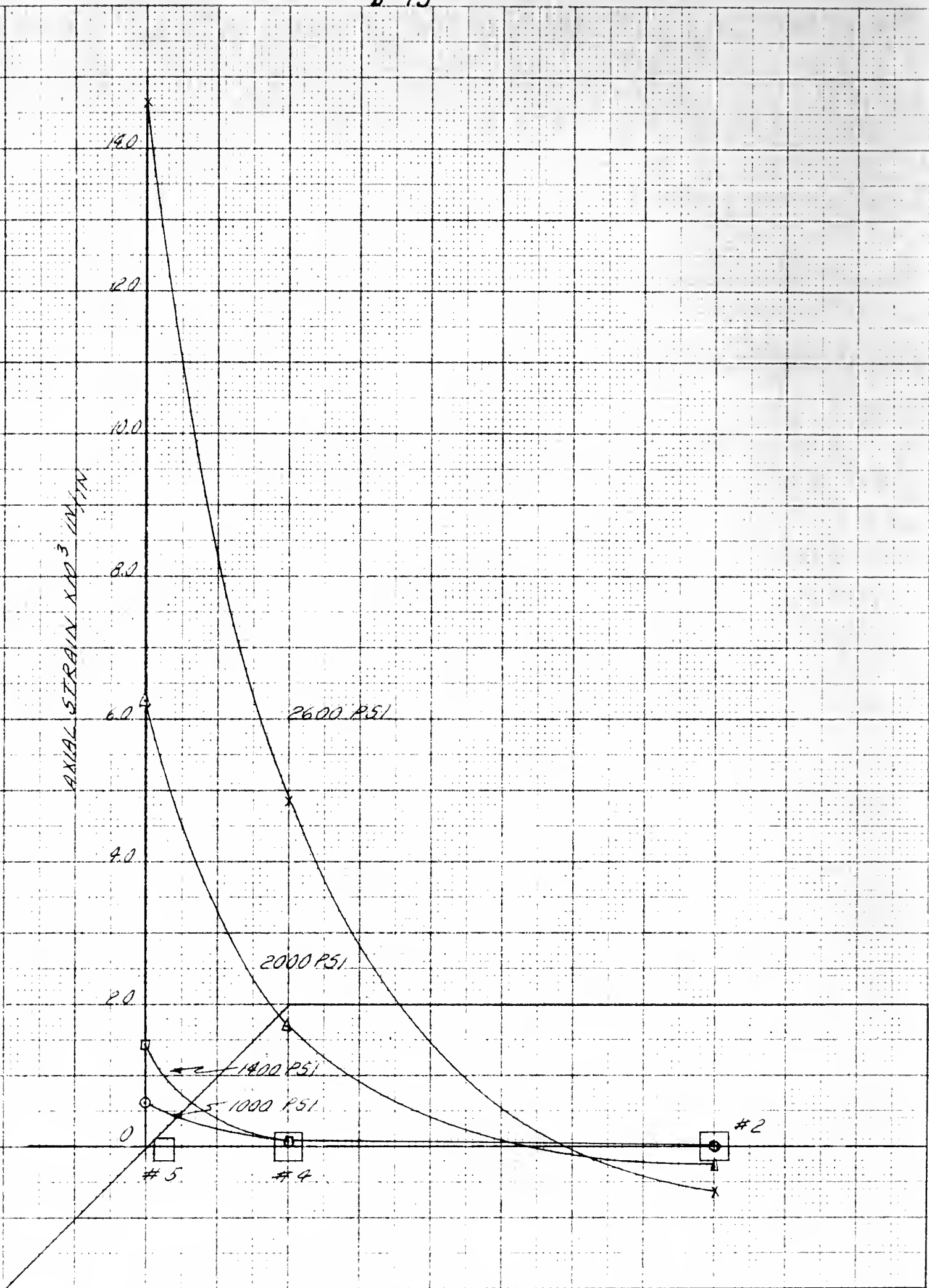


FIG. 43  
AXIAL STRAIN VS. AXIAL POSITION  
TEST NO. II

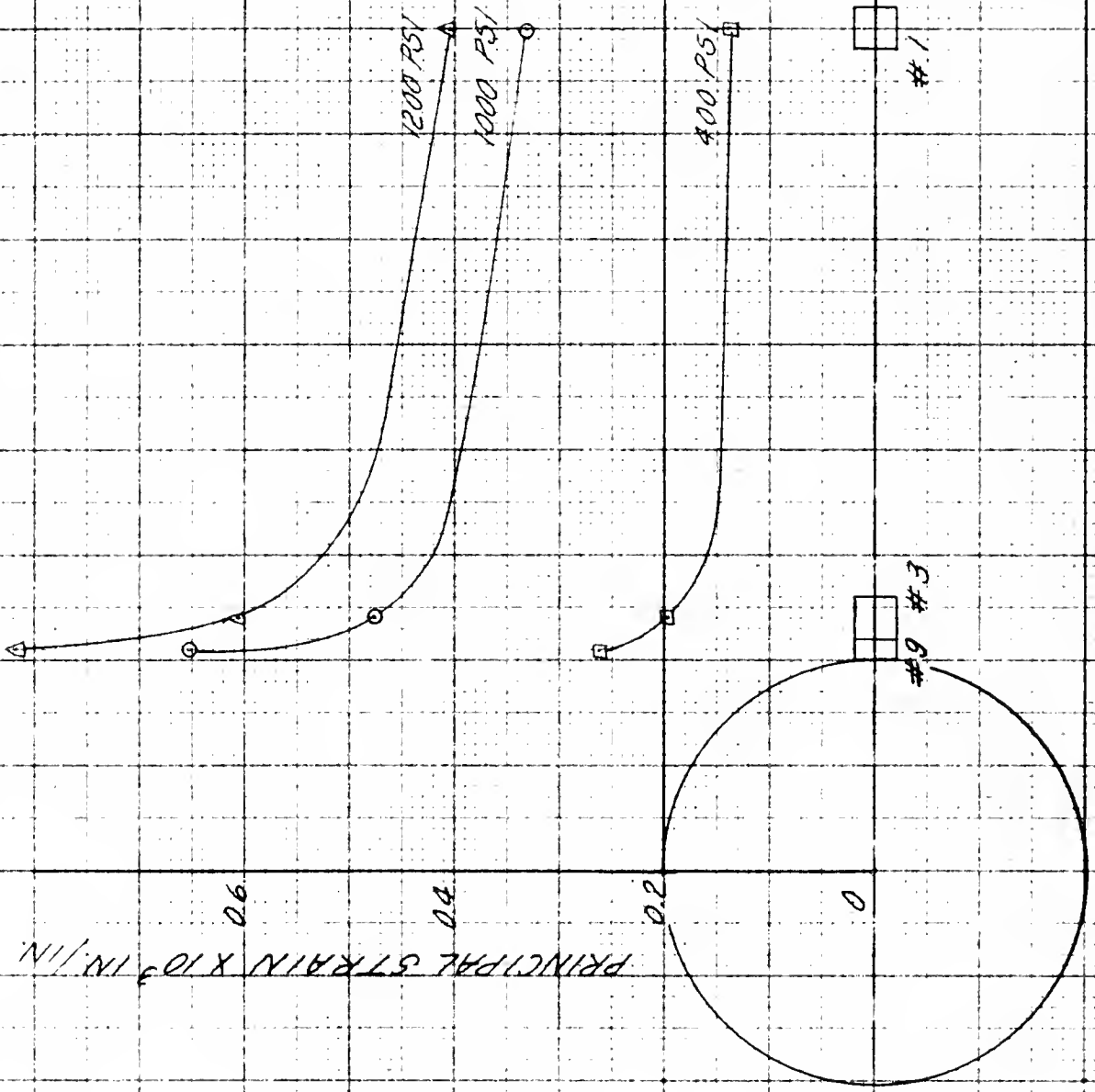


FIG 44  
PRINCIPAL STRAIN VS. AXIAL POSITION  
TEST NO. II

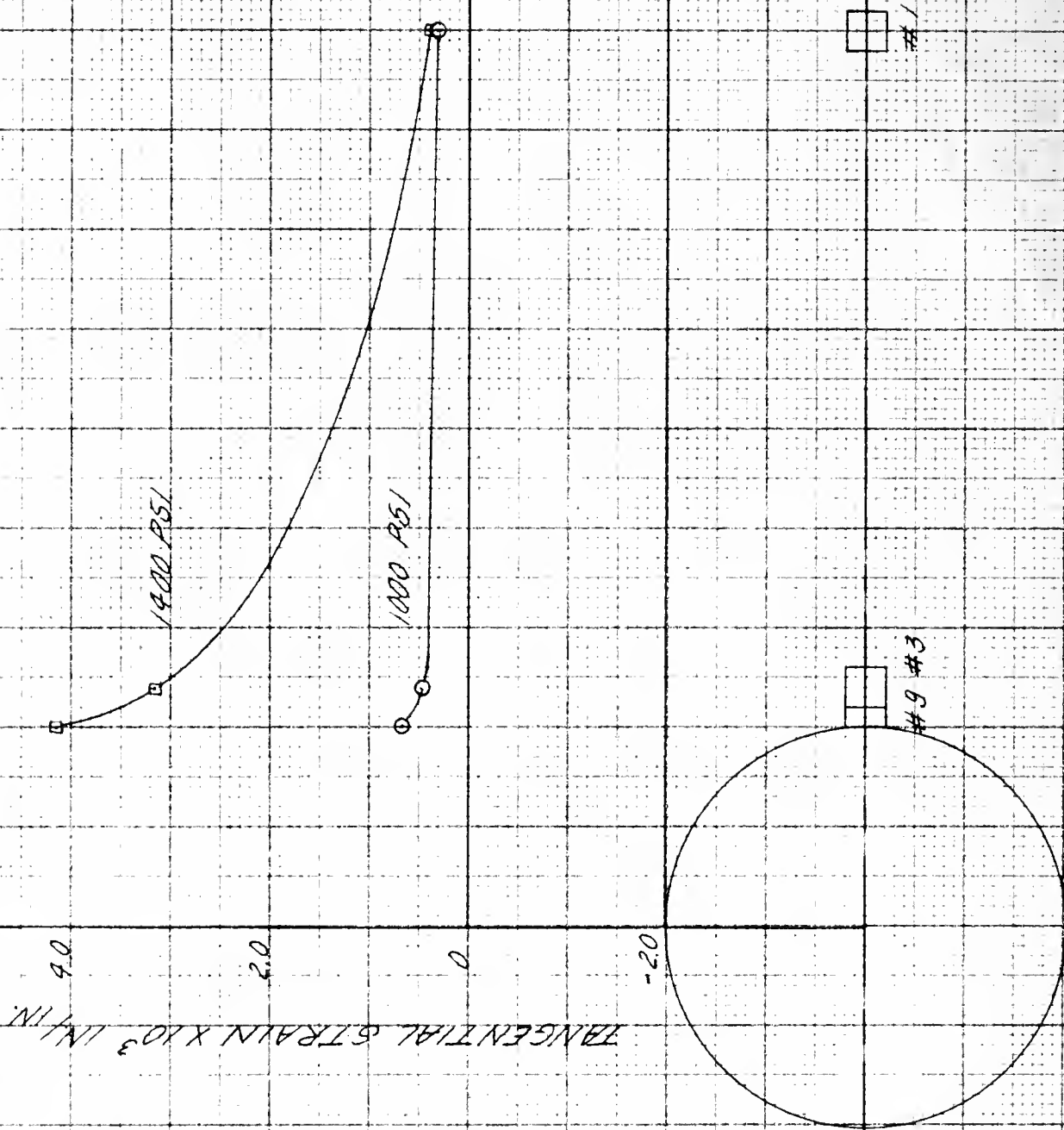


FIG 45  
TANGENTIAL STRAIN VS AXIAL POSITION  
TEST NO. II



AXIAL STRAIN  $\times 10^3$  IN/IN

4.0

2.0

0

-2.0

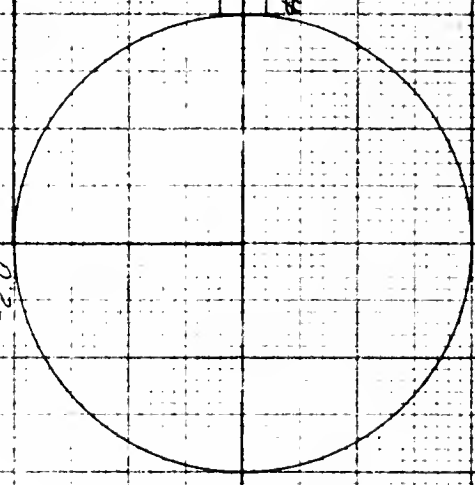
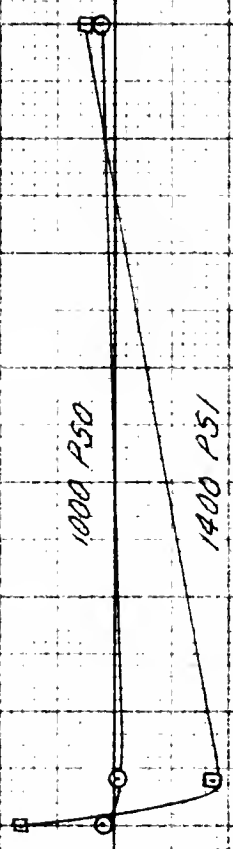


FIG. 46  
AXIAL STRAIN VS. AXIAL POSITION  
TEST NO. II

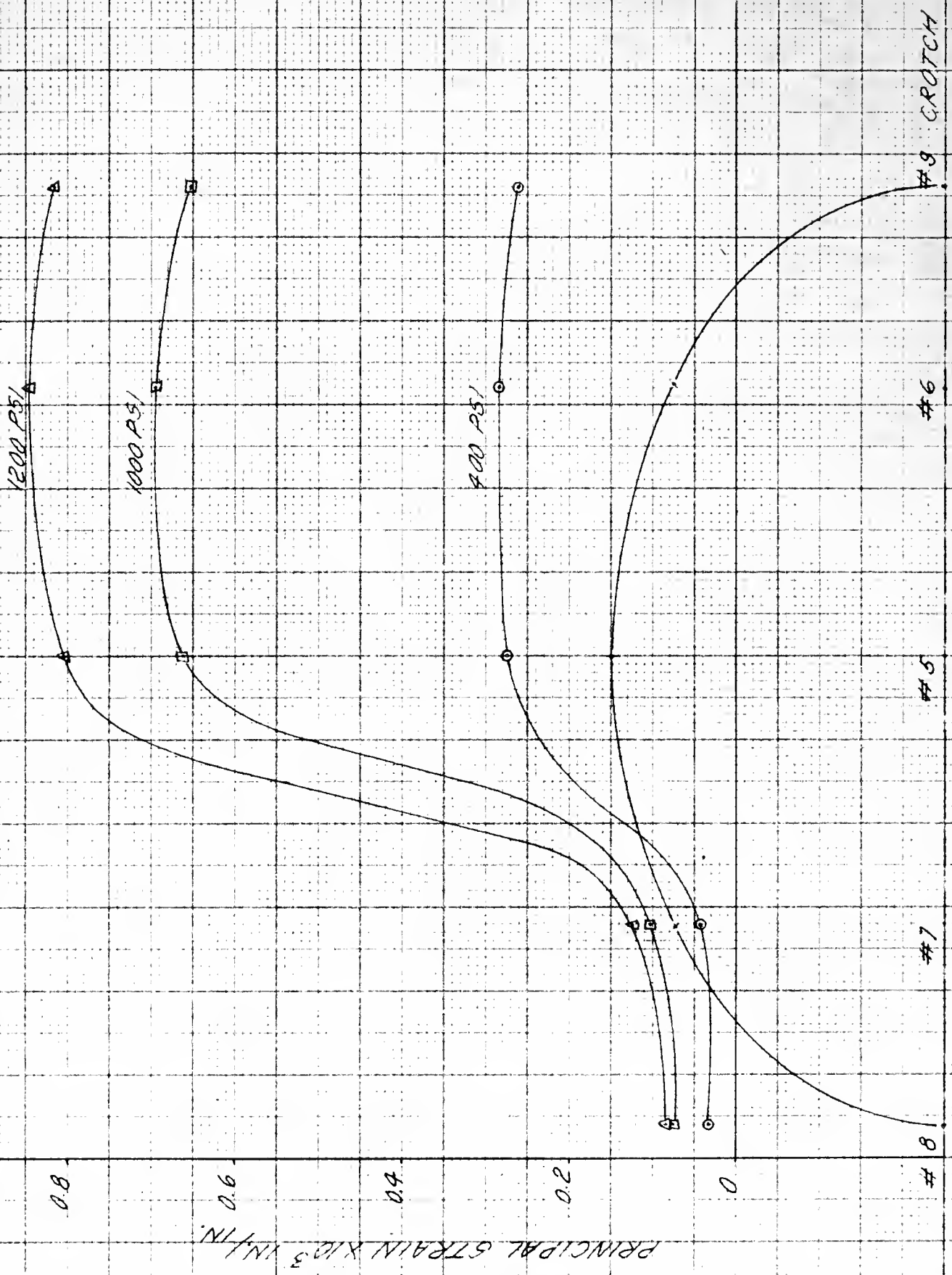


FIG. 47  
PRINCIPAL STRAIN VS. POSITION ON INTERSECTION  
TEST NO. II

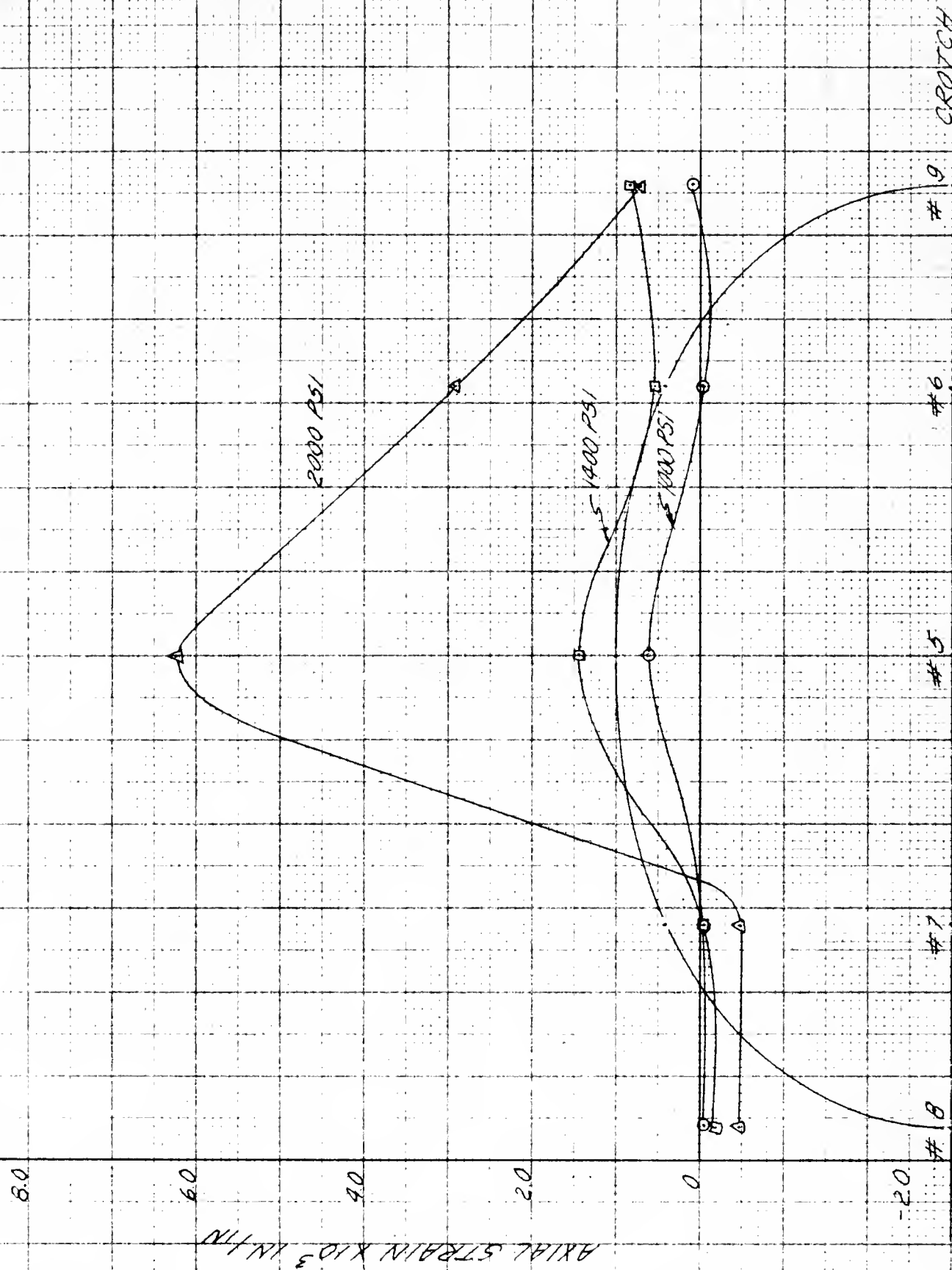


FIG. 48  
AXIAL STRAIN VS. POSITION ON INTERSECTION  
TEST NO. II

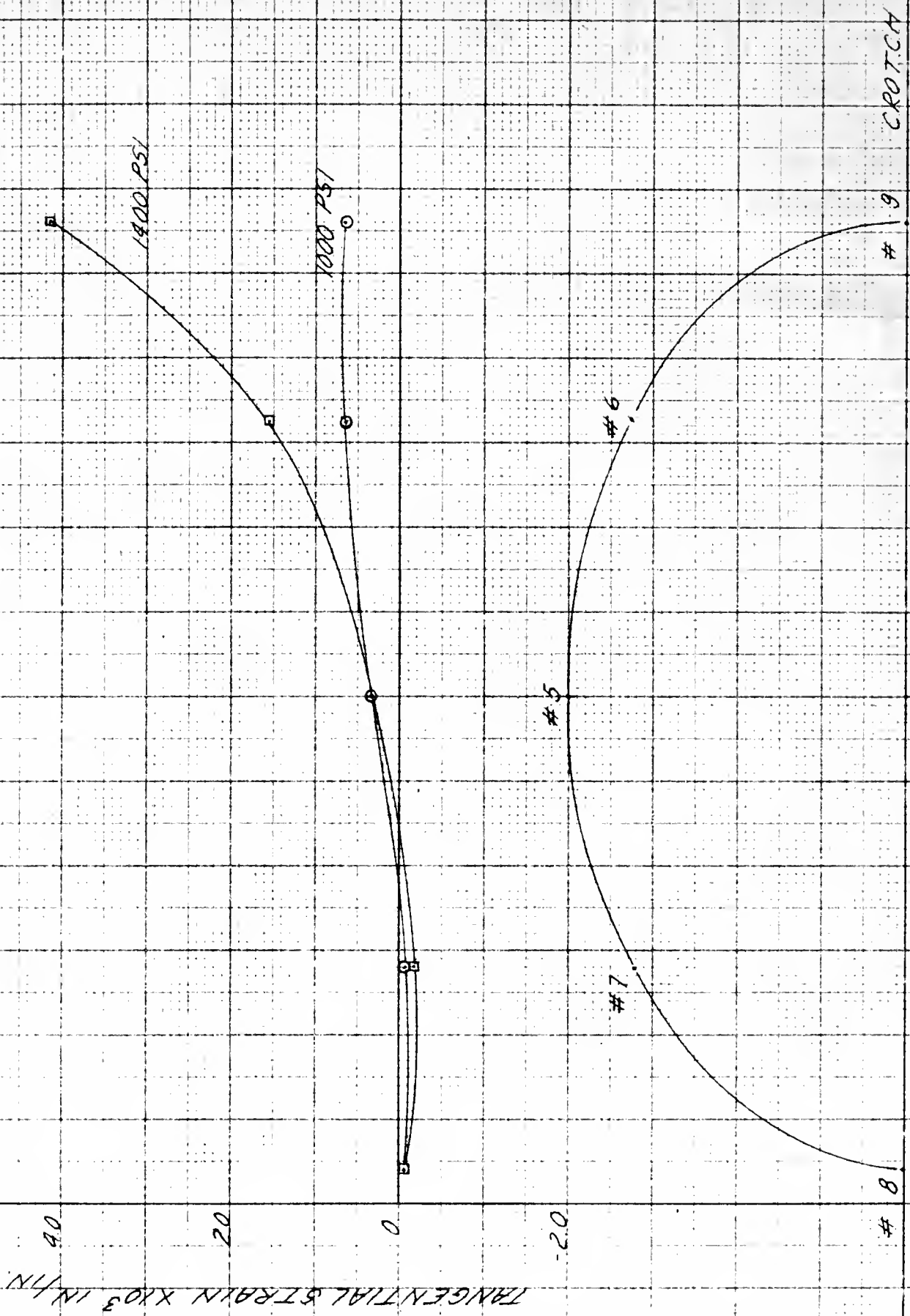
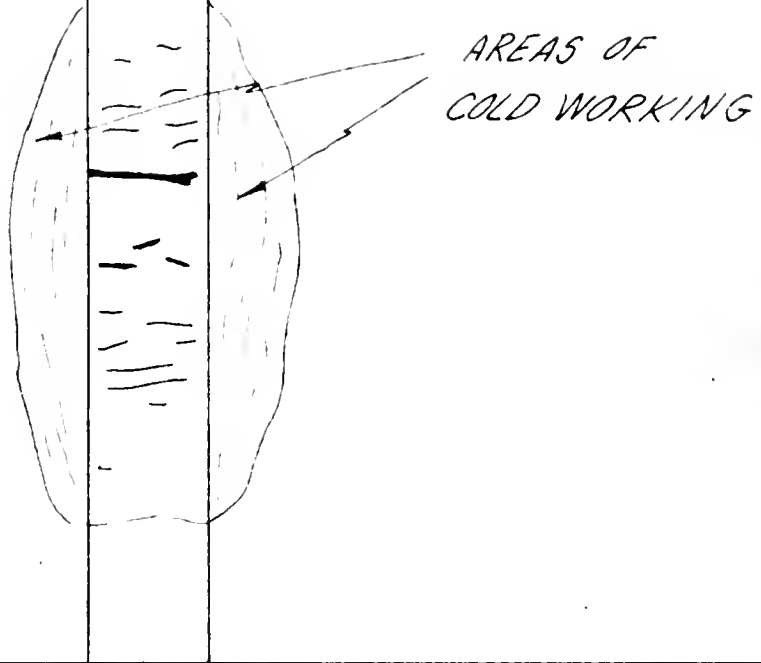
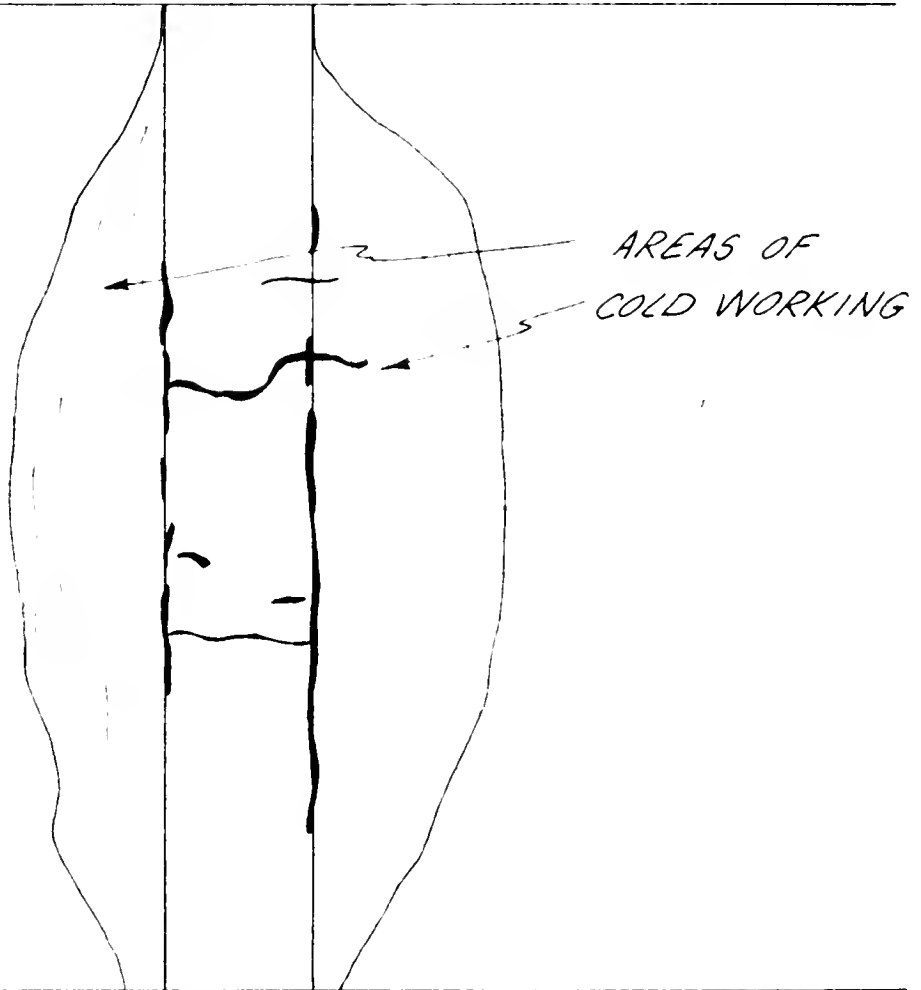


FIG. 99  
TANGENTIAL STRAIN VS POSITION ON INTERSECTION  
TEST NO. II



# I



# II

FIG. 50  
SKETCHES OF BREAKS IN WELDS



7 Thesis 11370  
7 T23 Teig  
Stress distribution  
in two intersecting  
cylinders under  
pressure.

Thesis 11370  
T23 Teig  
Stress distribution  
in two intersecting  
cylinders under  
pressure.

thesT23

Stress distribution in two intersecting



3 2768 002 03432 4

DUDLEY KNOX LIBRARY